Magnetic circuit: a case study

https://www.digikey.co.uk/en/maker/projects/85v-260vac-to-5vdc-2.5a-flyback-switching-power-supply/848a9fa1b7d44244805e0540e3a14441?utm_campaign=an_ac-to-dc_flyback_switc&utm_content=digikey&utm_medium=social&utm_source=twitter

Core: Ferrite, EE-20-10-6 (B66311G0000X187)
Primary Winding: 2.88 mH (124 turns of 0.2 mm wire)
Gap: ~0.25 mm (mathematically)
Secondary Winding: 6 turns of 2 * 0.7 mm wires (two 0.7 mm wires in parallel)

Usually, EE cores come with no gap (a gap between the two middle legs of the core). Therefore, you have to grind the middle EE legs equally to build a gap, but making such a gap accurately and winding the transformer by hand and without any error is difficult. The easy solution is to use an LCR meter. First, wind the primary and assemble the transformer (without any gap). Then measure the inductance of the primary. Naturally, the inductance would be higher than 2.88 mH. Therefore, you have to grind the middle leg of the EE ferrite and build a gap, then assemble the transformer again and measure the inductance of the primary. As a result, simply increase the gap and continuously measure the primary inductance till it gets as close as possible to 2.88 mH. A little tolerance from 2.88 mH is fine and does not make any difference. Figure shows the EE core and the gap. This is the simplest flyback transformer with one primary and one secondary winding.

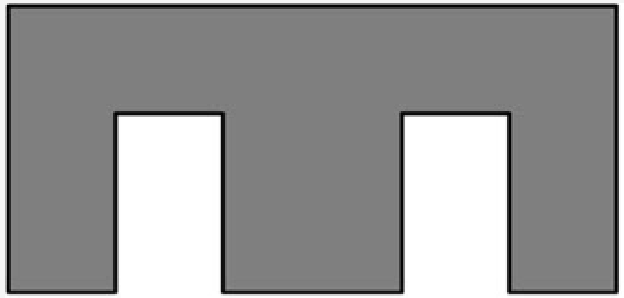

single E core with no gap

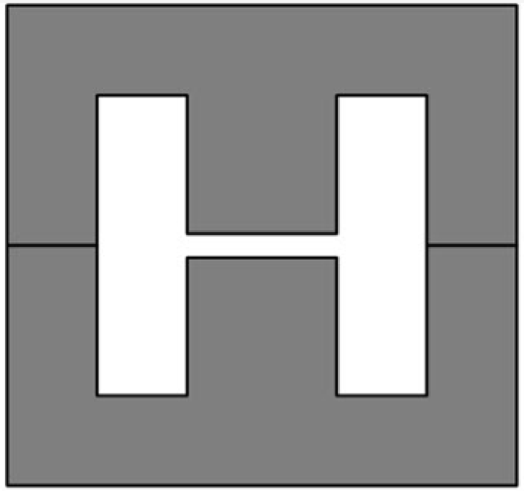

EE core, with a gap on the middle legs

Ferrite E-core used in this case study

https://www.farnell.com/datasheets/1756165.pdf

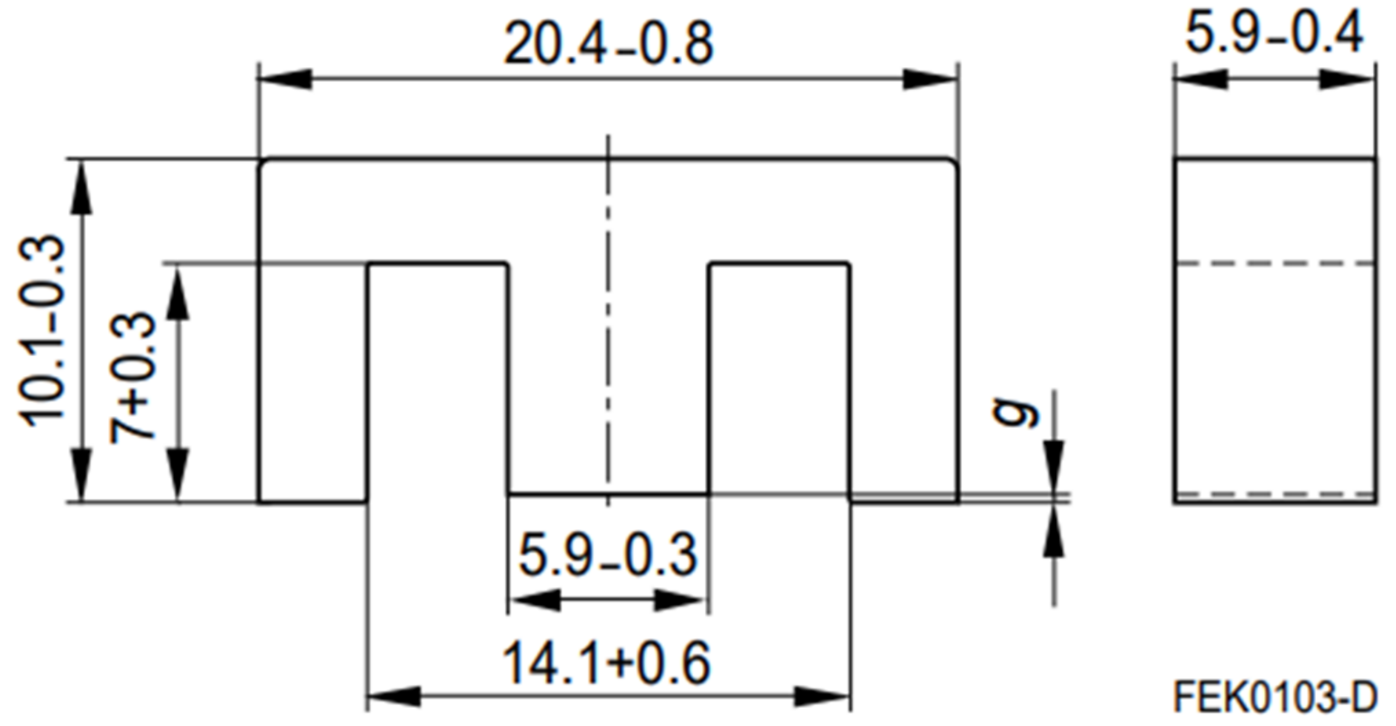

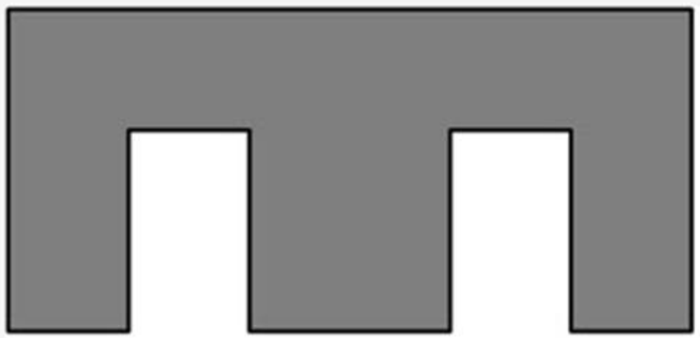

single E core with no gap

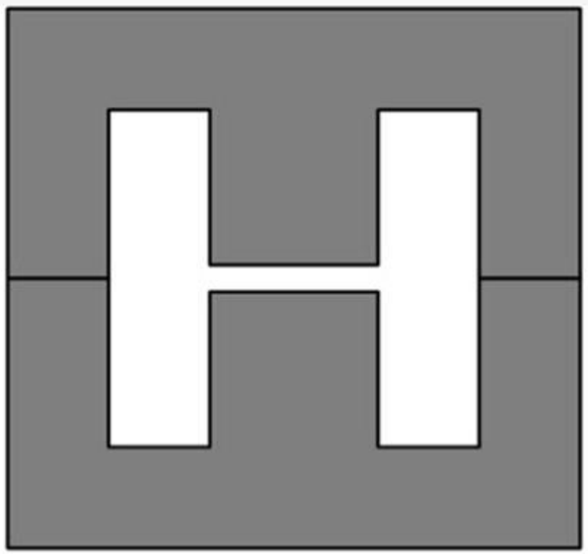

EE core, with a gap on the middle legs

Ferrite cores

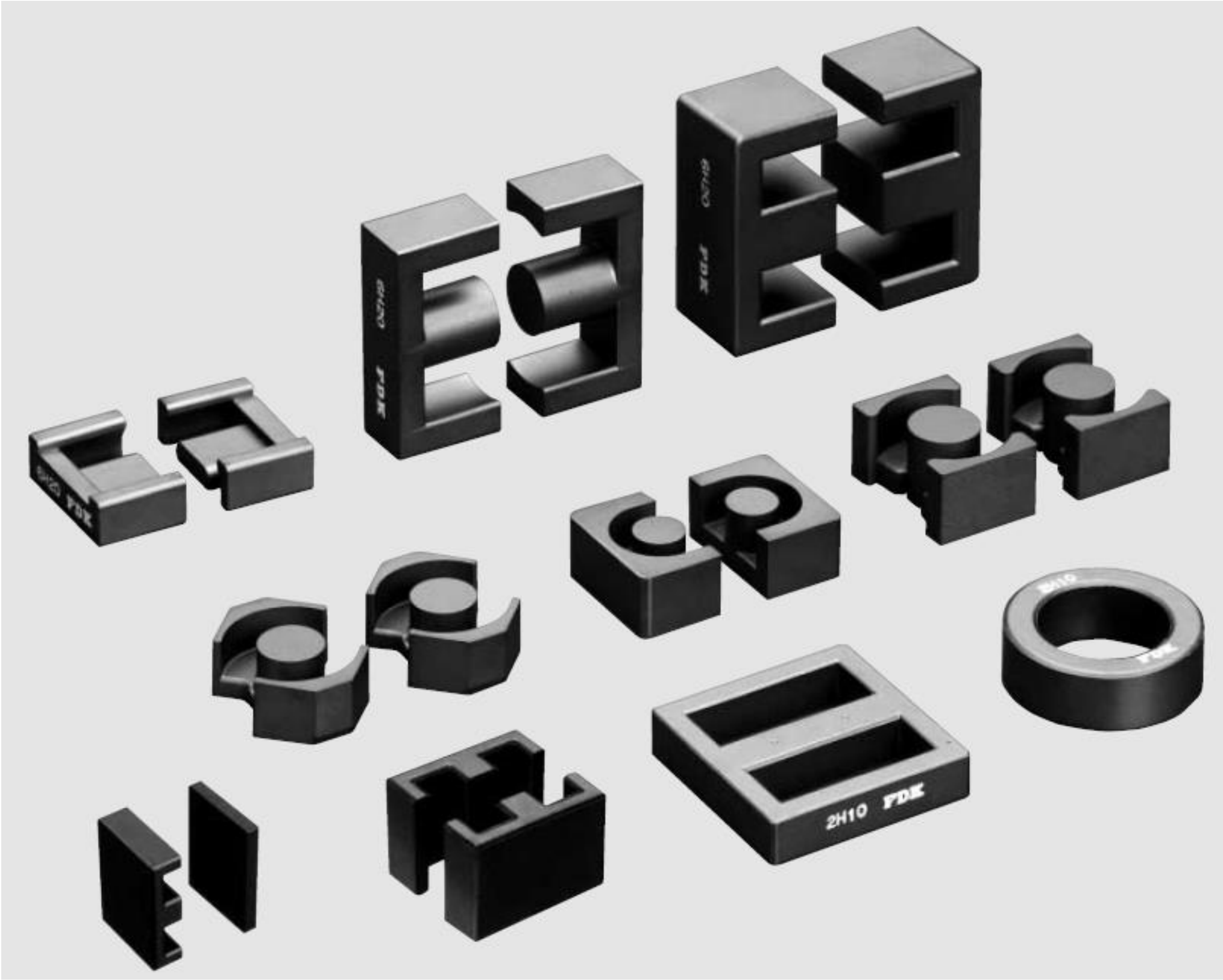

Laminated steel cores

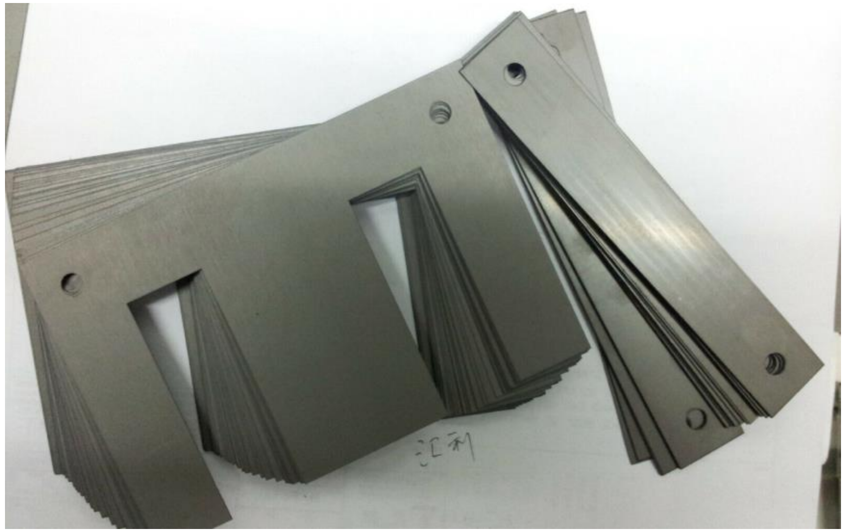

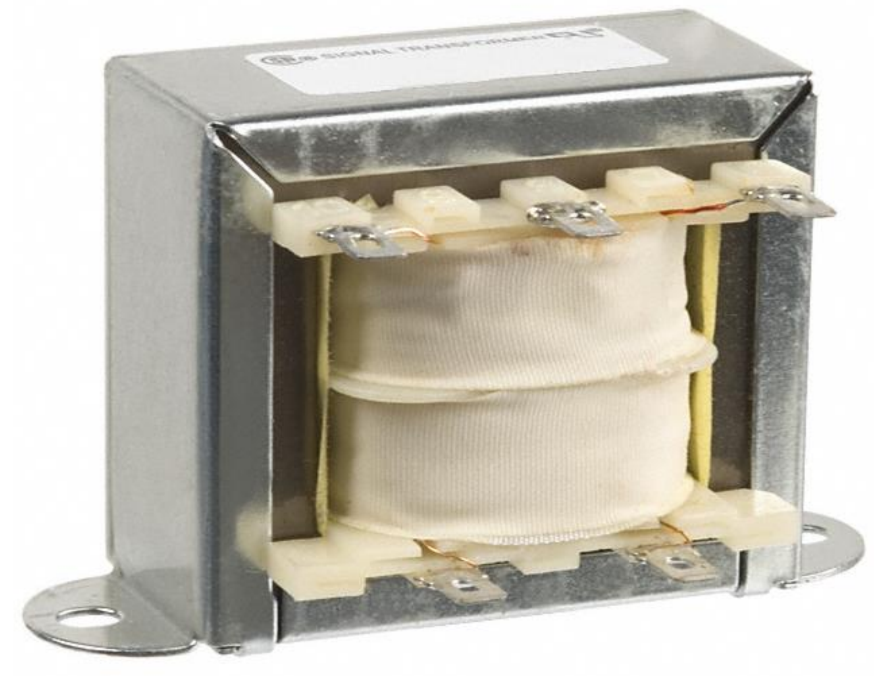

Design equations and magnetic circuit segments

$$R_i = \frac{l_i}{\mu_0 \mu_i S_i}$$

$$\Phi = \frac{\sum_i I_i \times N_i}{\sum_i \frac{l_i}{\mu_0 \mu_i S_i}} = \frac{\sum_i \mathrm{MMF}_i}{\sum_i R_i} - \text{single loop (otherwise use KVL and KCL)}$$

$$B_i = \frac{\Phi}{S_i}$$

$$H_i = \frac{\Phi}{\mu_0 \mu_i S_i}$$

$$L = \frac{N^2}{R_{total}}$$

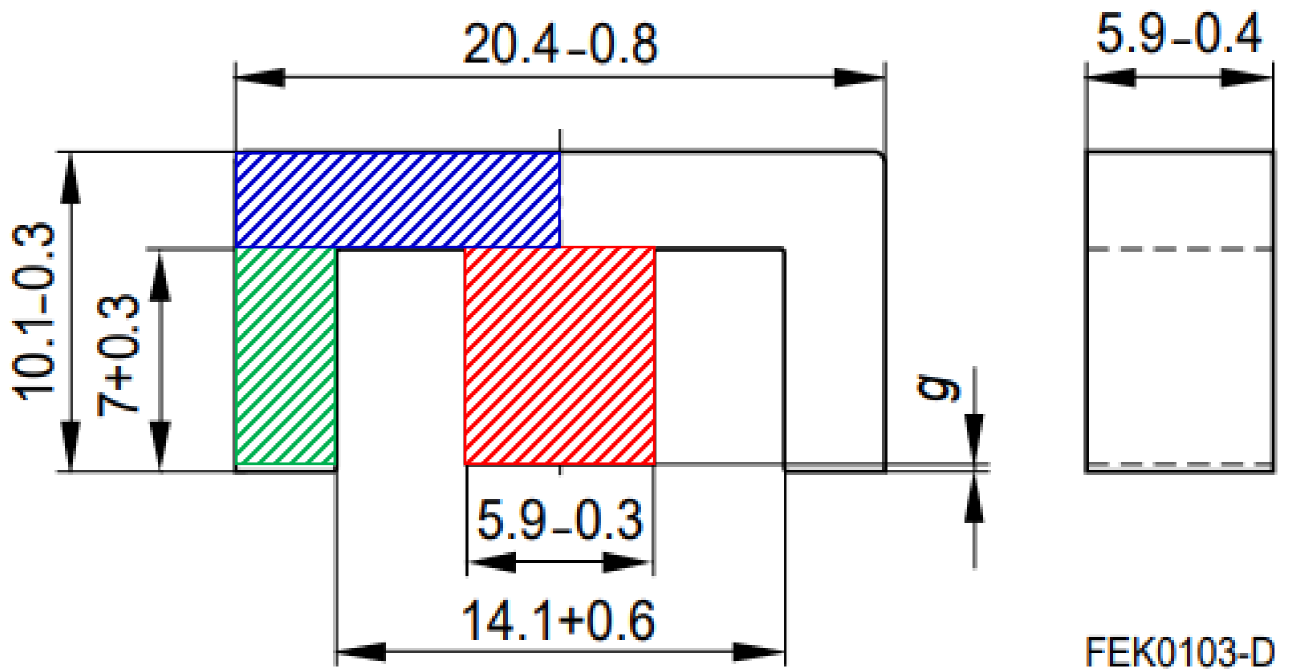

Magnetic saturation is an asymptotic state. Therefore, it is indicated for which **H** (1000 A/m) the induction (flux density) **B** was measured when approaching its saturation value.

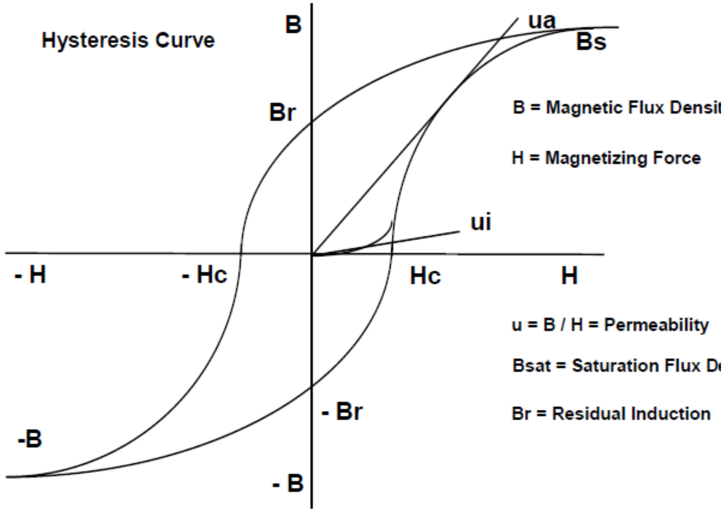

Materials are only ferromagnetic below their corresponding **Curie temperatures.**

Standard material characteristics (Power material)

Property	Symbol		Condition	Unit	6H10	6H20	6H40	6H41	6H42	7H10	7H20
AC initial permeability	μi		0.1 MHz	—	2500	2300	2400	2500	3400	1500	1000
Saturation magnetic flux density	Bs (1000 A/m)		23 °C	mT	510	510	530	530	530	480	480
			100 °C		390	390	430	430	430	380	380
Residual magnetic flux density	Br		23 °C	mT	110	130	110	110	110	150	130
Coercivity	Hc		23 °C	A/m	13	13	10	10	10	30	25
Relative loss factor	tanδ/μi		0.1 MHz	×10⁻⁶	<5	<5	<3	<3	<3	<5	<4
Core loss	200 mT	25 kHz	23 °C	kW/m³	—	—	90	75	60	—	—
			40 °C		—	—	75	60	50	—	—
			60 °C		65	80	60	50	40	—	—
			80 °C		55	65	50	40	45	—	—
			100 °C		80	55	40	45	55	—	—
		100 kHz	23 °C	kW/m³	—	—	650	550	450	—	—
			40 °C		—	—	550	450	350	—	—
			60 °C		450	550	450	350	300	—	—
			80 °C		400	450	350	300	325	—	—
			100 °C		500	400	300	325	375	—	—
	50 mT	500 kHz	60 °C	kW/m³	—	—	—	—	—	100	50
			80 °C		—	—	—	—	—	80	40
			100 °C		—	—	—	—	—	100	50
		1 MHz	60 °C	kW/m³	—	—	—	—	—	400	200
			80 °C		—	—	—	—	—	400	200
			100 °C		—	—	—	—	—	500	250
Temperature coefficient	αμr		20 °C~80 °C	×10⁻⁶	8	8	8	8	8	8	8
Curie temperature	Tc		—	°C	>200	>200	>200	>200	>200	>200	>200
Resistivity	ρ		—	Ω · m	3	3	2	2	2	5	5
Apparent density	d		—	×10³ kg/m³	4.8	4.8	4.9	4.9	4.9	4.8	4.8

Note: 1) The values were obtained with toroidal cores (FR25/15/5).
2) The values were obtained at 23±2 °C unless otherwise specified.
3) Initial permeability was measured at 10kHz, 0.8A/m.

Ferrite cores

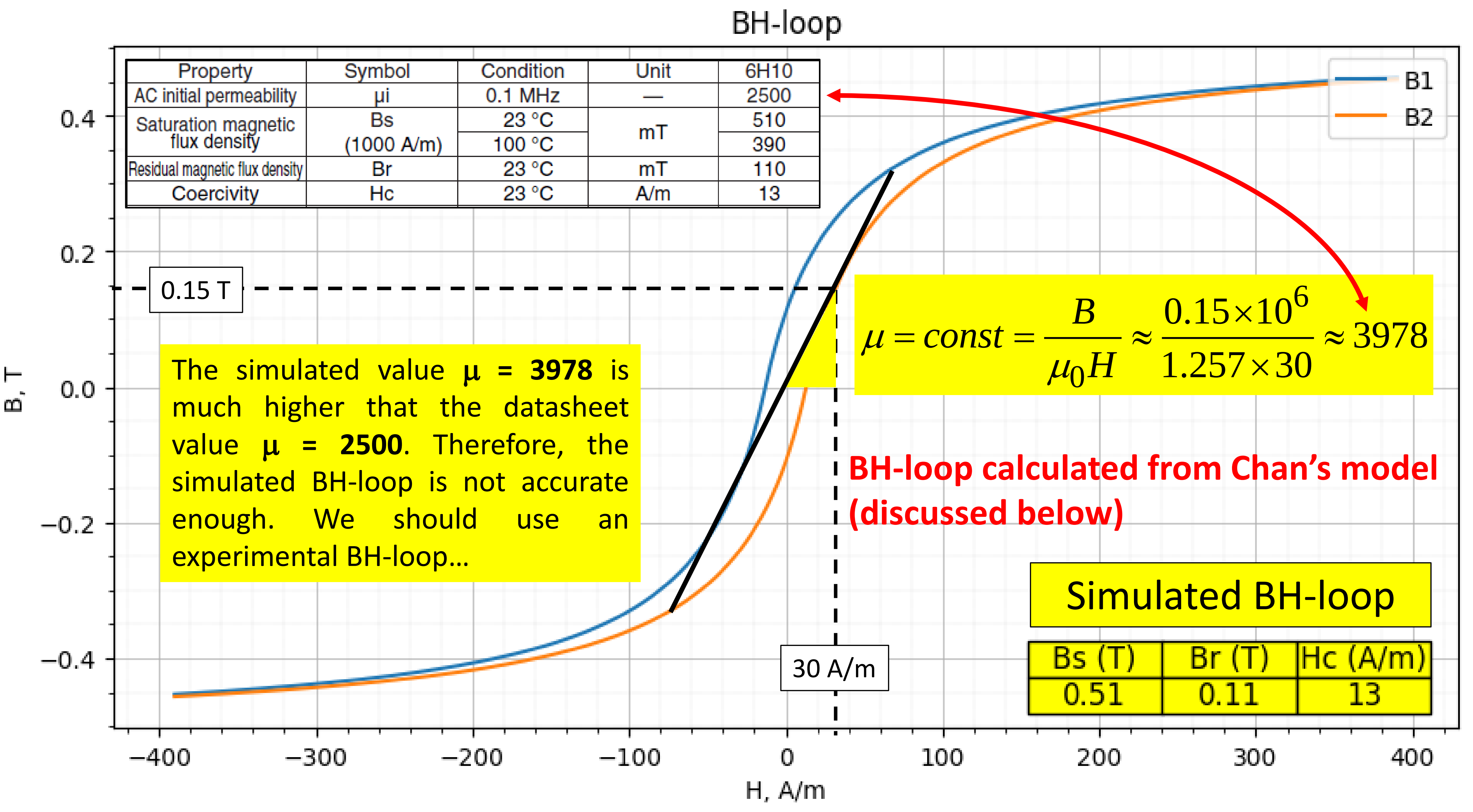
BH-loop

Property	Symbol	Condition	Unit	6H10
AC initial permeability	μi	0.1 MHz	—	2500
Saturation magnetic flux density	Bs (1000 A/m)	23 °C	mT	510
		100 °C		390
Residual magnetic flux density	Br	23 °C	mT	110
Coercivity	Hc	23 °C	A/m	13

B1
B2
0.15 T
30 A/m
The simulated value **μ = 3978** is much higher that the datasheet value **μ = 2500**. Therefore, the simulated BH-loop is not accurate enough. We should use an experimental BH-loop…

$$\mu = const = \frac{B}{\mu_0 H} \approx \frac{0.15\times 10^6}{1.257\times 30} \approx 3978$$

BH-loop calculated from Chan's model (discussed below)
Simulated BH-loop

Bs (T)	Br (T)	Hc (A/m)
0.51	0.11	13

B, T
0.4
0.2
0.0
−0.2
−0.4
H, A/m
−400
−300
−200
−100
0
100
200
300
400

The saturation properties of a magnetic core are equally if not more important than dimensions, AL value and core loss and should also be specified measured and monitored. In many applications if the core saturates, the inductance and impedance of the component decreases and causes the circuit currents to escalate. Excessive currents can cause other circuit components (semiconductor switches, diodes, capacitors) to fail. The saturated core is hard to determine as the root cause since this failure mode typically exhibits no permanent damage to the ferrite core and the magnetic component.

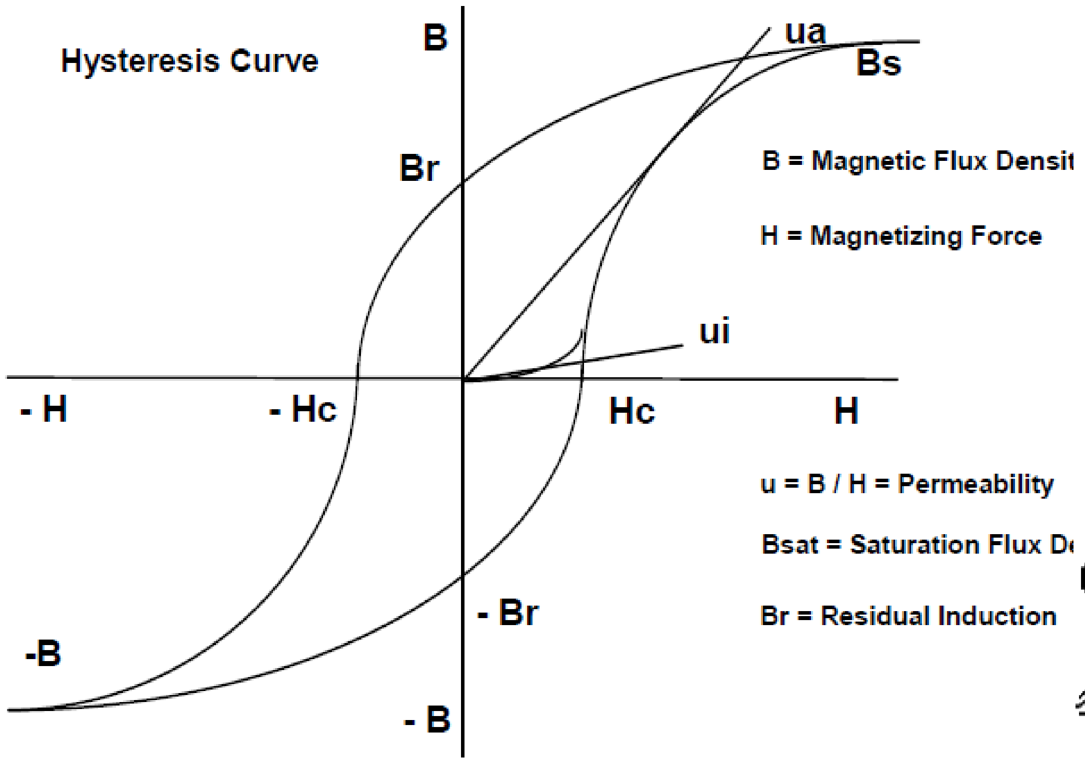

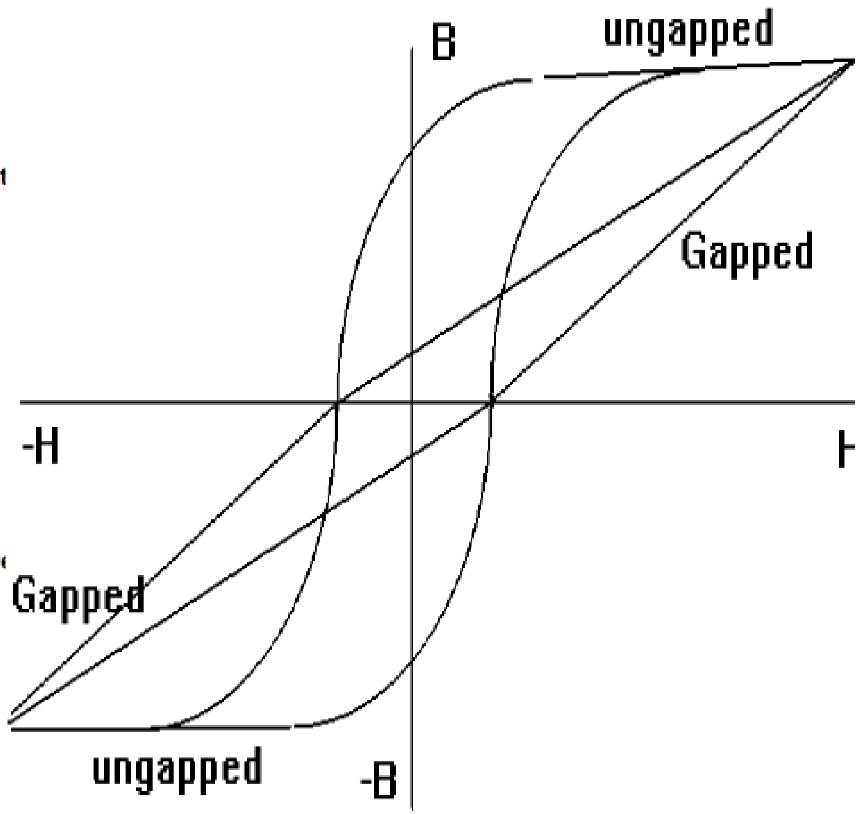

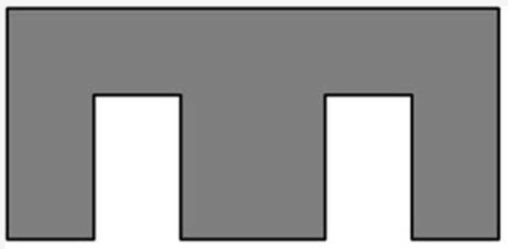

single E core with no gap

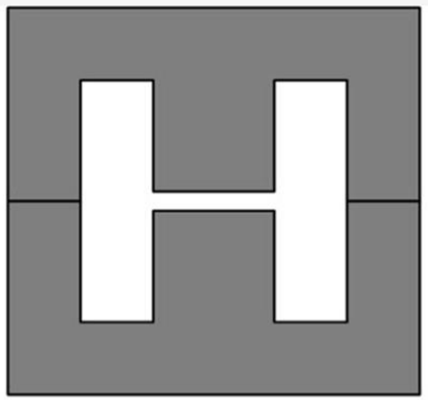

EE core, with a gap on the middle legs

The slope of flux density (B) divided by magnetizing force (H) is the effective permeability. Permeability is a materials ability to conduct magnetic flux relative to air and is proportional to a components inductance. Note that as the material saturates the slope of B/H decreases, thus the inductance of a component decreases. Introducing an air gap in the magnetic flux path sheers the hysteresis loop so that it requires more magnetizing force to saturate the core. The more air gap introduced into the flux path the lower the permeability (ratio of B/H). Note that the saturation flux density is unchanged even though a gapped core requires more magnetizing force before reaching saturation.

https://www.farnell.com/datasheets/1756165.pdf

Ungapped

Material	A_L value nH	μ_e	P_V W/set	Ordering code
N30	2150 +30/–20%	2460		B66311G0000X130
N27	1300 +30/–20%	1490	< 0.27 (200 mT, 25 kHz, 100 °C)	B66311G0000X127
N87	1470 +30/–20%	1680	< 0.75 (200 mT, 100 kHz, 100 °C)	B66311G0000X187

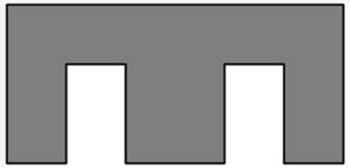

single E core with no gap

A_L	Inductance factor; $A_L = L/N^2$	nH

Gapped

Material	g mm (Total gap!)	A_L value approx. nH	μ_e	Ordering code ** = 27 (N27) = 87 (N87)
N27, N87	0.09 ±0.01	363	415	B66311G0090X1**
	0.17 ±0.02	227	259	B66311G0170X1**
	0.25 ±0.02	171	195	B66311G0250X1**
	0.50 ±0.05	103	118	B66311G0500X1**

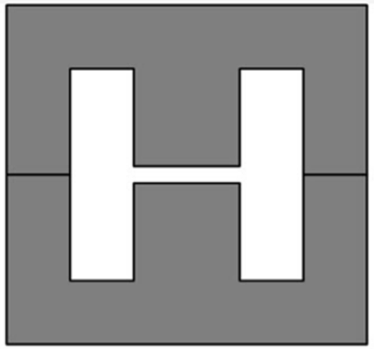

EE core, with a gap on the middle legs

The A_L value in the table applies to a core set comprising one ungapped core (dimension g = 0) and one gapped core (dimension g > 0).

Cross-sections

18.59 mm²

18.29 mm²

34.81 mm²

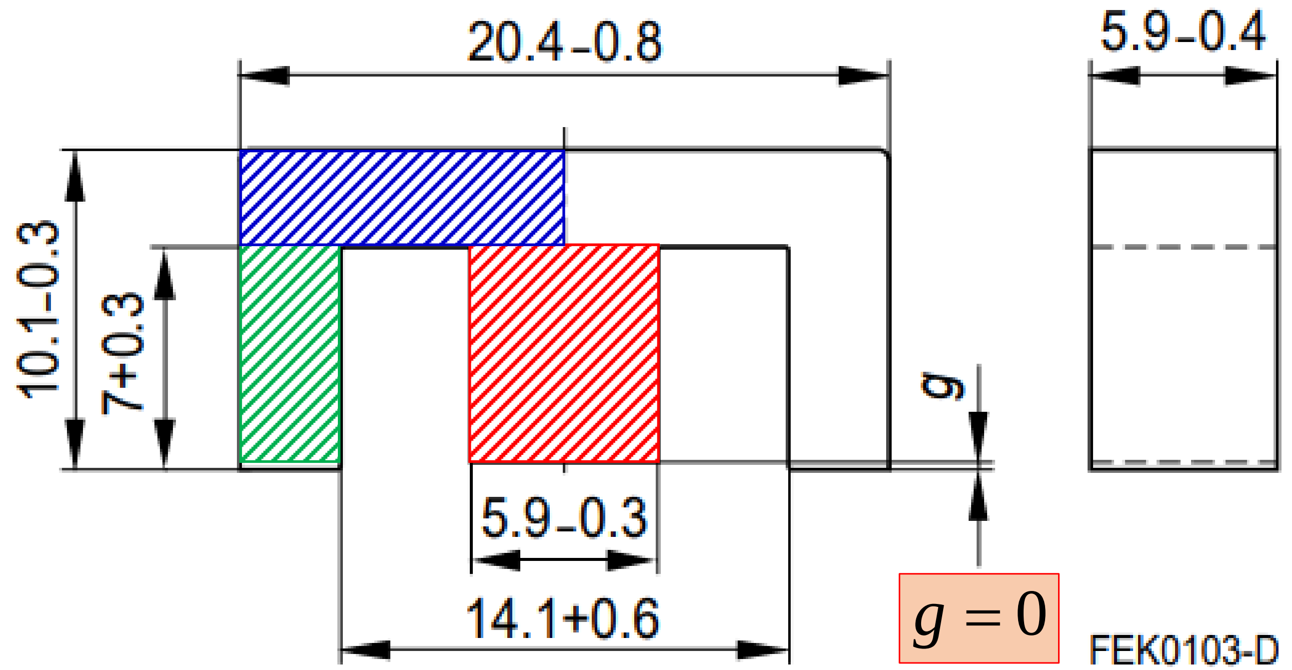

$$R_{red} = \frac{7\times10^3}{\mu_0\times\mu\times34.81}\approx9.53\times10^4$$

$$R_{blue} = \frac{10.2\times10^3}{\mu_0\times\mu\times18.29}\approx2.64\times10^5$$

$$R_{green} = \frac{7\times10^3}{\mu_0\times\mu\times18.59}\approx1.78\times10^5$$

$$\mu_0 = 1.25663706212\times10^{-6}$$

$$\mu = 1680$$

18.59 mm²

18.29 mm²

34.81 mm²

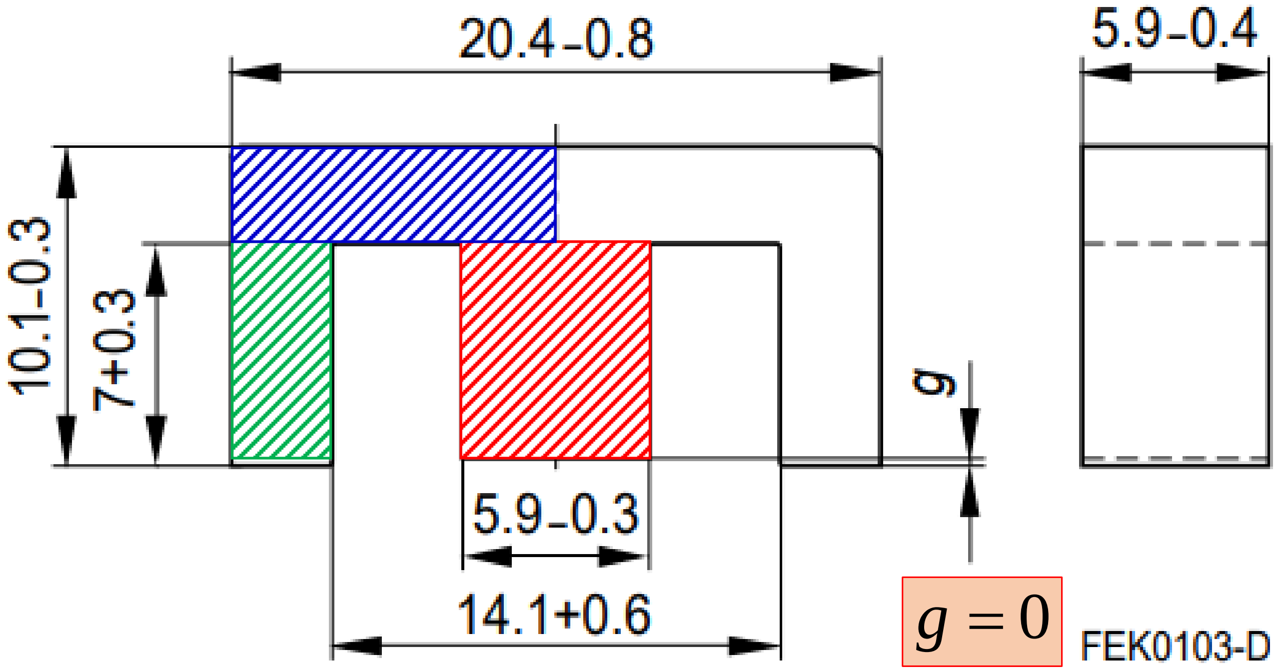

$$R_{red} = \frac{7\times10^3}{\mu_0 \times \mu \times 34.81} \approx 9.53\times10^4$$

$$R_{blue} = \frac{10.2\times10^3}{\mu_0 \times \mu \times 18.29} \approx 2.64\times10^5$$

$$R_{green} = \frac{7\times10^3}{\mu_0 \times \mu \times 18.59} \approx 1.78\times10^5$$

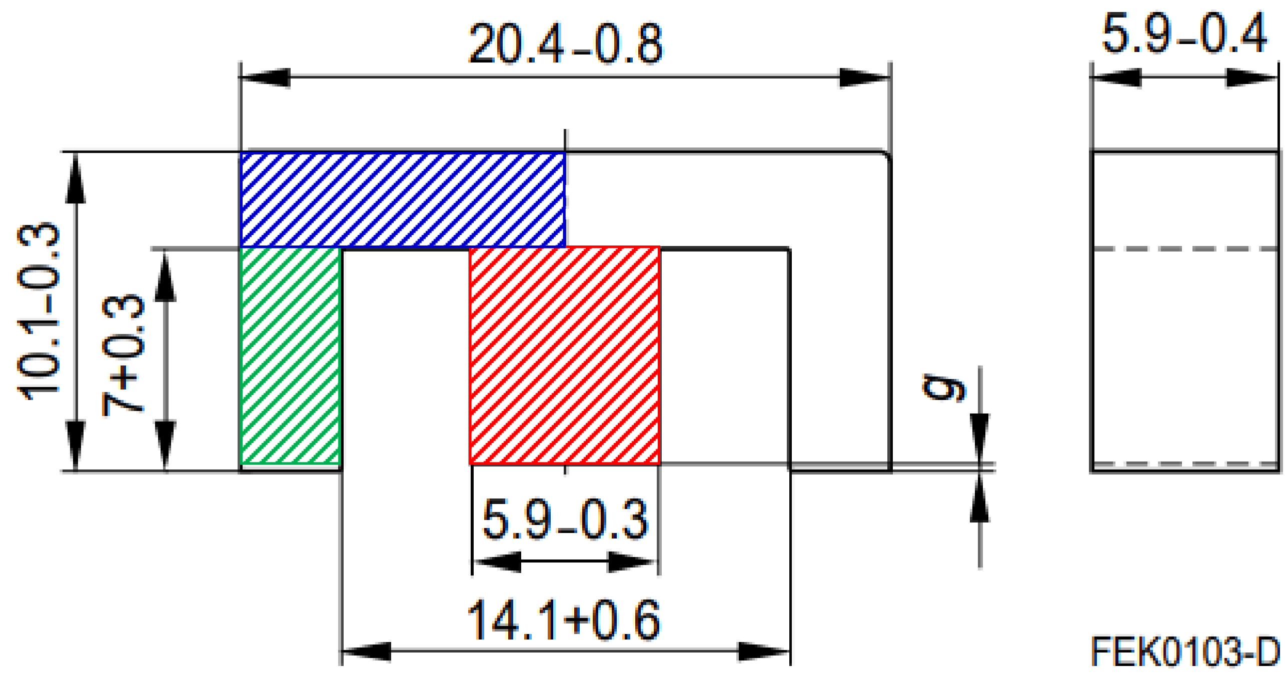

$$\boxed{R_{total} = 2R_{red} + R_{blue} + R_{green} \approx 6.33\times10^5}$$

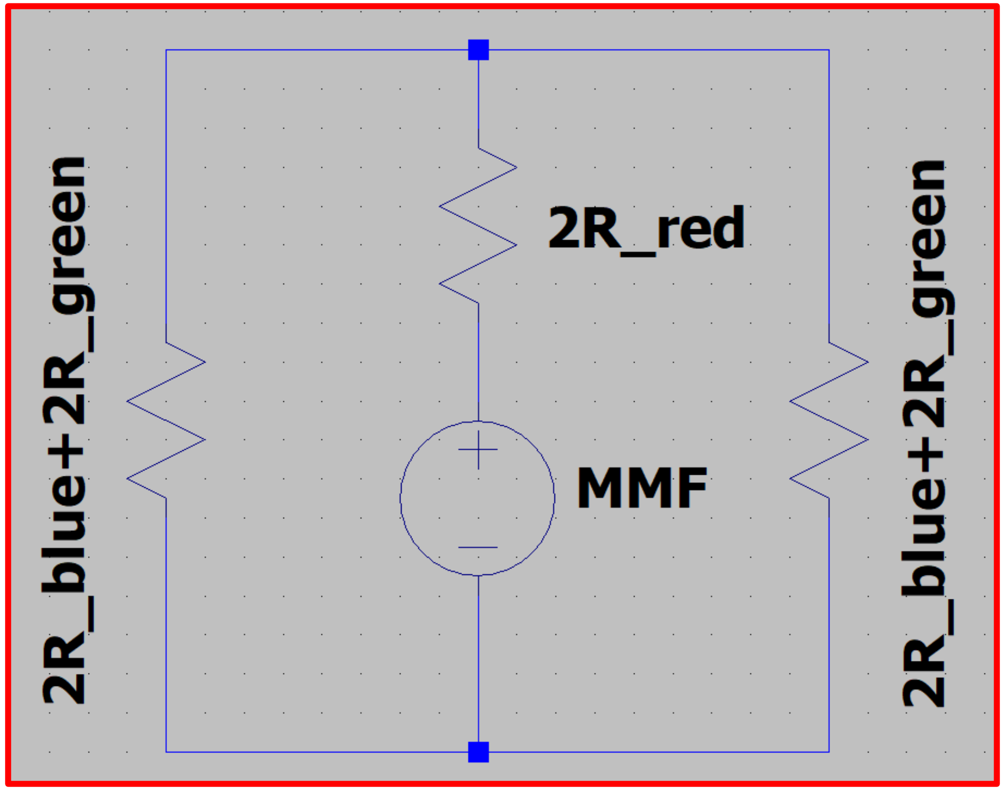

$$\boxed{g = 0}$$

$$\boxed{L = \left.\frac{N^2}{R_{total}}\right|_{N=124} \approx 24.3 \text{ mH}}$$

Ungapped

Material	A_L value nH	μ_e	P_V W/set	Ordering code
N30	2150 +30/–20%	2460		B66311G0000X130
N27	1300 +30/–20%	1490	< 0.27 (200 mT, 25 kHz, 100 °C)	B66311G0000X127
N87	1470 +30/–20%	1680	< 0.75 (200 mT, 100 kHz, 100 °C)	B66311G0000X187

↓

A_L	Inductance factor; $A_L = L/N^2$	nH

↓

For $N = 124$: $18.1\ \mathrm{mH} < L < 29.38\ \mathrm{mH}$

$$\boxed{g = 0} \qquad \boxed{L = \left.\frac{N^2}{R_{total}}\right|_{N=124} \approx 24.3\ \mathrm{mH}}$$

$$R_{red} = \frac{7\times10^3}{\mu_0\times\mu\times34.81} \approx 9.53\times10^4$$

$$\mu_0 = 1.25663706212\times10^{-6}$$
$$\mu = 1680$$

$$R_{blue} = \frac{10.2\times10^3}{\mu_0\times\mu\times18.29} \approx 2.64\times10^5$$

$$R_{gap} = \frac{0.25\times10^3}{\mu_0\times34.81} \approx 5.72\times10^6$$

$$R_{green} = \frac{7\times10^3}{\mu_0\times\mu\times18.59} \approx 1.78\times10^5$$

18.59 mm²

18.29 mm²

34.81 mm²

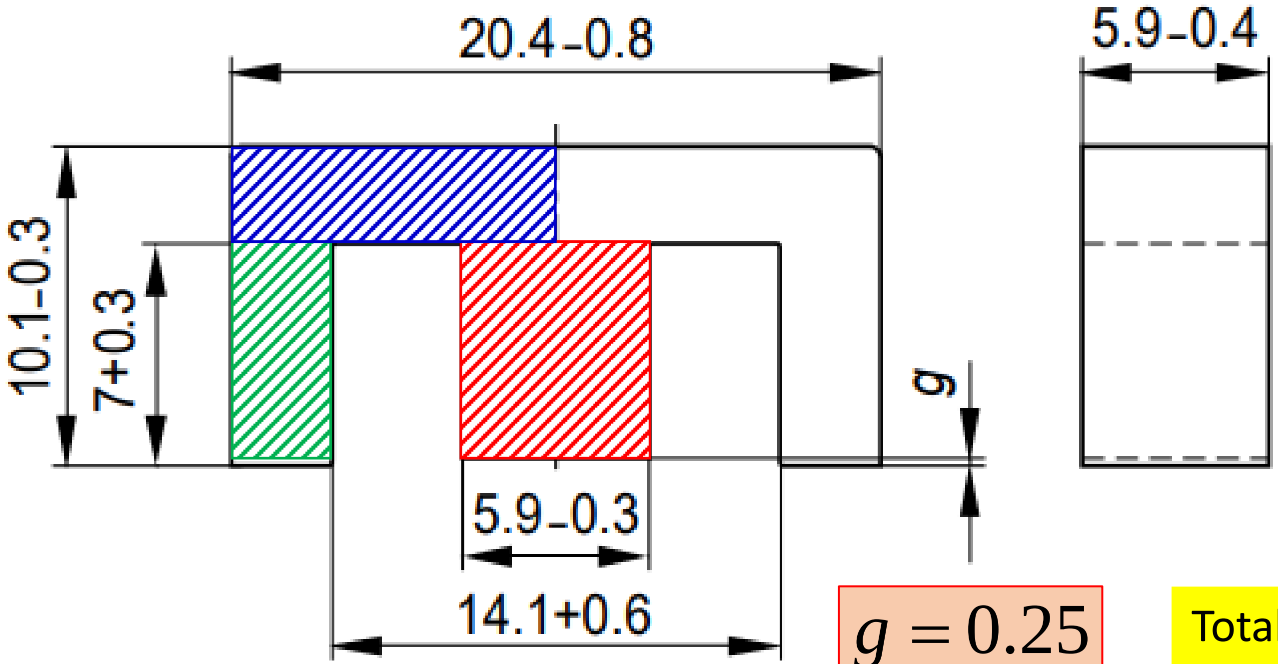

$g = 0.25$

Total gap!

$$R_{red} = \frac{7\times10^3}{\mu_0 \times \mu \times 34.81} \approx 9.53\times10^4$$

$$R_{blue} = \frac{10.2\times10^3}{\mu_0 \times \mu \times 18.29} \approx 2.64\times10^5$$

$$R_{green} = \frac{7\times10^3}{\mu_0 \times \mu \times 18.59} \approx 1.78\times10^5$$

$$R_{gap} = \frac{0.25\times10^3}{\mu_0 \times 34.81} \approx 5.72\times10^6$$

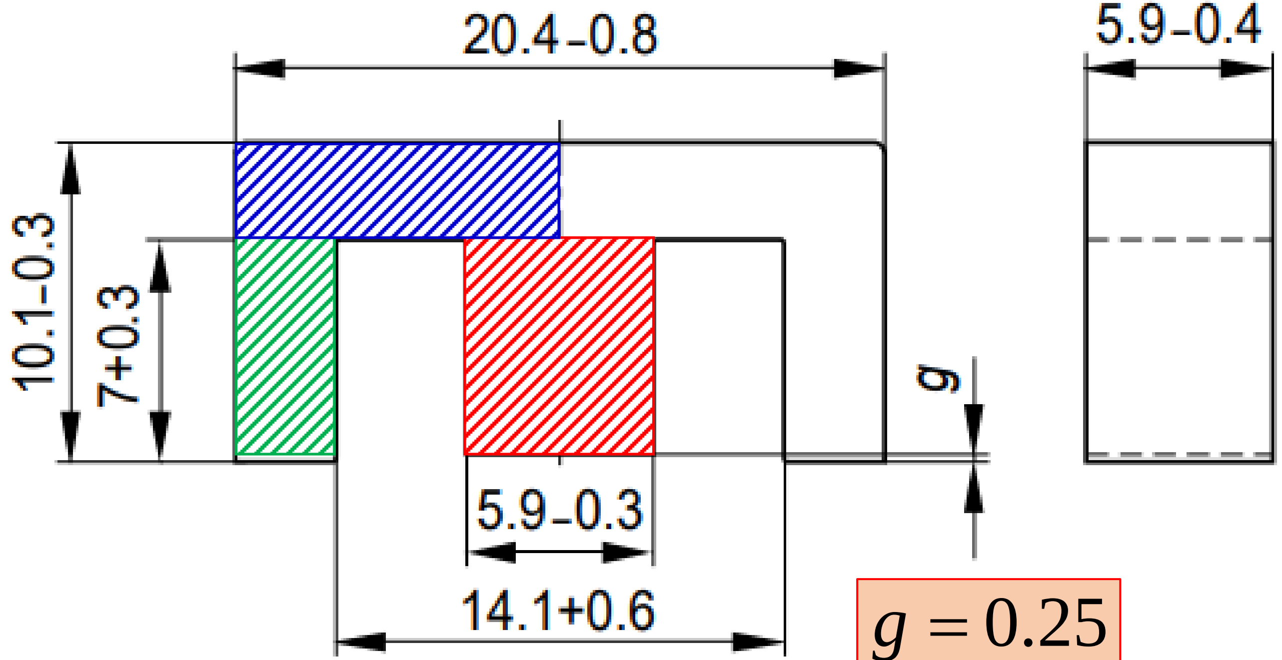

$$\boxed{g = 0.25}$$

$$\boxed{R_{total} = 2R_{red} + R_{gap} + R_{blue} + R_{green} \approx 6.35\times10^6}$$

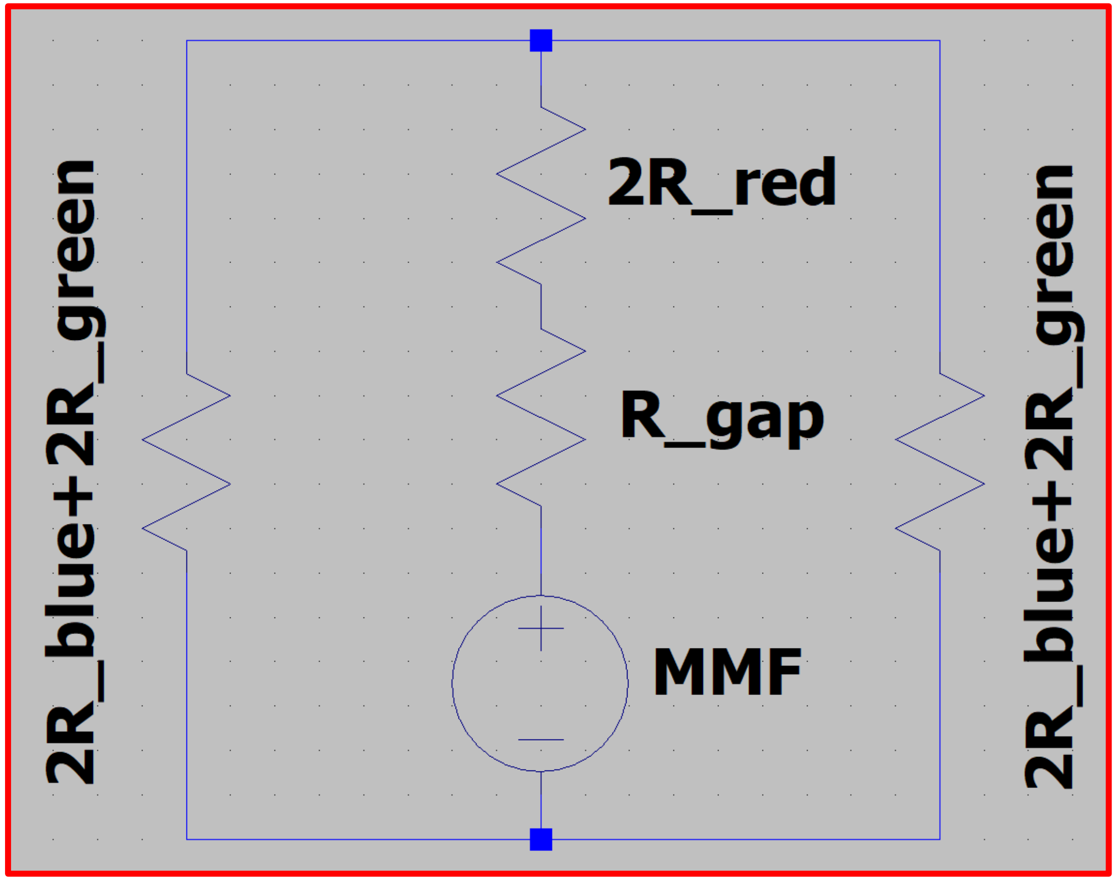

$$\boxed{L = \left.\frac{N^2}{R_{total}}\right|_{N=124} \approx 2.4 \text{ mH}}$$

Gapped

Material	g mm	A_L value approx. nH	μ_e	Ordering code ** = 27 (N27) = 87 (N87)
N27, N87	0.09 ±0.01	363	415	B66311G0090X1**
	0.17 ±0.02	227	259	B66311G0170X1**
	0.25 ±0.02	171	195	B66311G0250X1**
	0.50 ±0.05	103	118	B66311G0500X1**

A_L	Inductance factor; $A_L = L/N^2$	nH

For $N = 124$: $L = 2.63\ \mathrm{mH}$

$$\boxed{g = 0.25}$$

$$\boxed{L = \left.\frac{N^2}{R_{total}}\right|_{N=124} \approx 2.4\ \mathrm{mH}}$$

https://www.farnell.com/datasheets/1756165.pdf

Calculation factors (for formulas, see *"E cores: general information"*)

Material	Relationship between air gap – A_L value		Calculation of saturation current			
	K1 (25 °C)	K2 (25 °C)	K3 (25 °C)	K4 (25 °C)	K3 (100 °C)	K4 (100 °C)
N27	61.6	–0.737	88.1	–0.847	80.9	–0.865
N87	61.6	–0.737	88.5	–0.796	78.4	–0.873

Validity range: K1, K2: 0.05 mm < s < 1.50 mm
K3, K4: 50 nH < A_L < 430 nH

Calculation formulae a) and b) apply to the A_L value under the following measuring conditions:

Measuring flux density $\hat{B} \leq 0.25$ mT, measuring frequency f = 10 kHz,
measuring temperature T = 25 ±3 °C, measuring coil: N = 100 turns, fully wound

a) Air gap and A_L value

The typical A_L value tabulated in the individual data sheets refers to a core set comprising a gapped core with dimension „g" and an ungapped core with „g" approx. 0.

By inserting the core-specific constants K1 and K2, a nominal A_L value can be calculated for the materials N27 and N87 within the relevant quoted air-gap validity range:

$$s = \left(\frac{A_L}{K1}\right)^{\frac{1}{K2}} \qquad s = [\mathrm{mm}] \quad A_L = [\mathrm{nH}]$$

https://www.farnell.com/datasheets/1756165.pdf

Calculation factors (for formulas, see *"E cores: general information"*)

Material	Relationship between air gap – A_L value		Calculation of saturation current			
	K1 (25 °C)	K2 (25 °C)	K3 (25 °C)	K4 (25 °C)	K3 (100 °C)	K4 (100 °C)
N27	61.6	–0.737	88.1	–0.847	80.9	–0.865
N87	61.6	–0.737	88.5	–0.796	78.4	–0.873

Validity range: K1, K2: 0.05 mm < s < 1.50 mm
K3, K4: 50 nH < A_L < 430 nH

b) DC magnetic bias I_{DC}

By using the core-shape-related factors K3 and K4, nominal values can be determined for the DC magnetic biasing characteristic of E, ETD and EFD cores made of N27 and N87 and ELP cores made of N87 at temperature 25 °C and 100 °C.

The direct current I_{DC} at which the A_L value drops by 10% compared to the A_L value without magnetic biasing (I_{DC} = 0 A) is determined for a coil with 100 turns.

Calculation of I_{DC} at T = 25 °C:
The factors K3 and K4 for T = 25 °C and the A_L value without magnetic biasing are inserted into the equation for the calculation.

For $A_L = 171$ (gaped) and $N = 100$: $I_{DC} \approx 0.5$ A

Calculation of I_{DC} at T = 100 °C:

The factors K3 and K4 for T = 100 °C are inserted into the equation for the calculation. The value for T = 25 °C without magnetic biasing should be used here as the A_L value.

$$I_{DC} = \left(\frac{0.9 \cdot A_L}{K3}\right)^{\frac{1}{K4}}$$

I_{DC} = [A]
A_L = [nH] (without magnetic biasing)

18.59 mm²

18.29 mm²

34.81 mm²

$g = 0.25$

$\boxed{R_{total} \approx 6.35 \times 10^6}$

$L = \frac{N^2}{R_{total}}$

$I = 0.5\ \mathrm{A}$ – beggining of the saturation

$$\Phi_{red} = \frac{I \times N \times 10^{-6}}{6.35} = \frac{0.5 \times 100 \times 10^{-6}}{6.35} \approx 7.87 \times 10^{-6}\,\mathrm{Wb}$$

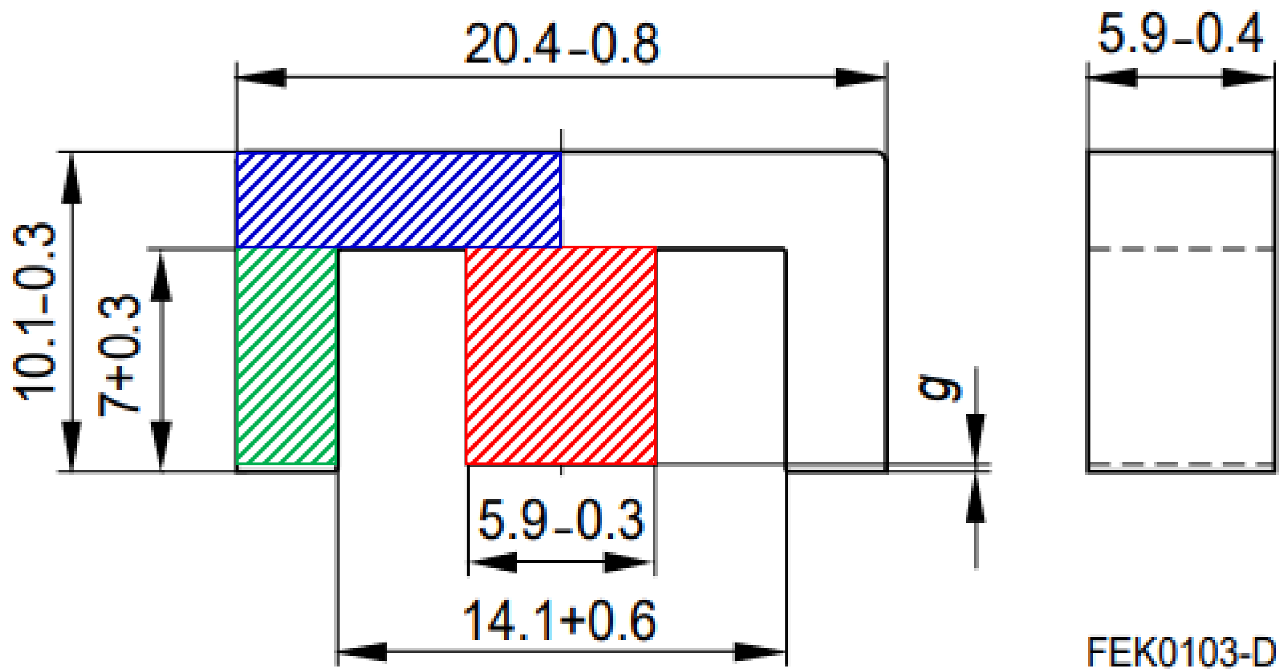

$$B_{red} = \frac{\Phi_{red}}{S_{red}} \approx 0.23\ \mathrm{T}$$

$$B_{blue} = \frac{(\Phi_{red}/2)}{S_{blue}} \approx 0.22\ \mathrm{T}$$

$$B_{green} = \frac{(\Phi_{red}/2)}{S_{green}} \approx 0.21\ \mathrm{T}$$

All parts are approximately at the same magnetic condition

Simulating Non-linear Transformers in LTspice

https://www.allaboutcircuits.com/technical-articles/simulating-non-linear-transformers-in-ltspice/

Chan's model: https://ieeexplore.ieee.org/document/75630

The two hysteresis loop branches can be modeled with two equations. One for the upper branch and for the lower one:

$$B_+(H) = B_s \frac{H + H_c}{|H + H_c| + H_c(\frac{B_s}{B_r} - 1)}, B_-(H) = B_s \frac{H - H_c}{|H - H_c| + H_c(\frac{B_s}{B_r} - 1)}$$

The Chan model shows that it is possible to model hysteresis using three magnetic parameters.

- Coercive force (amps-turns/m), Hc.
- Remnant flux density (T), Br.
- Saturation flux density (T), Bs.

Besides, we need to consider the physical aspects of the transformer:

- Magnetic Length (Lm), in meters
- Length of the gap (Lg), in meters
- Cross-sectional area (A), in square meters
- Number of turns (N)

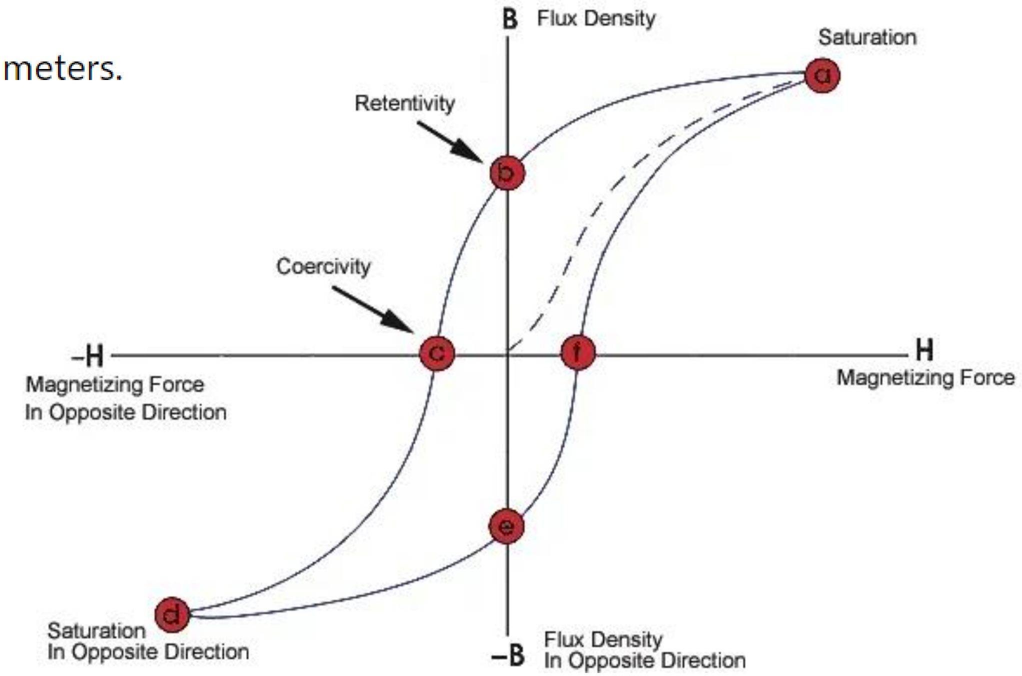

Chan's model: https://ieeexplore.ieee.org/document/75630

In the case of a transformer where the windings surround a magnetic material, the core, the relation between the flux and current is no longer linear. Two additional magnetic quantities, the magnetic field, H, induced in the core, and the magnetic induction or flux density, B, must be computed. The magnetic field in the core is obtained by summing up the contributions H_i of each winding:

$$H = \sum_{i=1}^{n} \frac{\kappa_i N_i I_i}{l_{\text{mag}}} \tag{3}$$

where N_i is the number of turns in winding i, $0 \leq \kappa_i \leq 1$ is the coupling of the winding to the core, I_i is the current through winding i, and l_{mag} is the effective magnetic path length of the core. In the above equation H is expressed in (ampere-turns/meters), the International System unit. The flux density, B, can be equated to the magnetic field, H, by the permeability, $\mu = \mu_r \mu_0$, of the magnetic material

$$B = \mu_r \mu_0 H = \frac{\phi}{A}. \tag{4}$$

Furthermore, B is not only a nonlinear function of H, but depends on the history of the magnetic fields applied to the core:

$$B = B(H, \text{history}). \tag{5}$$

Python program for Chan's model for simulating a BH-loop

```
#
# Simulating a BH-loop using Chan's model: https://ieeexplore.ieee.org/document/75630
# Dr. Dmitriy Makhnovskiy, City College Plymouth, England
# 23.02.2024
#

import tkinter as tk
from tkinter import messagebox
import matplotlib.pyplot as plt
import csv
import logging

….. (algorithm)…….
```

(see Appendix and GitHub)

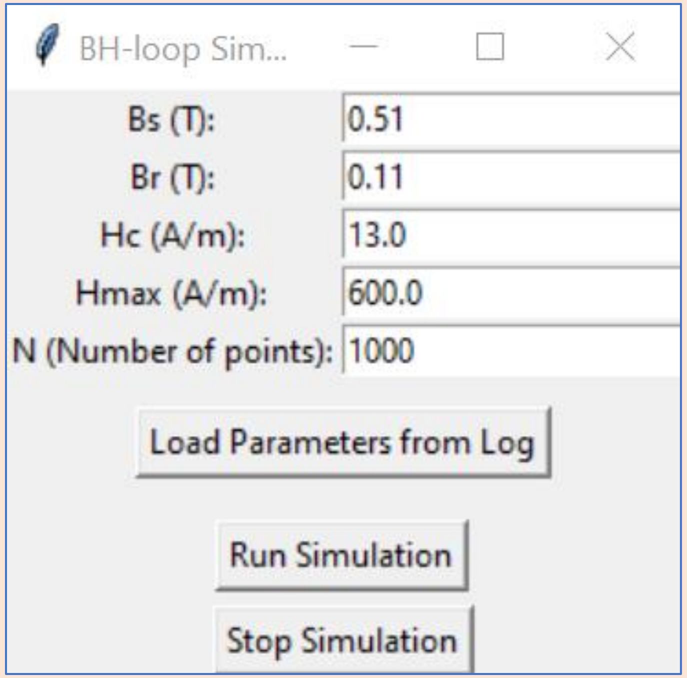

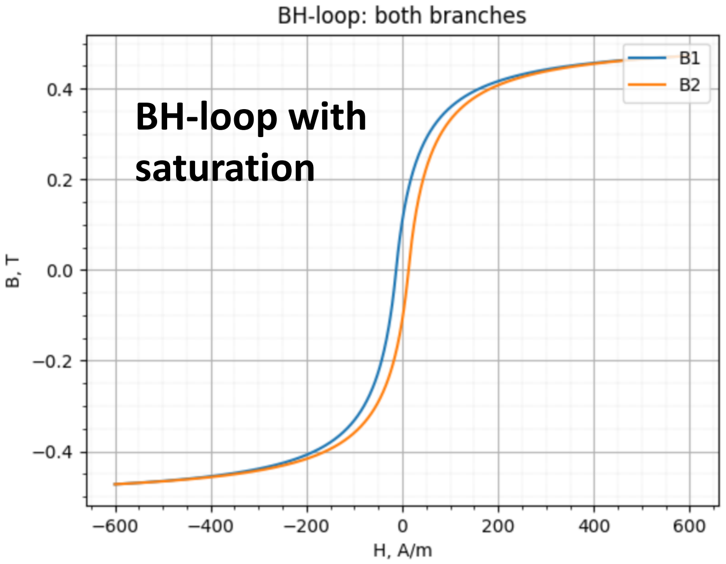

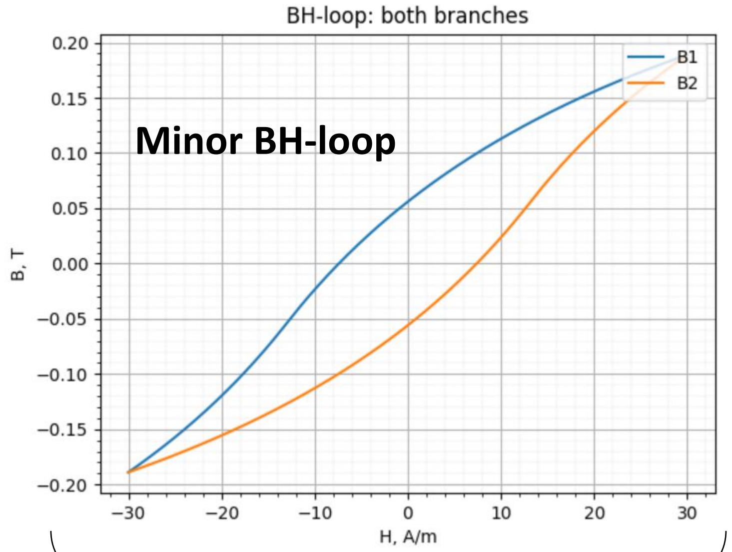

Smaller field range

Project on GitHub: https://github.com/DmitriyMakhnovskiy/Chan_BH-loop_model

In Chan's paper, they don't explain how to solve differential equations with nonlinear inductors. Their main goal was to propose a fairly simple model of hysteresis, including minor BH-loops. This model is then used by the LTspice simulator in its internal procedures for numerically solving differential equations.

https://www.allaboutcircuits.com/technical-articles/simulating-non-linear-transformers-in-ltspice/

L_{l1} – *primary leakage inductance*
L_{l2} – *secondary leakage inductance*

$$\begin{bmatrix} v_1(t) \\ v_2(t) \end{bmatrix} = \begin{bmatrix} L_{11} & L_{12} \\ L_{12} & L_{22} \end{bmatrix} \frac{d}{dt} \begin{bmatrix} i_1(t) \\ i_2(t) \end{bmatrix}$$

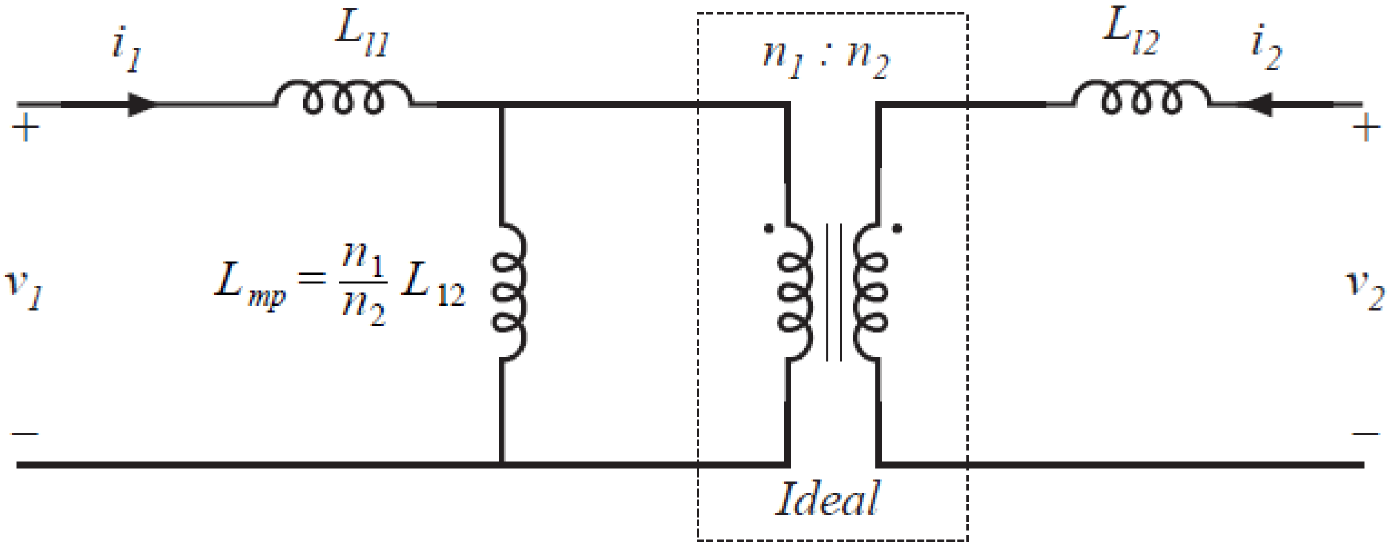

mutual inductance

$$L_{12} = \frac{n_1 n_2}{R} = \frac{n_2}{n_1} L_{mp}$$

Leakage inductances should not depend on the core magnetic properties

primary and secondary self-inductances

$$L_{11} = L_{l1} + \frac{n_1}{n_2} L_{12}$$

$$L_{22} = L_{l2} + \frac{n_2}{n_1} L_{12}$$

effective turns ratio $\quad n_e = \sqrt{\frac{L_{22}}{L_{11}}}$

coupling coefficient $\quad k = \frac{L_{12}}{\sqrt{L_{11} L_{22}}}$

LTspice does not allow to simulate arbitrary coupled inductors, there are some workarounds to get non-linear transformers simulated. The easiest way is to model a perfect transformer using dependent sources and then, add in parallel the non-ideal inductor (Chan's model discussed above).

https://www.allaboutcircuits.com/technical-articles/simulating-non-linear-transformers-in-ltspice/

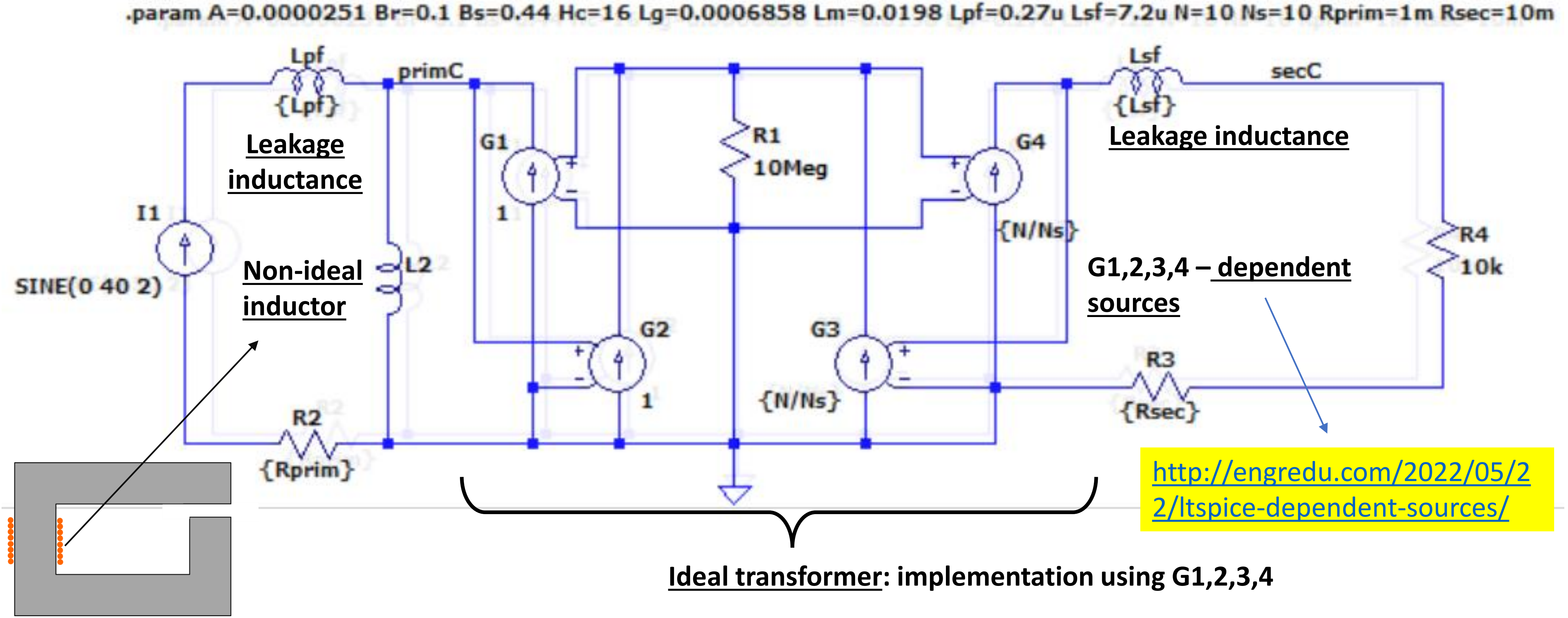

LTspice does not allow to simulate arbitrary coupled inductors, there are some workarounds to get non-linear transformers simulated. The easiest way is to model a perfect transformer using dependent sources and then, add in parallel the non-ideal inductor.

https://www.allaboutcircuits.com/technical-articles/simulating-non-linear-transformers-in-ltspice/

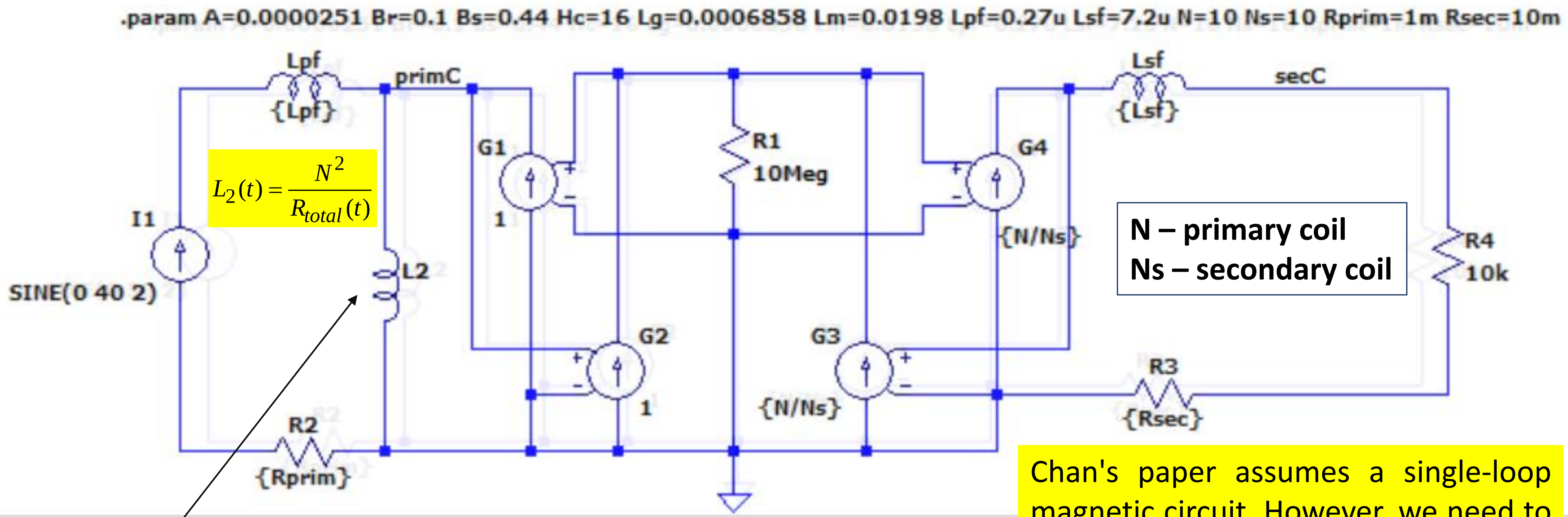

$$L_2(t) = \frac{N^2}{R_{total}(t)}$$

N – primary coil
Ns – secondary coil

Chan's paper assumes a single-loop magnetic circuit. However, we need to understand how to provide these parameters if the circuit has branches.

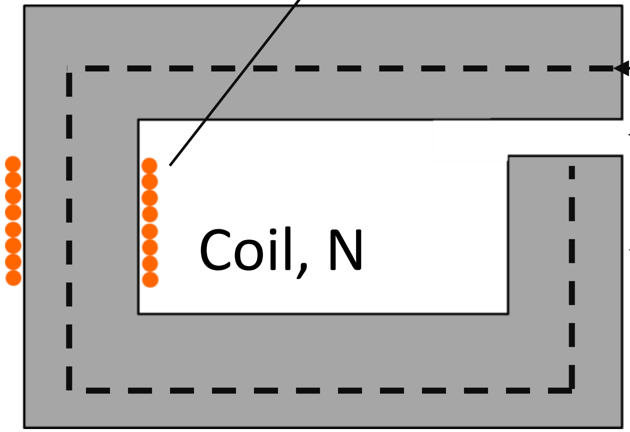

- Magnetic Length (Lm), in meters
- Length of the gap (Lg), in meters
- Cross-sectional area (A), in square meters
- Number of turns (N)

$$V(t) = -\frac{d\Phi(t)}{dt} = -\frac{d(L(t)\times I(t))}{dt} = -L(t)\times\frac{dI(t)}{dt} - I(t)\times\frac{dL(t)}{dt} -$$ self-inductance voltage

$$\mu(t) = \mu(H(t)) = \frac{1}{\mu_0}\times\left.\frac{dB(H)}{dH}\right|_{H(t)} -$$ incremental permeability from BH-loop

$$H(t) = C\times I(t) -$$ coil magnetising force; C is a constant

$$R_{total}(t) = \frac{(l/S)_{eff}}{\mu_0\mu(t)} + R_{gap} -$$ total reluctance

$(l/S)_{eff}$ – geometrical factor of the magnetic circuit

$$L(t) = \frac{N^2}{R_{total}(t)} -$$ non-linear coil inductance

We assume that all sections of the magnetic circuit at each moment of time have the same magnetic induction.

See the previous slide:

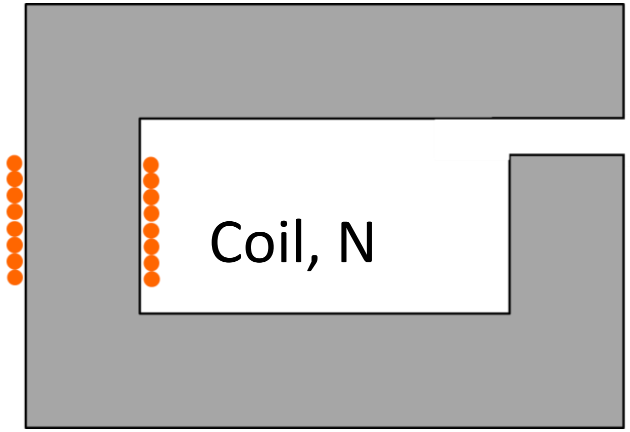

In the model for LTspice:

$$H(t) \approx \frac{I(t)\times N}{L_m}$$

$$R_{total}(t) = \frac{(L_m/A)}{\mu_0\mu(t)} + \frac{(L_g/A)}{\mu_0}$$

$$L_2(t) = \frac{N^2}{R_{total}(t)} -$$ in circuit

N – primary coil turns

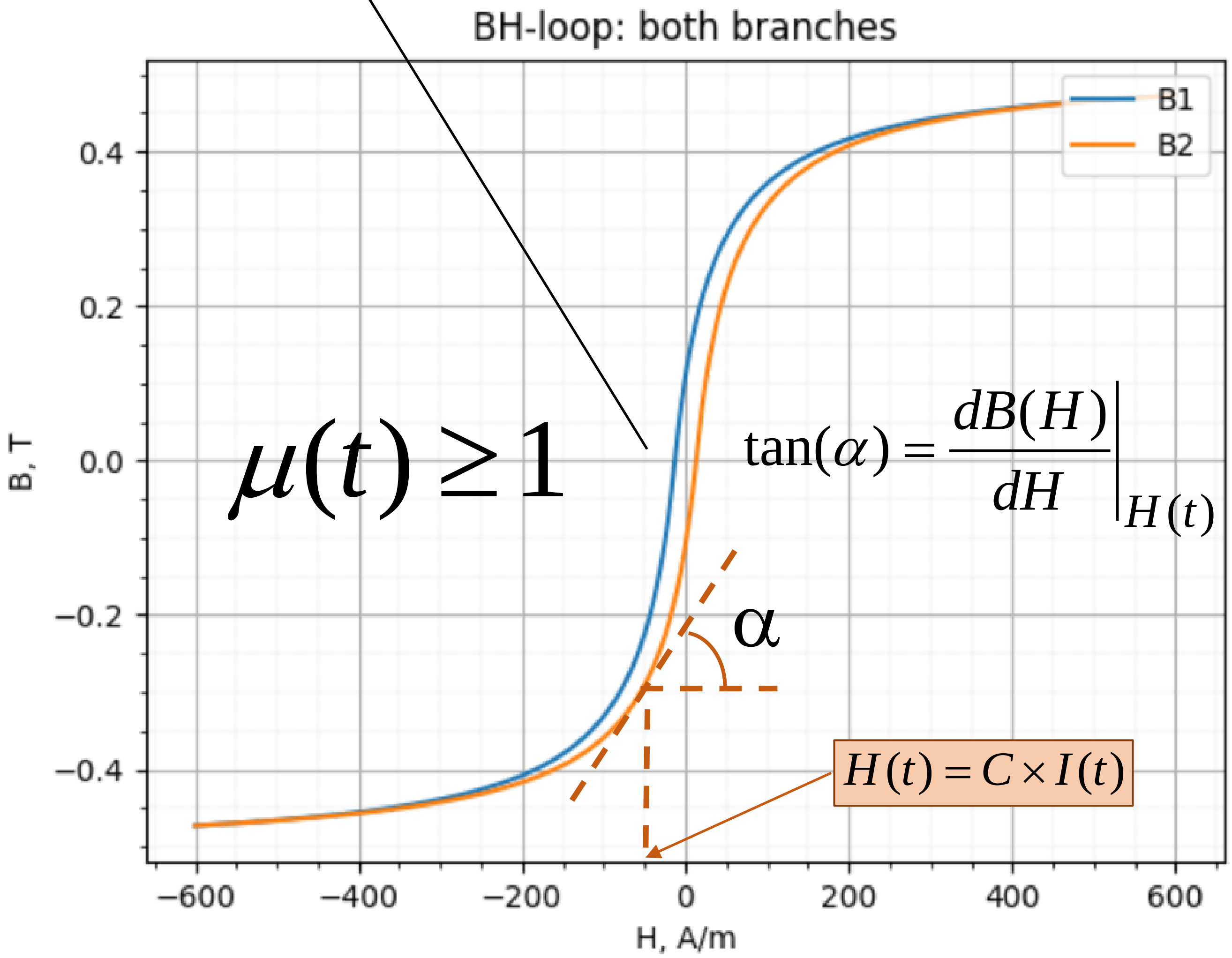

Chan's model used in LTspice assumes a single loop magnetic circuit. In our case, we have a branched circuit. However, note that the sum of the cross sections of the blue and red segments is very close to the cross section of the red segment (as it should be). Therefore, this branched circuit can be replaced by a single loop circuit with the cross-section of 34.81 mm^2 and the length equal to twice the length of all segments, minus the gap. **Thus, we get for LTspice:** $L_m = 4.82\times10^{-2}$ m, $L_g = 2.5\times10^{-4}$ m, $A = 3.48\times10^{-5}$ m^2. Other magnetic parameters were not provided for our E-shape core. So, we will use some typical values: $B_s = 0.5$ T, $B_r = 0.1$ T, and $H_c = 10$ A/m.

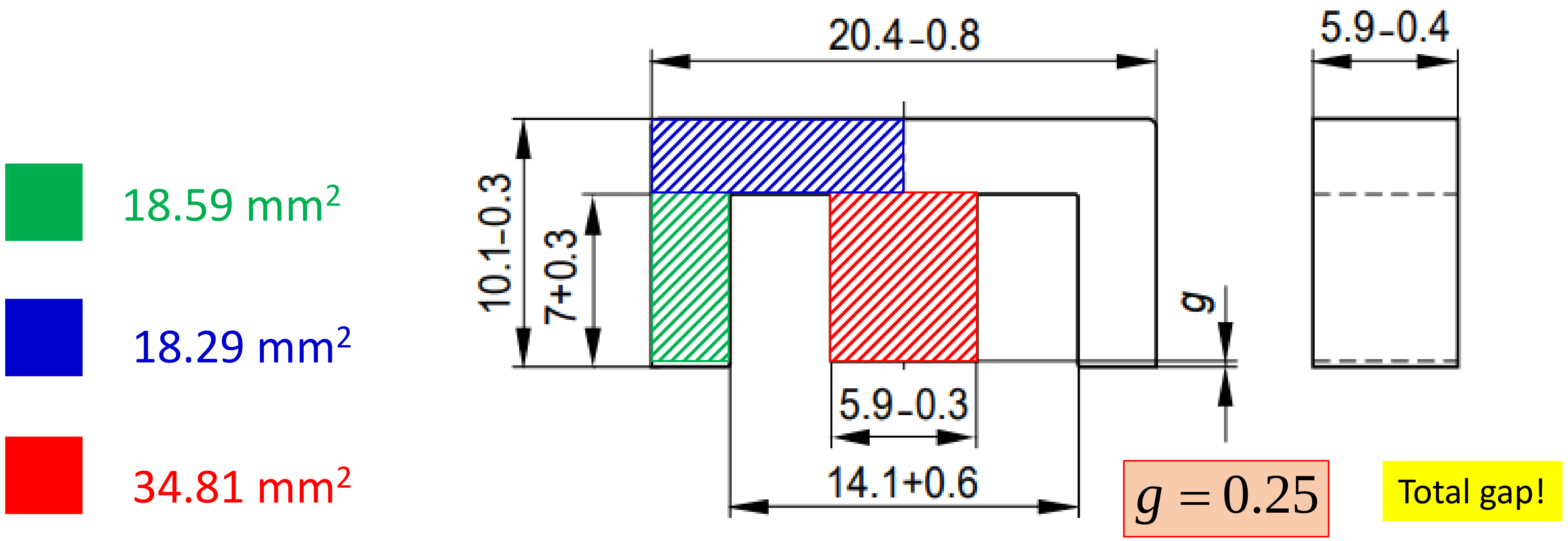

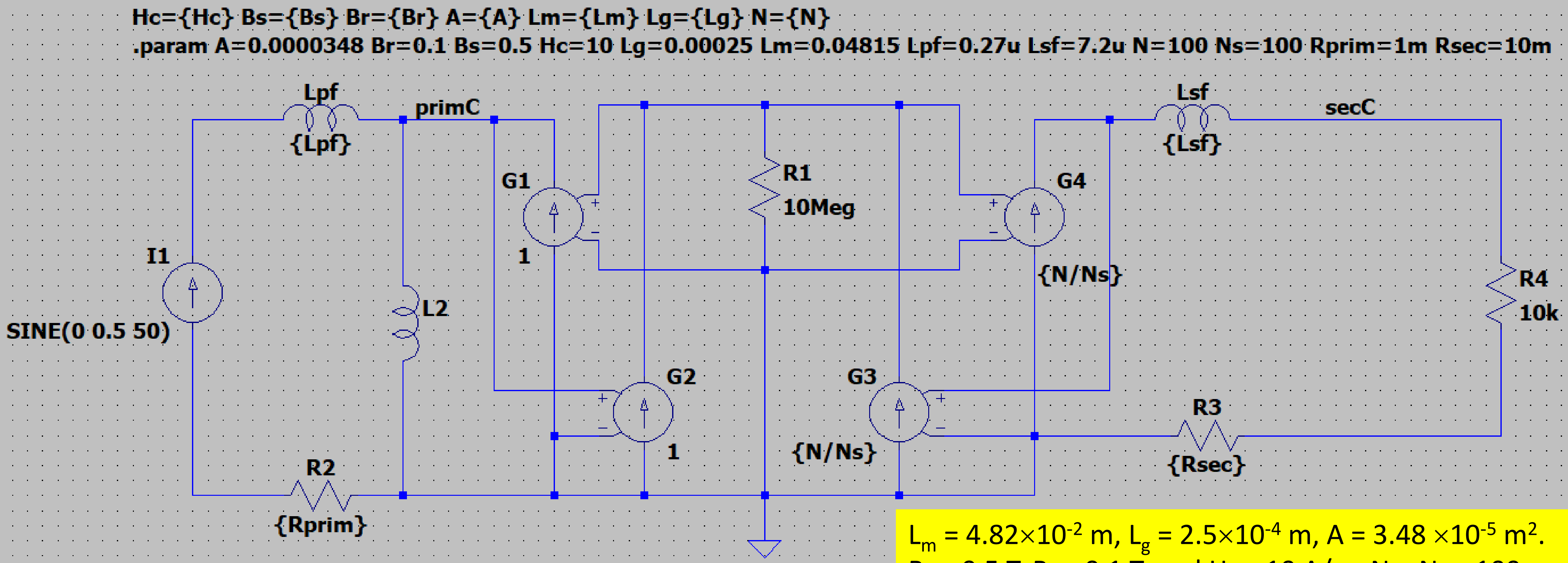

$L_m = 4.82\times10^{-2}$ m, $L_g = 2.5\times10^{-4}$ m, $A = 3.48\times10^{-5}$ m^2. $B_s = 0.5$ T, $B_r = 0.1$ T, and $H_c = 10$ A/m, $N = N_s = 100$

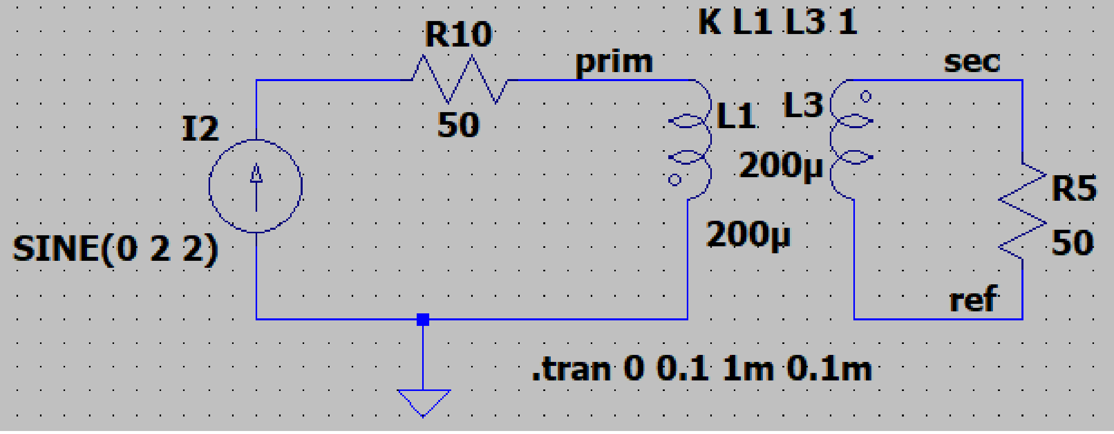

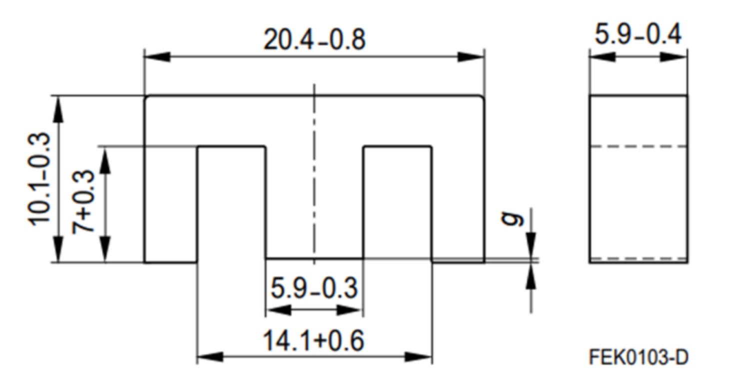

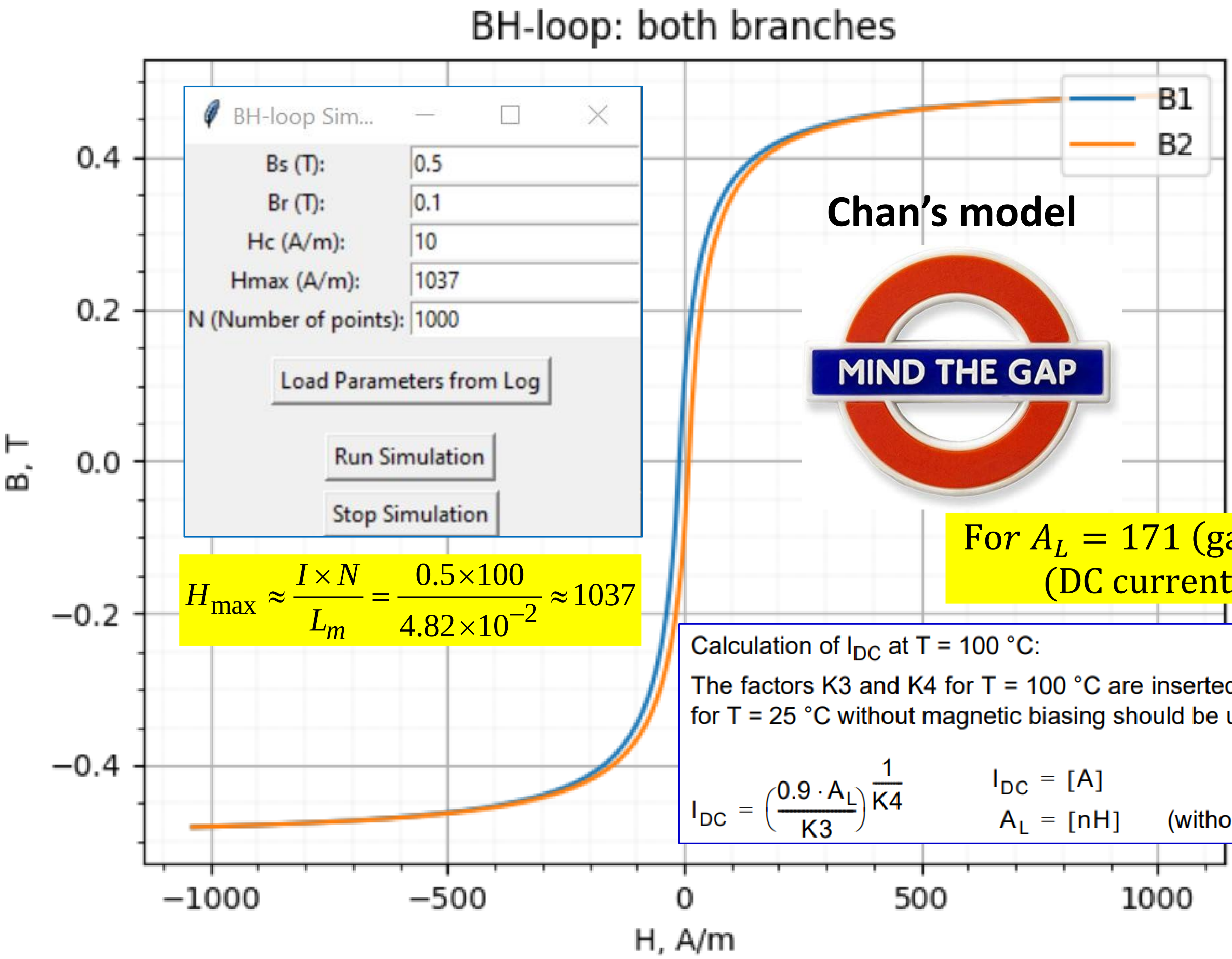

Chan's model

MIND THE GAP

$$H_{\max} \approx \frac{I \times N}{L_m} = \frac{0.5 \times 100}{4.82 \times 10^{-2}} \approx 1037$$

The hysteresis BH-loop, calculated without a gap **(see in the Figure)**, is already highly saturated even with an AC excitation current of 0.5 A. **However, introducing a gap will significantly reduce the magnetic flux density inside the core, resulting in an unsaturated loop.** This aligns well with the calculations we have performed for this core.

For $A_L = 171$ (gaped) and $N = 100$: $I_{DC} \approx 0.5$ A
(DC current just before the saturation)

Calculation of I_{DC} at T = 100 °C:

The factors K3 and K4 for T = 100 °C are inserted into the equation for the calculation. The value for T = 25 °C without magnetic biasing should be used here as the A_L value.

$$I_{DC} = \left(\frac{0.9 \cdot A_L}{K3}\right)^{\frac{1}{K4}}$$

I_{DC} = [A]
A_L = [nH] (without magnetic biasing)

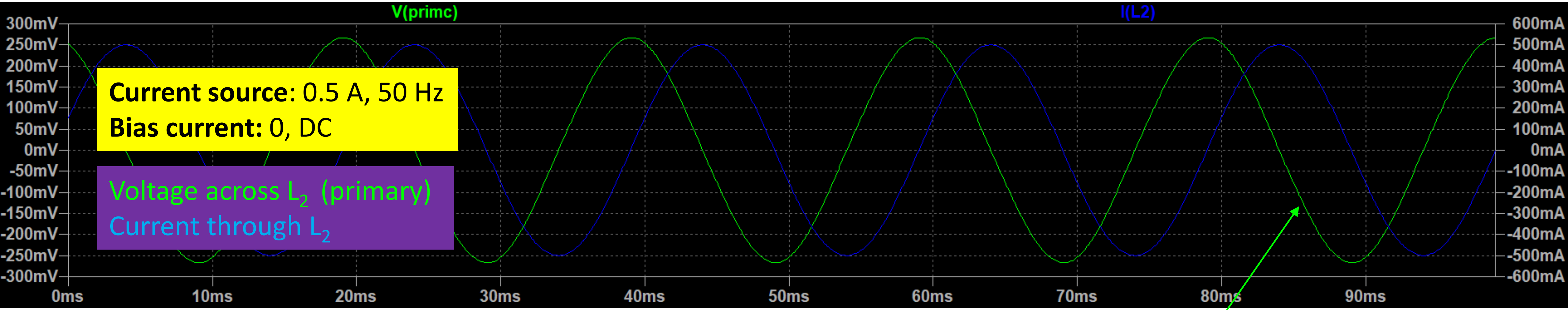

$L_m = 4.82\times10^{-2}$ m, $L_g = 2.5\times10^{-4}$ m, $A = 3.48\times10^{-5}$ m^2.
$B_s = 0.5$ T, $B_r = 0.1$ T, and $H_c = 10$ A/m, $N = N_s = 100$

There is still no visible distortion of the primary voltage

Very strong non-linear distortions of the primary voltage

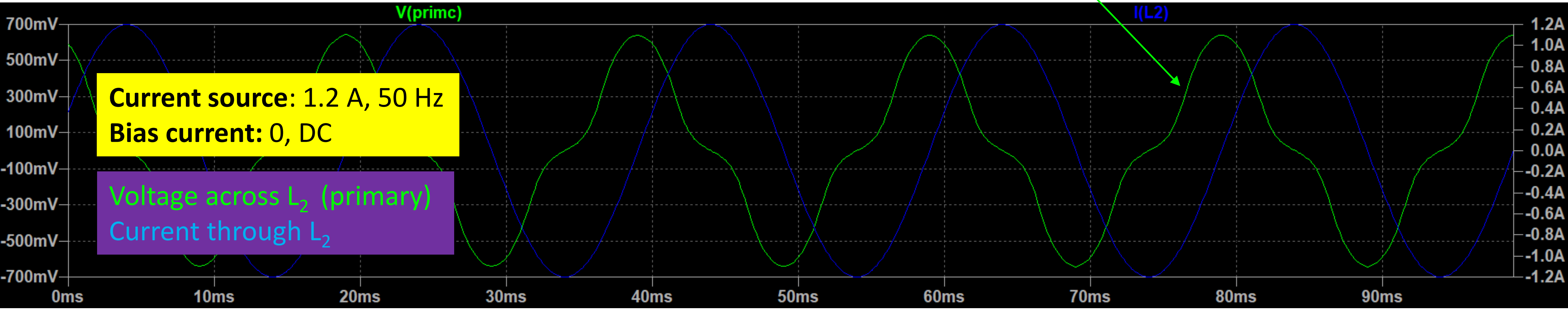

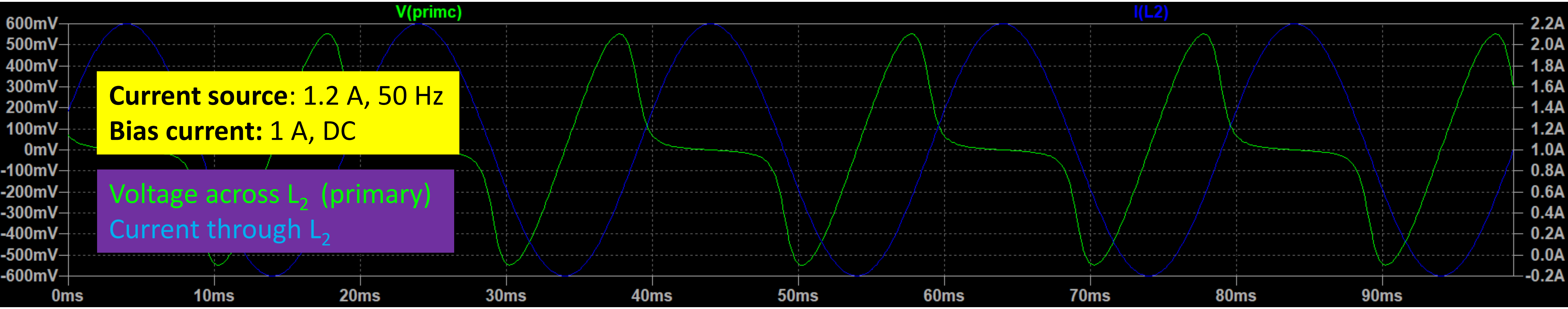

$L_m = 4.82\times10^{-2}$ m, $L_g = 2.5\times10^{-4}$ m, $A = 3.48\times10^{-5}$ m^2.
$B_s = 0.5$ T, $B_r = 0.1$ T, and $H_c = 10$ A/m, $N = N_s = 100$

The core is fully saturated by the bias current 5 A. Magnetic permeability is close to 1. Low non-linear distortions.

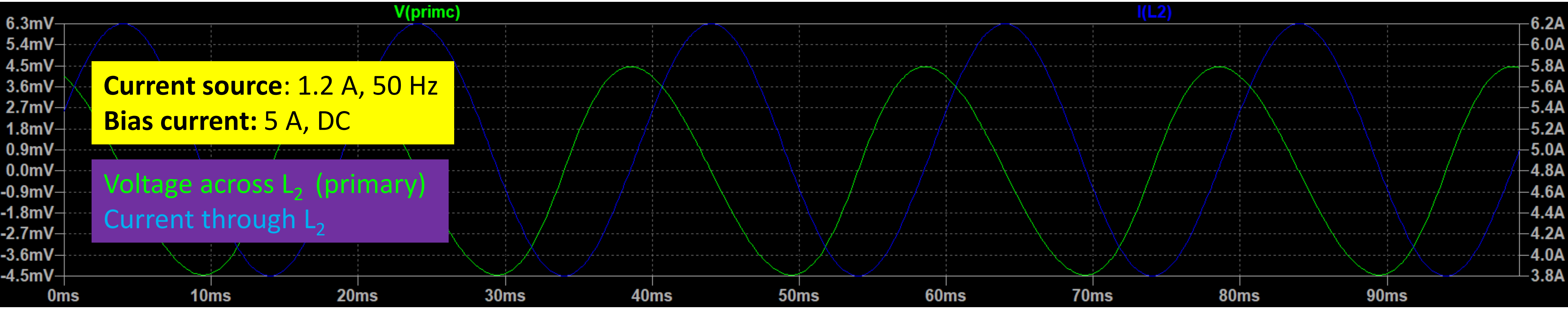

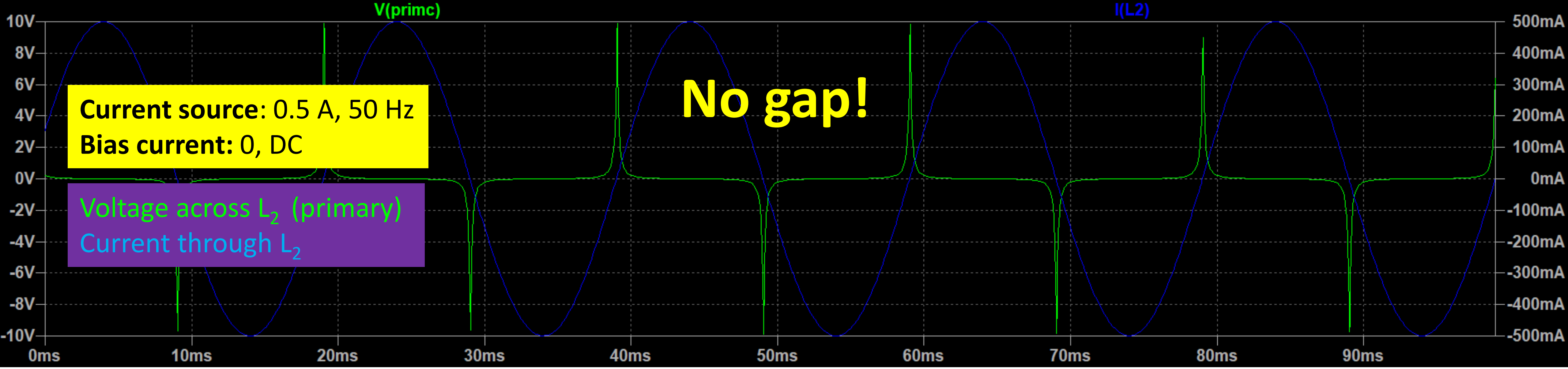

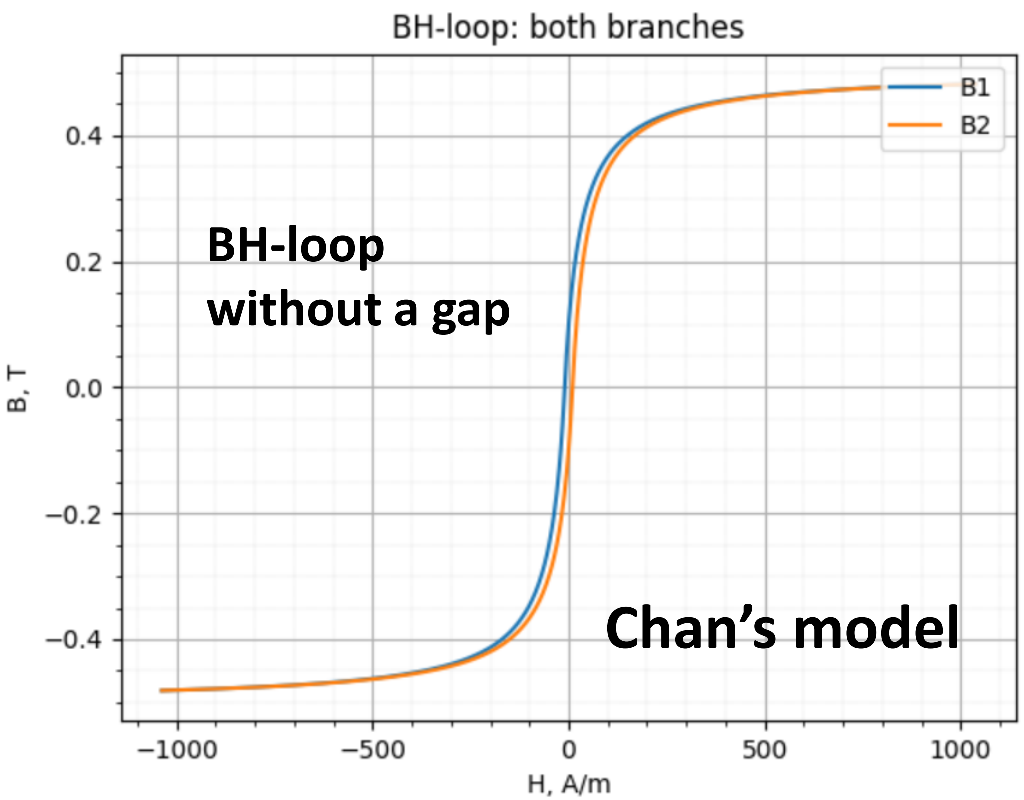

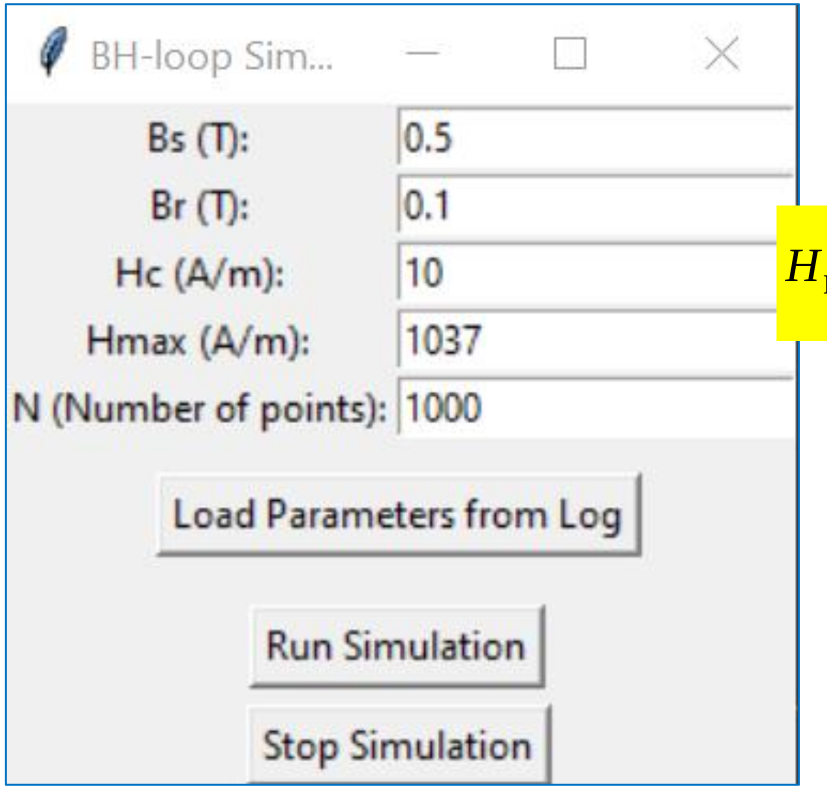

$$H_{\max} \approx \frac{I \times N}{L_m} = \frac{0.5 \times 100}{4.82 \times 10^{-2}} \approx 1037$$

Ferrites and accessories

E 20/10/6 (EF 20)
Core and accessories

Series/Type: **B66311, B66206**
Date: June 2013

E 20/10/6 (EF 20)

Core **B66311**

- To IEC 61246
- Delivery mode: single units

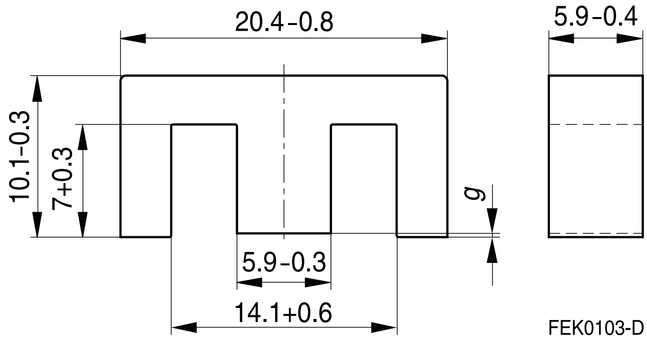

Magnetic characteristics (per set)

$\Sigma l/A$ = 1.44 mm^{-1}
l_e = 46.3 mm
A_e = 32.1 mm^2
A_{min} = 31.9 mm^2
V_e = 1490 mm^3

Approx. weight 7.3 g/set

Ungapped

Material	A_L value nH	μ_e	P_V W/set	Ordering code
N30	2150 +30/–20%	2460		B66311G0000X130
N27	1300 +30/–20%	1490	< 0.27 (200 mT, 25 kHz, 100 °C)	B66311G0000X127
N87	1470 +30/–20%	1680	< 0.75 (200 mT, 100 kHz, 100 °C)	B66311G0000X187

Gapped

Material	g mm	A_L value approx. nH	μ_e	Ordering code ** = 27 (N27) = 87 (N87)
N27, N87	0.09 ±0.01	363	415	B66311G0090X1**
	0.17 ±0.02	227	259	B66311G0170X1**
	0.25 ±0.02	171	195	B66311G0250X1**
	0.50 ±0.05	103	118	B66311G0500X1**

The A_L value in the table applies to a core set comprising one ungapped core (dimension g = 0) and one gapped core (dimension g > 0).

Calculation factors (for formulas, see *"E cores: general information"*)

Material	Relationship between air gap – A_L value		Calculation of saturation current			
	K1 (25 °C)	K2 (25 °C)	K3 (25 °C)	K4 (25 °C)	K3 (100 °C)	K4 (100 °C)
N27	61.6	–0.737	88.1	–0.847	80.9	–0.865
N87	61.6	–0.737	88.5	–0.796	78.4	–0.873

Validity range: K1, K2: 0.05 mm < s < 1.50 mm
K3, K4: 50 nH < A_L < 430 nH

Coil former (magnetic axis horizontal or vertical)

Material: GFR polyterephthalate (UL 94 V-0, insulation class to IEC 60085: F ≙ max. operating temperature 155 °C), color code black
Valox 420-SE0® [E45329 (M)], GE PLASTICS B V
Solderability: to IEC 60068-2-20, test Ta, method 1 (aging 3): 235 °C, 2 s
Resistance to soldering heat: to IEC 60068-2-20, test Tb, method 1B: 350 °C, 3.5 s
Winding: see Data Book 2013, chapter “Processing notes, 2.1”

Squared pins. For matching yoke see next page.

Version	Sections	A_N mm²	l_N mm	A_R value μΩ	Pins	Ordering code
Horizontal	1	34	41.2	42	10	B66206B1110T001
Vertical	1	34	41.2	42	10	B66206W1110T001

Horizontal version

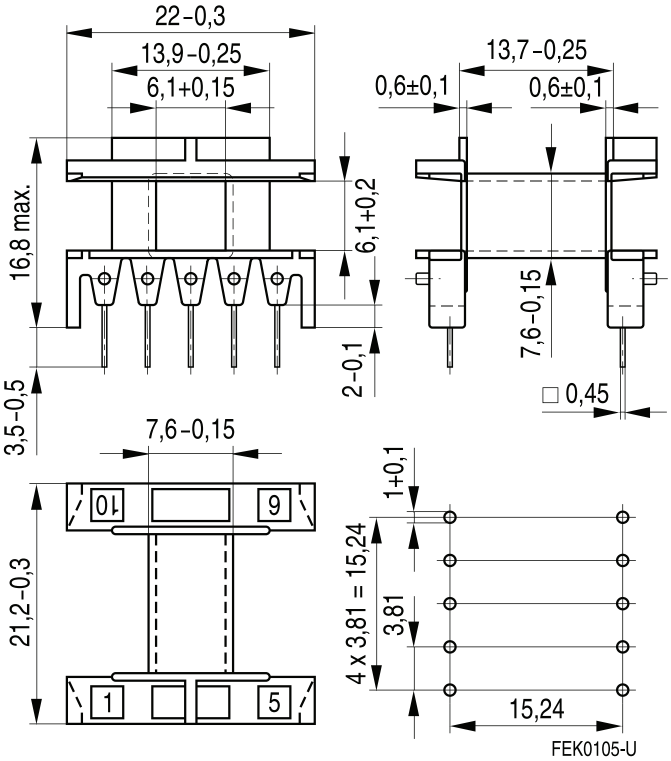

Hole arrangement
View in mounting direction

Vertical version

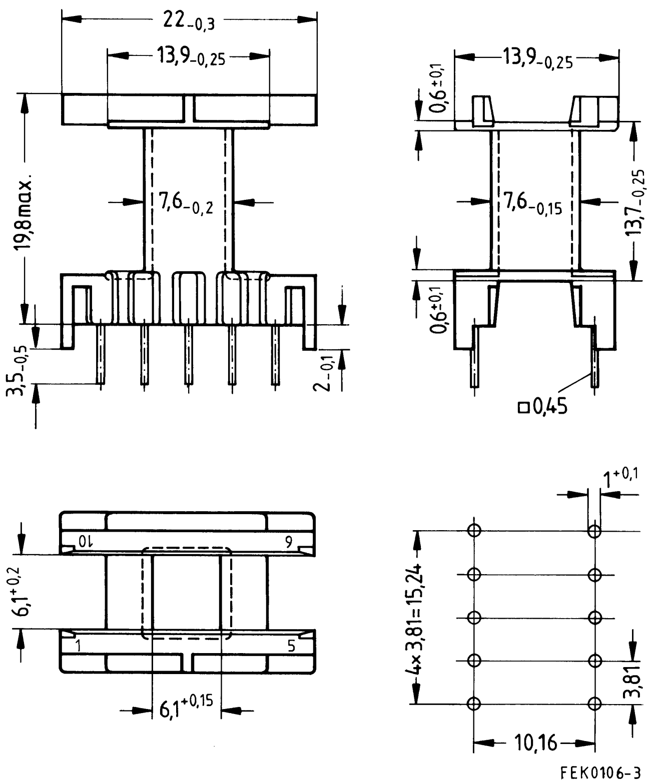

Hole arrangement
View in mounting direction

Coil former (with right-angle pins)

Material: GFR polyterephthalate (UL 94 V-0, insulation class to IEC 60085:
F ≙ max. operating temperature 155 °C), color code black
Pocan B4235® [E245249 (M)], LANXESS AG
Solderability: to IEC 60068-2-20, test Ta, method 1 (aging 3): 235 °C, 2 s
Resistance to soldering heat: to IEC 60068-2-20, test Tb, method 1B: 350 °C, 3.5 s
Winding: see Data Book 2013, chapter “Processing notes, 2.1”

Squared pins.

Yoke

Material: Stainless spring steel (0.2 mm)

Coil former						Ordering code
Figure	Sections	A_N mm^2	l_N mm	A_R value $\mu\Omega$	Pins	
1	1	34	41.2	42	12	B66206C1012T001
2	1	34	41.2	42	14	B66206C1014T001
3	Yoke (ordering code per piece, 2 are required)					B66206A2010X000

Figure 1, coil former (12 pins)

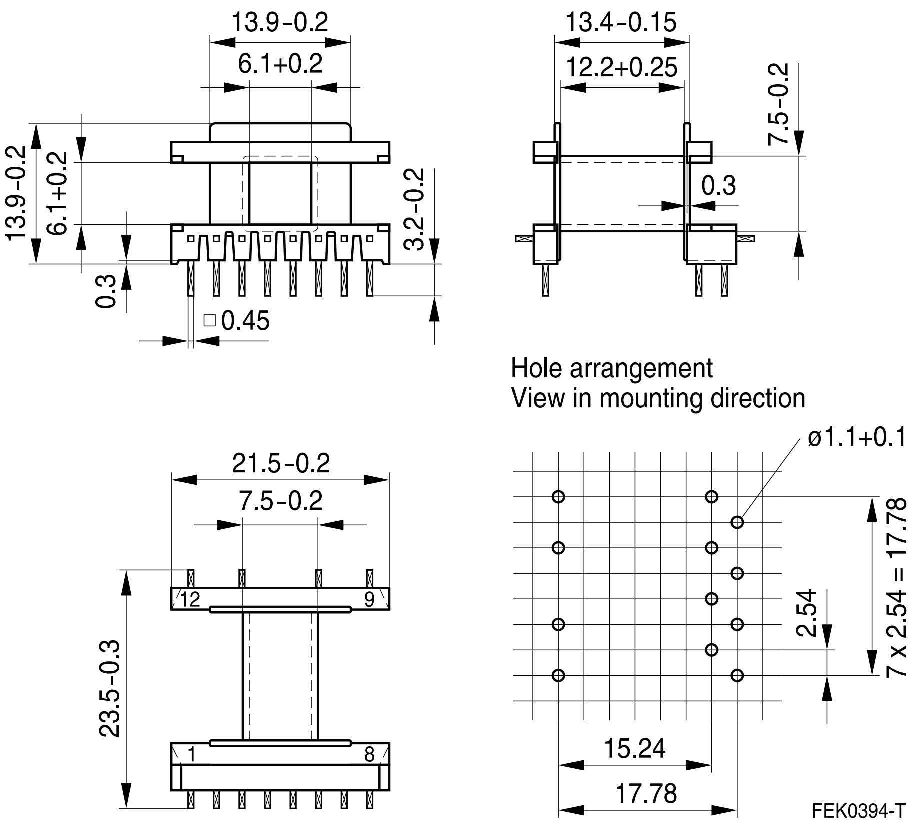

Figure 2, coil former (14 pins)

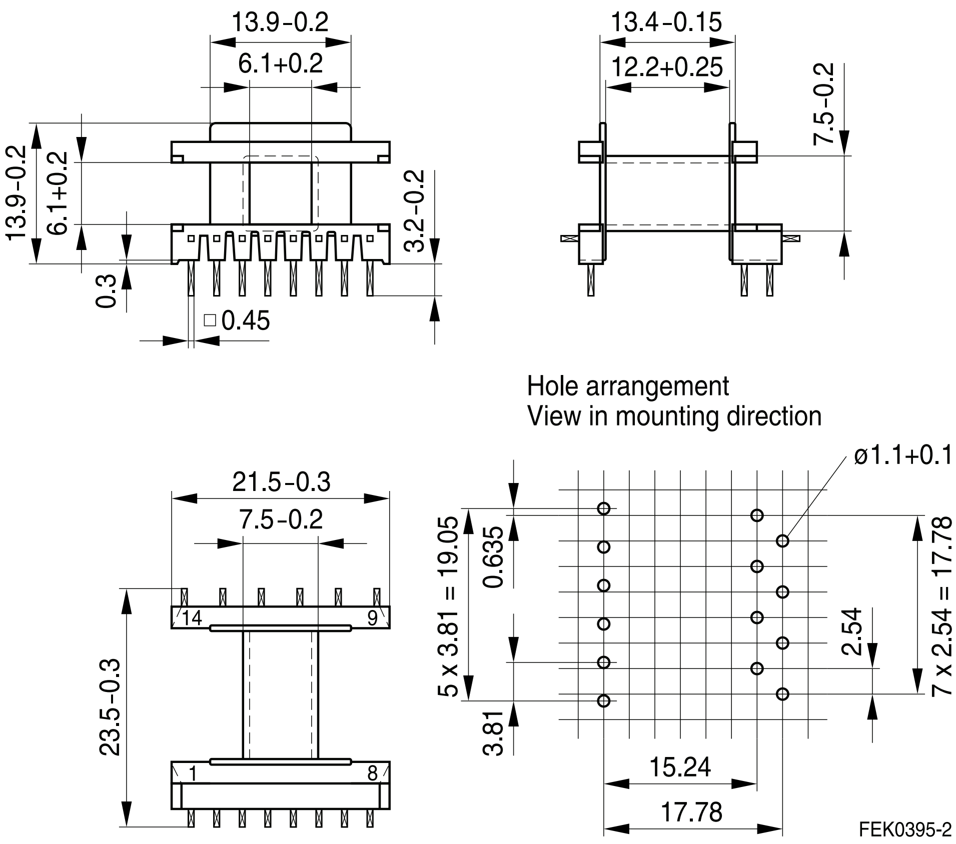

Figure 3, Yoke

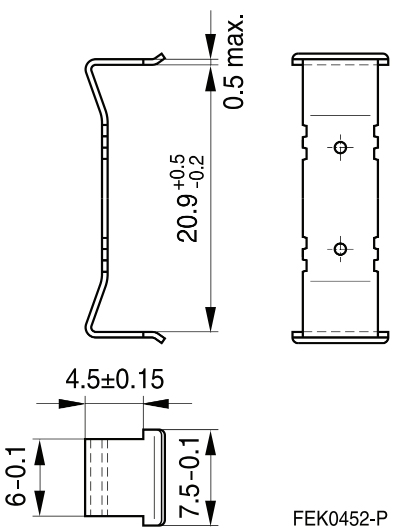

Coil former for luminaires

- Also to be used without clamps

Material: GFR polyterephthalate (UL 94 V-0, insulation class to IEC 60085:
H ≙ max. operating temperature 180 °C), color code black
Rynite FR 530® [E41938 (M)], E I DUPONT DE NEMOURS & CO INC

Solderability: to IEC 60068-2-20, test Ta, method 1 (aging 3): 235 °C, 2 s

Resistance to soldering heat: to IEC 60068-2-20, test Tb, method 1B: 350 °C, 3.5 s

Winding: see Data Book 2013, chapter “Processing notes, 2.1”

Squared pins.

Yoke

Material: Nickel silver (0.3 mm)

Sections	A_N mm^2	l_N mm	A_R value µΩ	Pins	Ordering code
1	32.7	42.3	44.5	6	B66206J1106T001
2	30.7	42.3	34.4	6	B66206K1106T002
Yoke					B66206A2001X000

Coil former

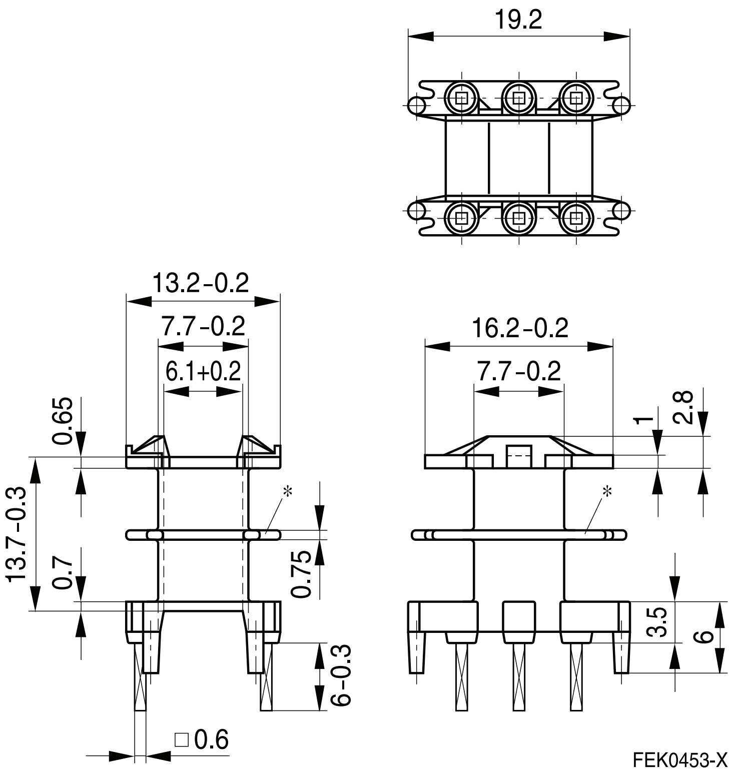

FEK0453-X

Yoke

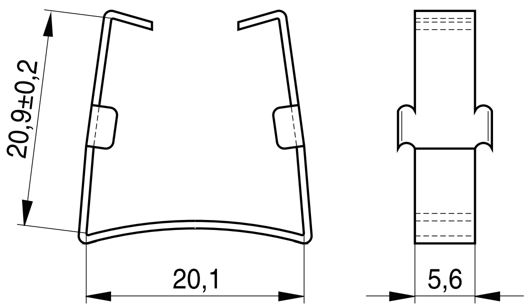

FEK0322-W

Hole arrangement
View in mounting direction

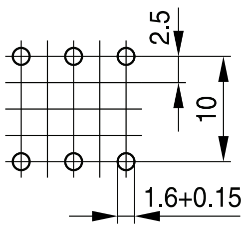

FEK0234-E

* Omitted for one-section version.

Mechanical stress and mounting

Ferrite cores have to meet mechanical requirements during assembling and for a growing number of applications. Since ferrites are ceramic materials one has to be aware of the special behavior under mechanical load.

As valid for any ceramic material, ferrite cores are brittle and sensitive to any shock, fast changing or tensile load. Especially high cooling rates under ultrasonic cleaning and high static or cyclic loads can cause cracks or failure of the ferrite cores.

For detailed information see chapter *"Definitions"*, section 8.1.

Effects of core combination on A_L value

Stresses in the core affect not only the mechanical but also the magnetic properties. It is apparent that the initial permeability is dependent on the stress state of the core. The higher the stresses are in the core, the lower is the value for the initial permeability. Thus the embedding medium should have the greatest possible elasticity.

For detailed information see chapter *"Definitions"*, section 8.2.

Heating up

Ferrites can run hot during operation at higher flux densities and higher frequencies.

NiZn-materials

The magnetic properties of NiZn-materials can change irreversible in high magnetic fields.

Processing notes

- The start of the winding process should be soft. Else the flanges may be destroid.
- To strong winding forces may blast the flanges or squeeze the tube that the cores can no more be mount.
- To long soldering time at high temperature (>300 °C) may effect coplanarity or pin arrangement.
- Not following the processing notes for soldering of the J-leg terminals may cause solderability problems at the transformer because of pollution with Sn oxyd of the tin bath or burned insulation of the wire. For detailed information see chapter *"Processing notes"*, section 8.2.
- The dimensions of the hole arrangement have fixed values and should be understood as a recommendation for drilling the printed circuit board. For dimensioning the pins, the group of holes can only be seen under certain conditions, as they fit into the given hole arrangement. To avoid problems when mounting the transformer, the manufacturing tolerances for positioning the customers' drilling process must be considered by increasing the hole diameter.

Symbols and terms

Symbol	Meaning	Unit
A	Cross section of coil	mm^2
A_e	Effective magnetic cross section	mm^2
A_L	Inductance factor; $A_L = L/N^2$	nH
A_{L1}	Minimum inductance at defined high saturation ($\triangleq \mu_a$)	nH
A_{min}	Minimum core cross section	mm^2
A_N	Winding cross section	mm^2
A_R	Resistance factor; $A_R = R_{Cu}/N^2$	$\mu\Omega = 10^{-6}\ \Omega$
B	RMS value of magnetic flux density	Vs/m^2, mT
ΔB	Flux density deviation	Vs/m^2, mT
$\hat{B}$	Peak value of magnetic flux density	Vs/m^2, mT
$\Delta\hat{B}$	Peak value of flux density deviation	Vs/m^2, mT
B_{DC}	DC magnetic flux density	Vs/m^2, mT
B_R	Remanent flux density	Vs/m^2, mT
B_S	Saturation magnetization	Vs/m^2, mT
C_0	Winding capacitance	F = As/V
CDF	Core distortion factor	$mm^{-4.5}$
DF	Relative disaccommodation coefficient $DF = d/\mu_i$	
d	Disaccommodation coefficient	
E_a	Activation energy	J
f	Frequency	s^{-1}, Hz
f_{cutoff}	Cut-off frequency	s^{-1}, Hz
f_{max}	Upper frequency limit	s^{-1}, Hz
f_{min}	Lower frequency limit	s^{-1}, Hz
f_r	Resonance frequency	s^{-1}, Hz
f_{Cu}	Copper filling factor	
g	Air gap	mm
H	RMS value of magnetic field strength	A/m
$\hat{H}$	Peak value of magnetic field strength	A/m
H_{DC}	DC field strength	A/m
H_c	Coercive field strength	A/m
h	Hysteresis coefficient of material	10^{-6} cm/A
h/μ_i^2	Relative hysteresis coefficient	10^{-6} cm/A
I	RMS value of current	A
I_{DC}	Direct current	A
$\hat{I}$	Peak value of current	A
J	Polarization	Vs/m^2
k	Boltzmann constant	J/K
k_3	Third harmonic distortion	
k_{3c}	Circuit third harmonic distortion	
L	Inductance	H = Vs/A

Symbols and terms

Symbol	Meaning	Unit
$\Delta L/L$	Relative inductance change	H
L_0	Inductance of coil without core	H
L_H	Main inductance	H
L_p	Parallel inductance	H
L_{rev}	Reversible inductance	H
L_s	Series inductance	H
l_e	Effective magnetic path length	mm
l_N	Average length of turn	mm
N	Number of turns	
P_{Cu}	Copper (winding) losses	W
P_{trans}	Transferrable power	W
P_V	Relative core losses	mW/g
PF	Performance factor	
Q	Quality factor ($Q = \omega L/R_s = 1/\tan \delta_L$)	
R	Resistance	Ω
R_{Cu}	Copper (winding) resistance (f = 0)	Ω
R_h	Hysteresis loss resistance of a core	Ω
ΔR_h	R_h change	Ω
R_i	Internal resistance	Ω
R_p	Parallel loss resistance of a core	Ω
R_s	Series loss resistance of a core	Ω
R_{th}	Thermal resistance	K/W
R_V	Effective loss resistance of a core	Ω
s	Total air gap	mm
T	Temperature	°C
ΔT	Temperature difference	K
T_C	Curie temperature	°C
t	Time	s
t_v	Pulse duty factor	
$\tan \delta$	Loss factor	
$\tan \delta_L$	Loss factor of coil	
$\tan \delta_r$	(Residual) loss factor at $H \rightarrow 0$	
$\tan \delta_e$	Relative loss factor	
$\tan \delta_h$	Hysteresis loss factor	
$\tan \delta/\mu_i$	Relative loss factor of material at $H \rightarrow 0$	
U	RMS value of voltage	V
Û	Peak value of voltage	V
V_e	Effective magnetic volume	mm^3
Z	Complex impedance	Ω
Z_n	Normalized impedance $\lvert Z\rvert_n = \lvert Z\rvert /N^2 \times \varepsilon\ (l_e/A_e)$	Ω/mm

Symbols and terms

Symbol	Meaning	Unit
α	Temperature coefficient (TK)	1/K
α_F	Relative temperature coefficient of material	1/K
α_e	Temperature coefficient of effective permeability	1/K
ε_r	Relative permittivity	
Φ	Magnetic flux	Vs
η	Efficiency of a transformer	
η_B	Hysteresis material constant	mT^{-1}
η_i	Hysteresis core constant	$A^{-1}H^{-1/2}$
λ_s	Magnetostriction at saturation magnetization	
μ	Relative complex permeability	
μ_0	Magnetic field constant	Vs/Am
μ_a	Relative amplitude permeability	
μ_{app}	Relative apparent permeability	
μ_e	Relative effective permeability	
μ_i	Relative initial permeability	
μ_p'	Relative real (inductive) component of $\overline{\mu}$ (for parallel components)	
μ_p''	Relative imaginary (loss) component of $\overline{\mu}$ (for parallel components)	
μ_r	Relative permeability	
μ_{rev}	Relative reversible permeability	
μ_s'	Relative real (inductive) component of $\overline{\mu}$ (for series components)	
μ_s''	Relative imaginary (loss) component of $\overline{\mu}$ (for series components)	
μ_{tot}	Relative total permeability derived from the static magnetization curve	
ρ	Resistivity	Ωm^{-1}
$\Sigma l/A$	Magnetic form factor	mm^{-1}
τ_{Cu}	DC time constant $\tau_{Cu} = L/R_{Cu} = A_L/A_R$	s
ω	Angular frequency; $\omega = 2\,\Pi f$	s^{-1}

All dimensions are given in mm.

SMD Surface-mount device

Important notes

The following applies to all products named in this publication:

1. Some parts of this publication contain **statements about the suitability of our products for certain areas of application**. These statements are based on our knowledge of typical requirements that are often placed on our products in the areas of application concerned. We nevertheless expressly point out **that such statements cannot be regarded as binding statements about the suitability of our products for a particular customer application**. As a rule, EPCOS is either unfamiliar with individual customer applications or less familiar with them than the customers themselves. For these reasons, it is always ultimately incumbent on the customer to check and decide whether an EPCOS product with the properties described in the product specification is suitable for use in a particular customer application.
2. We also point out that **in individual cases, a malfunction of electronic components or failure before the end of their usual service life cannot be completely ruled out in the current state of the art, even if they are operated as specified**. In customer applications requiring a very high level of operational safety and especially in customer applications in which the malfunction or failure of an electronic component could endanger human life or health (e.g. in accident prevention or lifesaving systems), it must therefore be ensured by means of suitable design of the customer application or other action taken by the customer (e.g. installation of protective circuitry or redundancy) that no injury or damage is sustained by third parties in the event of malfunction or failure of an electronic component.
3. **The warnings, cautions and product-specific notes must be observed.**
4. In order to satisfy certain technical requirements, **some of the products described in this publication may contain substances subject to restrictions in certain jurisdictions (e.g. because they are classed as hazardous)**. Useful information on this will be found in our Material Data Sheets on the Internet (www.epcos.com/material). Should you have any more detailed questions, please contact our sales offices.
5. We constantly strive to improve our products. Consequently, **the products described in this publication may change from time to time**. The same is true of the corresponding product specifications. Please check therefore to what extent product descriptions and specifications contained in this publication are still applicable before or when you place an order. We also **reserve the right to discontinue production and delivery of products**. Consequently, we cannot guarantee that all products named in this publication will always be available. The aforementioned does not apply in the case of individual agreements deviating from the foregoing for customer-specific products.
6. Unless otherwise agreed in individual contracts, **all orders are subject to the current version of the "General Terms of Delivery for Products and Services in the Electrical Industry" published by the German Electrical and Electronics Industry Association (ZVEI)**.
7. The trade names EPCOS, BAOKE, Alu-X, CeraDiode, CeraLink, CSMP, CSSP, CTVS, DeltaCap, DigiSiMic, DSSP, FilterCap, FormFit, MiniBlue, MiniCell, MKD, MKK, MLSC, MotorCap, PCC, PhaseCap, PhaseCube, PhaseMod, PhiCap, SIFERRIT, SIFI, SIKOREL, SilverCap, SIMDAD, SiMic, SIMID, SineFormer, SIOV, SIP5D, SIP5K, ThermoFuse, WindCap are **trademarks registered or pending** in Europe and in other countries. Further information will be found on the Internet at www.epcos.com/trademarks.

Nonlinear Transformer Model for Circuit Simulation

John H. Chan, *Member, IEEE*, Andrei Vladimirescu, *Member, IEEE*, Xiao-Chun Gao, *Member, IEEE*, Peter Liebmann, and John Valainis, *Member, IEEE*

***Abstract*—A transformer model which consists of a nonlinear core with hysteresis and multiple windings is described as implemented in DSPICE, Daisy's proprietary version of the popular circuit simulator SPICE. The analytical formulation of the major and minor loops, and, the transition algorithm between hysteresis loops is described. The modeling of losses, and frequency and temperature dependence is also presented.**

I. Introduction

TRANSFORMERS differ from the ideal inductors supported by SPICE2 [1] due to the power loss incurred each cycle. An important loss factor is the hysteretic behavior of the flux density and magnetic field in the magnetic core. This paper presents an original approach of modeling a magnetic core in a circuit simulator and its implementation in DSPICE [2].

The addition of a nonlinear magnetic core model has been reported for several commercial versions of the SPICE simulator. The first reported magnetic model implementation [3] emphasizes the correctness of the hysteresis shape and partitions the loop in several regions. A disadvantage of the multiregion analytic description is the introduction of discontinuities at the transition points which have a negative impact on convergence. While SpicePlus [4] uses a multiregion formulation similar to Nitzan's, the magnetic model of PSpice [5] is based on the mathematical formulation reported by Jiles and Atherton [6]. The complexity of the latter makes it difficult to specify the core parameters for a desired hysteresis shape. IG-Spice [7] has also been reported to offer a magnetic model.

In contrast to previous implementations the nonlinear behavior of the new model is described by continuous piecewise-hyperbolic functions characterized by three parameters. These parameters are the same as the parameters published in catalogs of magnetic materials. A loop-traversing algorithm has been implemented which avoids discontinuities and eliminates both nonconvergence problems and the occurrence of erroneous voltage spikes during time-domain simulation. Both the functional representation of the loops and the traversing algorithm minimize the danger of nonconvergence which is apparent in previous models. The details of the hysteresis modeling are included in Section III.

The different effects included in the transformer model are presented in Section IV. In the large signal time-domain analysis the frequency dependent Eddy current losses in the core and wire losses are modeled. Additional effects such as wire skin effect and temperature dependence are also included. In the small signal ac analysis the transformer is modeled as frequency dependent lossy mutual inductors. For both analyses, air gap and the related fringe field effect are modeled by extending the magnetic path length of the core appropriately. In the transformer model library [8] parasitic capacitances and leakage inductances are added to the core and windings of the transformer.

The last section presents the simulation of a power circuit using the new transformer model. This example shows the accuracy of the new model as well as its usefulness in power circuit design.

Manuscript received May 9, 1988; revised February 2, 1990. This paper was recommended by Associate Editor R. K. Brayton.

J. H. Chan is with the University of Hong Kong, Hong Kong.

A. Vladimirescu is with Valid Logic Systems, San Jose, CA 95134.

X.-C. Gao is with Mentor Graphics, San Jose, CA 95112.

P. Liebmann is with Electrical Engineering Software, Santa Clara, CA 95051.

J. Valainis was with Daisy Systems Corp., Sunnyvale, CA. He is now with Valid Logic Systems, San Jose, CA 95134.

IEEE Log Number 9042075.

II. Basic Magnetics

The branch equation of an inductor is

$$V = \frac{d\phi}{dt} \tag{1}$$

where V is the voltage in volts, and, ϕ is the magnetic flux in Webers.

In the case of a coil, or inductor, with no magnetic material, the flux induced by the flow of current in the windings can be equated to the latter by a proportionality constant L

$$\phi = LI \tag{2}$$

where L is the inductance of the coil in Henries while I is the current in amperes. The inductance is a function of the geometry of the coil and the number of windings, and is independent of the current. Equations (1) and (2) describe the linear inductor supported in SPICE 2G6 [9].

In the case of a transformer where the windings surround a magnetic material, the core, the relation between the flux and current is no longer linear. Two additional magnetic quantities, the magnetic field, H, induced in the core, and the magnetic induction or flux density, B, must be computed. The magnetic field in the core is obtained by summing up the contributions H_i of each winding:

$$H = \sum_{i=1}^{n} \frac{\kappa_i N_i I_i}{l_{\text{mag}}} \tag{3}$$

where N_i is the number of turns in winding i, $0 \leq \kappa_i \leq 1$ is the coupling of the winding to the core, I_i is the current through winding i, and l_{mag} is the effective magnetic path length of the core. In the above equation H is expressed in (ampere-turns/meters), the International System unit. The flux density, B, can be equated to the magnetic field, H, by the permeability, $\mu = \mu_r \mu_0$, of the magnetic material

$$B = \mu_r \mu_0 H = \frac{\phi}{A}. \tag{4}$$

0278-0070/91/0400-0476$01.00 © 1991 IEEE

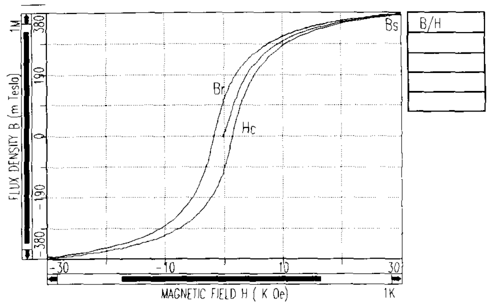

Fig. 1. Major magnetic hysteresis loop.

The above equation is valid only in the International System, where μ_0, the permeability of free space, is $4\pi \times 10^{-7}$ H/m; μ_r is the relative permeability of the material and is a function of H, H is measured in ampere-turns/meters, 1 A-turn/m = $4\pi 10^{-3}$Oe, A is the cross-sectional area in square meters, and B is the flux density in Tesla, 1 T = 10^4 G.

Furthermore, B is not only a nonlinear function of H, but depends on the history of the magnetic fields applied to the core:

$$B = B(H, \text{history}). \tag{5}$$

The result is a hysteresis curve in the B-H plane as shown in Fig. 1. These curves are the result of applying a sinusoidal current to a winding of a transformer and are studied in more detail in the following section. The amplitude of the current and the number of turns is chosen such that the field H, computed according to (3), is large enough to saturate the core.

The nonlinearity introduced by (4) can significantly change the circuit behavior compared to the linear case of (2). The voltage across a winding of the transformer results by solving (1), (3), and (4). The solution of these history-dependent time-varying nonlinear functions using the SPICE algorithms constitutes the major difficulty of the nonlinear core model implementation.

In circuit design it is often necessary to estimate the impedance of the windings of a transformer. For this purpose it is useful to define an equivalent inductance based on substitution of (3) and (4) in (2):

$$L_{eq} = \frac{4\pi 10^{-7} \mu_r(H) N^2 A}{l} \tag{6}$$

where L_{eq} is expressed in Henries, A in square meters, l in meters, and μ_r is averaged over the operating region of the core.

III. Hysteresis Modeling

A major hysteresis loop, shown in Fig. 1, is characterized by three parameters, H_c, B_r, and B_s. H_c, known as the coercive force, is given by the intersection of the major loop with the positive H axis. B_r, the remnant flux, is the intersection of the major loop with the positive B' axis. The limit of the magnetic flux density B when H increases is

$$\lim_{H \to \infty} B = \mu_0 H + B_s \tag{7}$$

which defines the saturation flux, B_s. For most fields encountered in practice the $\mu_0 H$ term is small compared to B_s. The major loop represents the envelope of all B-H curves and is attained when the current through the windings is large enough to saturate the core.

Several approaches to model the hysteresis curves of magnetic cores have been reported [3], [10]. Two hyperbolic curves have been found to fit well the experimental data measured for ferrites [11]. In our model the major loop is composed of two branches: a lower branch which applies for increasing fields H and an upper branch which applies for decreasing fields. The branch equations are defined below in terms of the flux $B' = B - \mu_0 H$.

The upper branch is given by:

$$B'_+(H) = B_s \frac{(H + H_c)}{|H + H_c| + H_c\left(\frac{B_s}{B_r} - 1\right)}. \tag{8a}$$

The lower branch is given by:

$$B'_-(H) = B_s \frac{(H - H_c)}{|H - H_c| + H_c\left(\frac{B_s}{B_r} - 1\right)}. \tag{8b}$$

Notice that we have inversion symmetry through the origin of the B', H plane. That is

$$B'_+(H) = -B'_-(-H). \tag{9}$$

The magnetization curve is the path in the H, B' plane which is followed if we start at $H = 0$, $B' = 0$, and increase or decrease the field without reversals. In the present model the magnetization curve is given by the average of the upper and lower branches of the major loop. Specifically:

$$B'_{mag}(H) = \frac{B'_+(H) + B'_-(H)}{2}. \tag{10}$$

Next we discuss the normal minor loops. These are the loops which are followed if H varies periodically from some $-H_{max}$ to H_{max} and back without any reversals of the direction of change of H except at the end points of the interval. The values of B' at the end points are denoted by $-B_{max}$ and B_{max}. The points $(-H_{max}, -B_{max})$ and (H_{max}, B_{max}) are called the extreme points of the minor loop.

In the current model the lower branch of a minor loop is obtained by translating the lower branch of the major loop vertically upward by some amount B_d where $0 \le B_d \le B_r$. The upper branch of the minor loop is obtained by translating the upper branch of the major loop downward by the same amount B_d. The intersection points of the upper and lower branches of the minor loop will lie on the magnetization curve $B_{mag}(H)$. These intersection points are just the extreme points of the minor loop.

The equations for a minor loop with a given value of B_d are

$$\text{upper branch: } B'(H) = B'_+(H) - B_d \tag{11a}$$

$$\text{lower branch: } B'(H) = B'_-(H) + B_d. \tag{11b}$$

Let us see how we move around in the (H, B') plane during a simulation. (Note that we always stay within the major loop.)

If we start from $H = 0$, $B' = 0$, represented by point A in Fig. 2, and increase H, we move along the magnetization curve, curve AFB in Fig. 2. Suppose that when H reaches 4 A-turns/m we begin to decrease H. We now move onto the upper branch of the minor loop at the upper extreme point which is located at the place where H begins to decrease, point B in Fig. 2. If H now decreases to exactly $-H_{max}$, $H_{max} = 4$ in our example, and then starts to increase again, we move onto the lower branch of

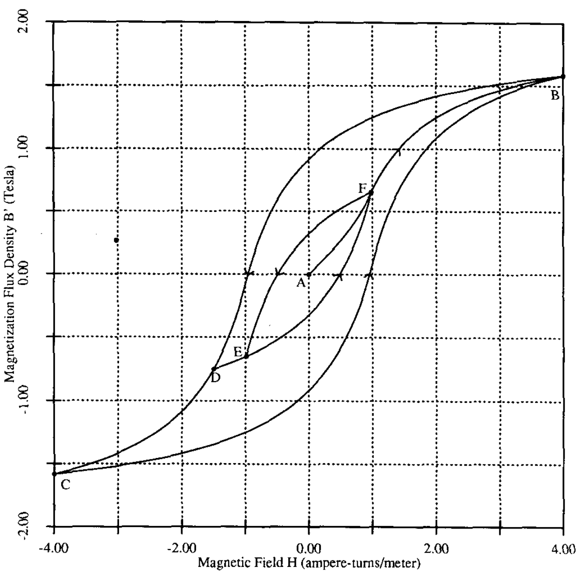

Fig. 2. Minor loops and magnetization curve (Case 1).

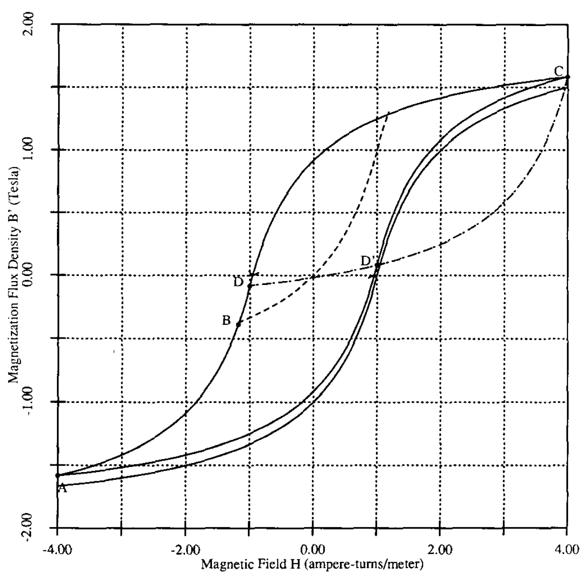

Fig. 3. Minor loop generation in Case 2.

the same minor loop. If we now continue to move periodically between $-H_{max}$ and H_{max} with no reversals in between, then we will stay on the same minor loop.

If we are moving along a minor loop and arrive at an extreme point but do not reverse the direction of change of H then we will move onto the magnetization curve again. Also note that each branch of a minor loop has a proper direction of motion. If we are on the lower branch then H must be increasing while on the upper branch H must be decreasing.

Next suppose that we are on a minor loop and reverse the direction of H at a point which is not an extreme point. Assume that we are moving along the upper branch of the outer minor loop shown in Fig. 2. We arrive at point D and H starts to increase. There are then two cases to be considered.

Case 1: As shown in the figure there is an extension of the lower branch of a valid minor loop, with $0 \le B_d \le B_r$, which passes through point D. In this case we follow the extension. This extension is given by the same analytical form as the lower branch of the minor loop but we have $H < -H_{max}$. For the main body of the minor loop we had the restriction $-H_{max} \le H \le H_{max}$. The valid minor loop has the extreme points E and F.

Case 2: The point where H changes direction does not lie on the extension of a normal minor loop with the proper direction of motion. This is the case when $B_d > B_r$. When $B_d = B_r$ the corresponding minor loop is a point at the origin; for larger values of B_d no minor loops exist. In Fig. 3 the dotted curve starting from point B is the vertical translate exactly by B_r of the lower branch of the major hysteresis loop. Thus there is no extension of a lower branch of a normal minor loop to follow when a reversal of the field occurs at points on the upper branch of the minor loop between B and C.

In this case the model uses a path constructed as follows. Suppose that we are at point D (between B and C) in Fig. 3 and H is increasing. We use a path which is a translate of the lower branch of the minor loop that D is on, defined by the extreme points A and C. We translate the lower branch of the minor loop in such a way that its lower extreme point A is translated to D. Let the coordinates of D be (H_D, B'_D). Then we note that because of the symmetry of the hysteresis loops, the point D' with coordinates $(-H_D, -B'_D)$ is on the lower branch of the same hysteresis loop that D is on. The extreme point $(-H_{max}, -B'_{max})$ is translated to D. Thus the translation vector is given by

$$(\Delta H, \Delta B') = (H_D + H_{max}, B'_D + B'_{max}). \qquad (12)$$

The translate of D' is thus

$$(-H_D, -B'_D) + (\Delta H, \Delta B') = (H_{max}, B'_{max}) \qquad (13)$$

which is the upper extreme point of the minor loop. Thus the translated lower branch intersects the upper branch of the minor loop at D and at its upper extreme point, C. This translated lower branch is the curve that we leave D on for increasing H and follow until H begins to decrease again or until we come to the upper extreme point.

If point D had been on a lower branch with H initially increasing but changing to decreasing at D, then the above discussion still holds with upper and lower, increasing and decreasing interchanged everywhere.

IV. Transformer Model

A. Windings, Cores, and Parasitics

Fig. 4 shows the equivalent model of a transformer including parasitics. The main component of a transformer is the magnetic core which has two or more windings. A basic transformer, e.g., TRF3 in Fig. 4, has a core, $B1$, and two or more windings, e.g., $Y1$, $Y2$, and $Y3$.

The core element statement contains such information as number of windings, magnetic length LM, cross-sectional area A, air gap LG, window height G, the frequency of signals, and the magnetization at time 0. Each core statement also contains the name of a core model. The core model statement defines B_r, B_s, and H_c and all coefficients of the modeled effects which are listed below. Each winding Y statement defines the number of

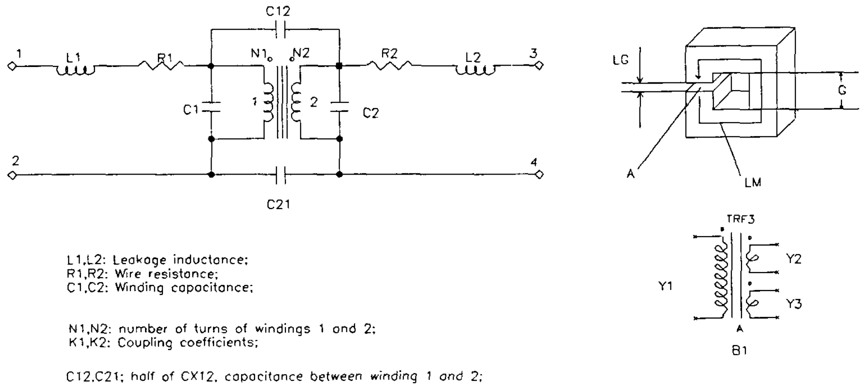

Fig. 4. Transformer equivalent model.

turns, the coupling coefficient, the name of the core it is wound on, and the initial current through the winding.

For a real transformer there are parasitic components associated with the main inductors and mutual inductances. Each winding has capacitances between turns of the winding. They are represented by $C1$ and $C2$ in Fig. 4 for a two winding transformer TRF1. $C12$ is the interwinding capacitance. The wire resistance is frequency dependent, and will be discussed later. The leakage inductance, which accounts for the flux that does not go through the magnetic core, and therefore, does not contribute to the mutual inductance, is separated out as $L1$ and $L2$ in Fig. 4. If the inductances of the two transformer windings are $Y1$ and $Y2$, then the coupling coefficient K for the mutual inductance between the two windings is

$$K = \sqrt{\frac{Y1\,Y2}{(Y1 + L1)(Y2 + L2)}}. \tag{14}$$

B. Frequency Behavior

The area enclosed by the hysteresis loop represents the energy loss to the core due to the irreversible movement of the magnetic domains in the core material and the Eddy current ohmic loss [6]. The energy loss to the core has a very pronounced frequency dependence. This dependency is modeled by modifying the effective H_c:

$$H_c' = H_c(f_1 + f_2 f^{f_3}) \tag{15}$$

where f is the operating frequency and f_1, f_2, f_3 are three empirical coefficients.

H_c increases with frequency and consequently the hysteresis loop widens. Therefore, the higher the frequency the more energy is dissipated due to core loss. The coefficients f_1, f_2, and f_3 are obtained by curve fitting the loss curves of core materials from data sheets. f_1 is usually 1.0 and f_3 is about 2.0. Since this is an empirical equation fitted to real loss data, all kinds of microscopic losses by the core are taken care of, such as the Eddy current loss.

Additional power loss is due to the ohmic loss of the windings. This wire loss is also frequency dependent due to the skin effect. The winding parasitic resistance is modified as

$$R_w' = R_w \frac{r^2}{r^2 - \left(r - \dfrac{504}{\sqrt{\sigma \mu_r f}}\right)^2} \tag{16}$$

where R_w is the resistance of the winding in ohms, r is the radius of the wire in meters, and σ is the conductivity of the wire in mho.

C. Temperature Behavior

The temperature dependence is modeled by a linear variation of the three basic parameters B_s, B_r, and H_c with temperature T. The temperature variation of the saturation flux density is expressed as

$$B_s' = B_s\big(1 + (T - T_{\text{nom}})TBS\big) \tag{17}$$

where T_{nom} is a reference temperature and TBS is the temperature coefficient for B_s. There are similar relations for B_r and H_c.

D. Air Gap

The air gap in the core can drastically change the shape of the hysteresis loop. A minute gap introduced into the core can prevent the core from saturating. The reason for this is that the permeability of air is so much smaller than that of the magnetic core material. The air gap effectively lengthens the magnetic path of the core:

$$L_m' = L_m + \mu_r L_g \tag{18}$$

where L_g is the length of the air gap.

However, the lengthening effect is not as large as indicated in (18) due to the fringe fields at the gap. An approximation for the fringe field effect [12] is to modify the above equation to

$$L_m' = \frac{L_m + \mu_r L_g}{1 + \dfrac{L_g}{\sqrt{A}} \ln\left(\dfrac{2G}{L_g}\right)} \tag{19}$$

where A is the cross-sectional area of the core and G is the window height of the core gap, as shown in Fig. 4.

E. Inrush Current

A high current may flow in a transformer winding upon initial connection to a sinusoidal voltage source. This potentially high current, termed inrush current [13], is a function of the phase shift of the sinusoidal source at time 0. The inrush current can be specified for each winding as an initial condition.

Often the core retains a residual magnetization. This magnetization can affect the turn-on behavior of the circuit by add-

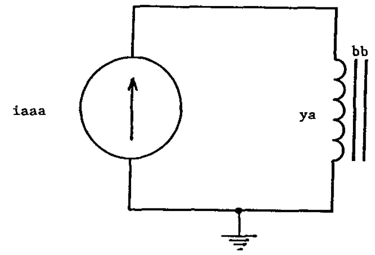


```
transformer test
.model core1 tfm bs = 2.0 br = 1.0; hc = 1.0 fc1 = 1.0 fc2 = 0.0
+ fc3 = 0.0 tbs = 0.0 tbr = 0.0 thc = 0.0
iaaa 0 1 sin(0.0 6.0 1e3 0.0 .4e3)
vaaa 1 2 0.0
ya 2 0 bb 1 1.0
bb 1 core1 lm = 1.0 a=1.0 lg=0.0
.tran .01 10.0 0.0 0.01
.print tran i(vaaa) b(bb)
.options limpts = 10000
.end
```

Fig. 5. Single-winding transformer circuit and DSPICE netlist.

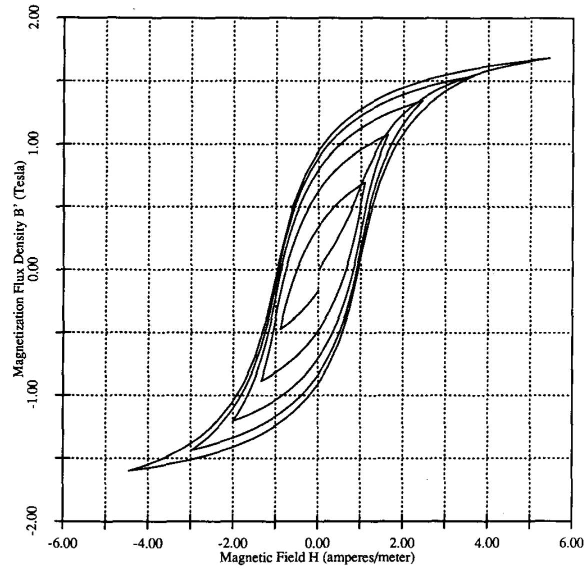

Fig. 6. (H, B') plane loops of single-winding transformer. Circuit for damped sinusoidal input.

ing another component to the inrush current. An initial flux density B_0 can be specified for each core in the circuit. B_0 together with the H determined from the initial currents establish the exact state of the transformer at time 0. The initial state of the transformer can be specified to be anywhere within the major loop of the core.

V. Results

Numerous circuits with magnetic core transformers have been simulated using DSPICE. These simulations using the transformer model described above have produced accurate results and have not caused convergence problems. The simulations of two magnetic circuits are presented below along with comments on the accuracy of the magnetic modeling.

The correctness of the model can be judged first for a simple one-winding transformer driven by a damped sine wave current source. The circuit is shown together with a SPICE netlist in Fig. 5. The hysteresis loops plotted in Fig. 6 show the smooth transition from one minor loop to another with no breaks or discontinuities.

A more representative circuit for the applications of a transformer model is a square wave power oscillator converter, also referred to as a Royer oscillator [14]. The circuit schematic is presented in Fig. 7. The heart of the circuit is the square hysteresis loop of the transformer core $B1$. The transformer core has five windings $Y1$ through $Y5$ with the specified polarity.

The circuit operates between two states. First assume that transistor $Q1$ is saturated and thus its collector, node 3, is at V_{cesat} (see Fig. 8). The saturation current flowing through $Y1$ produces, through inductive coupling, a voltage drop

$$V_{Y4} = \frac{n_4}{n_1} V_{Y1} \tag{20}$$

across $Y4$ which drives the base of $Q1$ positive and keeps $Q1$ in saturation. Due to the reverse polarity of $Y3$ the base of $Q2$ is driven negative and $Q2$ is turned off. Fig. 8 displays the plots

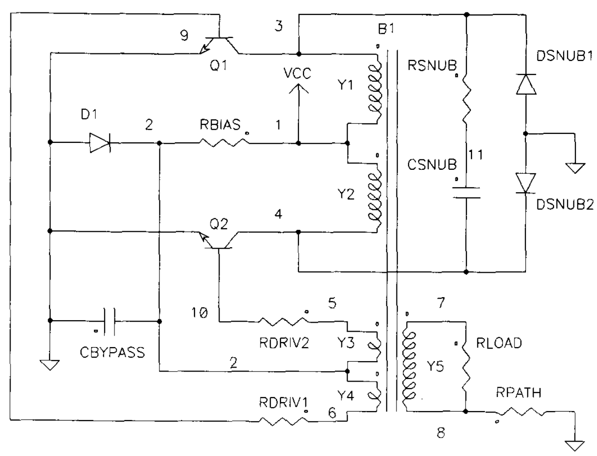

Fig. 7. Square wave power oscillator.

of the collector voltages of $Q1$ and $Q2$ as well as the flux density of the magnetic core versus time. The oscillation is centered around $V_{cc} = 12$ V with the collector of $Q1$ at V_{cesat} and the collector of $Q2$ at $2V_{cc} - V_{cesat}$. During the time that saturation current flows through $Q1$ the magnetic flux density in $B1$ decreases linearly with time because the voltage drop across $Y1$ is constant:

$$\frac{dB}{dt} = \frac{V_{Y1}}{n_1 A} = \frac{V_{cc} - V_{cesat}}{n_1 A} \tag{21}$$

Fig. 9 shows the plot of flux density in the (H, B') plane. B decreases linearly with time, as seen in Fig. 8, until it reaches the saturation value $-B_s$. At this point B cannot decrease any further and V_{Y1} falls to zero; this pulls the collector of $Q1$ to the supply V_{cc}. The current diverted through $R1$ flows partly in the base of $Q2$, turns it partially on, and generates a positive

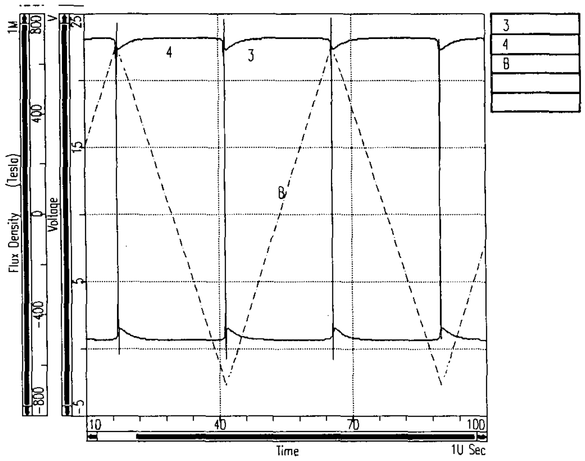

Fig. 8. Collector voltages of transistors $Q1$ and $Q2$, and magnetic flux density through core $B1$.

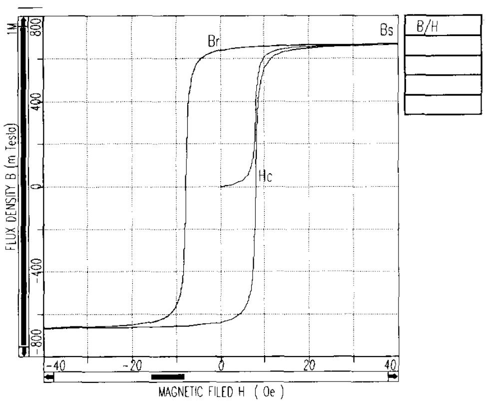

Fig. 9. (H, B') plane hysteresis loops of $B1$ during oscillations.

magnetic field in the core. A positive feedback effect leads to the saturation of $Q2$ and the cutoff of $Q1$. At the same time B increases at a constant slope toward B_s. When it reaches that point the circuit switches and the process continues periodically. The waveforms in Figs. 8 and 9 produced by DSPICE demonstrate the correct simulation of the Royer oscillator. The period of oscillation can be derived from (21) and is in agreement with the simulation results of Fig. 8:

$$T = \frac{4B_s n_1 A}{V_{cc} - V_{cesat}} = 45\ \mu s \tag{22}$$

for a magnetic core with $B_s = 0.675$ T, a cross section area $A = .05\ cm^2$, and 40 turns in the winding $Y1$. The supply voltage $V_{cc} = 12$ V.

VI. Conclusions

An extension of the applicability of SPICE2 to the systems and power electronics field has been described. The simulation capabilities are extended in DSPICE by supporting a transformer representation and a nonlinear magnetic core model.

Three new statements are used to specify a transformer in DSPICE: a core statement contains geometry information and the name of a core model, a model statement specifies the core hysteresis characteristics and coefficients for various effects, and, finally a winding statement defines the characteristics of each winding.

The most complex issue of the transformer implementation, the support of a nonlinear history dependent function in the context of the Newton–Raphson algorithm, has been presented in detail. The correctness of the algorithm has been verified by the results of a square wave oscillator simulation.

Acknowledgment

The authors would like to acknowledge the participation through suggestions and discussions of Daisy's technical specialists, application engineers, and DSPICE users.

References

[1] L. W. Nagel, "SPICE2: A simulation program with integrated circuit emphasis," ERL Memo ERL-M520, Univ. California, Berkeley, May 1975.

[2] ——, "Analog simulation tools," Daisy Systems Corp., Mountain View, 1988.

[3] D. Nitzan, "MTRAC: Computer program for the transient analysis of circuits including magnetic cores," *IEEE Trans. Magn.*, vol. MAG-5, pp. 524–533, Sept. 1969.

[4] M. Tabrizi, "Nonlinear magnetic model realistically simulates core behavior," *Powertech. Mag.*, Mar. 1988.

[5] ——, "PSpice," MicroSim Corp., Irvine, CA, 1989.

[6] D. C. Jiles and D. L. Atherton, "Theory of ferromagnetic hysteresis," *J. Magnet. and Magn. Mater.*, vol. 61, pp. 48–68, 1986.

[7] J. C. Bowers, "I-G SPICE—A circuit designer's dream," *Powerconversion Int.*, vol. 9, pp. 36–40, June 1983.

[8] ——, "Analog libraries," Daisy Systems Corp., Mountain View, 1988.

[9] A. Vladimirescu, K. Zhang, A. R. Newton, D. O. Pederson, A. Sangiovanni Vincentelli, "SPICE version 2G user's guide," Dept. EECS, Univ. California, Berkeley, 1982.

[10] M. K. El-Sharbiny, "Representation of magnetic characteristics by a sum of exponentials," *IEEE Trans. Magn.*, vol. MAG-9, pp. 60–61, Mar. 1973.

[11] D. R. Bennion, D. C. Hewitt, and D. Nitzan, *Digital Magnetic Logic*. New York: McGraw-Hill, 1969.

[12] W. T. McLyman, *Magnetic Core Selection for Transformers and Inductors*. New York: Marcel Dekker, 1982.

[13] S. A. Nasar, and L. E. Unnewehr, *Electromechanics and Electric Machines*. New York: Wiley, 1983.

[14] A. Pressman, *Switching and Linear Power Supply, Power Converter Design*. Rochelle Park, NJ: Hayden, 1977.

John Chan (M'84) received the B.A. and Ph.D. degrees in physics from the University of California, Berkeley, in 1970 and 1976, respectively.

He has worked at the Fairchild Research Center, Shiva Corp., and Daisy Systems Corp. on various aspects of analog simulation and device modeling. Currently he is teaching at the University of Hong Kong. His current interests include CAD for VLSI, analog simulation, and parallel algorithms.

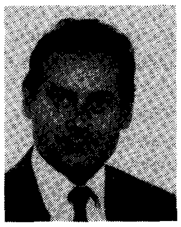

Andrei Vladimirescu (S'79–M'82) received the Diploma Engineering degree in electronics from the Polytechnic Institute in Bucharest, Romania, in 1971, and the M.S. and Ph.D. degrees in electrical engineering and computer sciences from the University of California, Berkeley, in 1980 and 1982, respectively.

From 1971 to 1977 he was with the Research and Development Center for Electronic Components, in Bucharest, Romania, where he worked in the areas of CAD tools and MOS IC design and modeling. In 1977 he joined the IC/CAD research group of the EECS Department, University of California, Berkeley, where he carried out research in the area of electrical simulation, specifically LSI electrical simulation on parallel computers and semiconductor device modeling. In 1983 he joined the Linear Signal-Processing Division of Analog Devices Inc., where he participated in the development of CAD tools for ASIC's, and then from 1984 to 1988 he was Research and Development director of the Analog Division at Daisy Systems Corp., where he led the development of Daisy's analog computer-aided engineering product and the research for a SPICE hardware accelerator. Since 1988, he has been Research and Development Director at Analog Design Tools Inc., and subsequently at Valid Logic Systems Inc. His current research interests are in the areas of computer simulation, including algorithmic issues, component and higher level modeling, analog hardware description languages, and mixed analog-digital and electrical-physical design tools.

Xiao-Chun Gao (M'88), photograph and biography not available at time of publication.

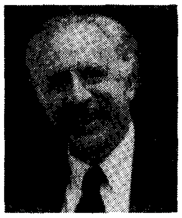

Peter Liebmann received the B.A. degree in mathematics from Clark University, and the Ph.D. degree in physical chemistry from New York University, in 1969.

From 1969 to 1980 he held research grants at various universities where he developed numerical techniques to facilitate the understanding of a variety of problems related to molecular biology, surface physics, and other quantum-chemical phenomena. He is presently Project Development Manager at Electrical Engineering Software, Santa Clara, CA. Before EES he worked at the Fairchild Research Center on the in-house circuit simulator, and afterwards, at Daisy Systems Corp. where he was the main contributor to the DSPICE simulation program.

John Valainis (M'90) received the B.S. degree in physics from Butler University, Indianapolis, IN, and the M.S. and Ph.D. degrees in physics from the California Institute of Technology, in 1975 and 1982, respectively.

He has been employed by Schlumberger Research Center, Palo Alto, CA, and Daisy/Cadnetix, Mountain View, CA. He is currently with Valid Logic Systems, San Jose, CA. His interests include CAD for VLSI, analog simulation, electromagnetic problems, and various aspects of physics.

```python
#
# Simulating a BH-loop using Chan's model: https://ieeexplore.ieee.org/document/75630
# Dr. Dmitriy Makhnovskiy, City College Plymouth, England
# 23.02.2024
#

import tkinter as tk
from tkinter import messagebox
import matplotlib.pyplot as plt
import csv
import logging

# Configure logging
logging.basicConfig(filename='simulation_log.log', level=logging.INFO, format='%(asctime)s - %(levelname)s: %(message)s')

def read_log_file():
    try:
        with open('simulation_log.log', 'r') as log_file:
            lines = log_file.readlines()
            params_found = False
            params = []
            for line in lines:
                if "Simulation parameters:" in line:
                    params = line.split(':')[1].strip().split(',')
                    if len(params) == 5:  # Ensure the correct number of parameters
                        params_found = True
            if params_found:
                entry_Bs.delete(0, tk.END)
                entry_Bs.insert(0, params[0].split('=')[1])
                entry_Br.delete(0, tk.END)
                entry_Br.insert(0, params[1].split('=')[1])
                entry_Hc.delete(0, tk.END)
                entry_Hc.insert(0, params[2].split('=')[1])
                entry_Hmax.delete(0, tk.END)
                entry_Hmax.insert(0, params[3].split('=')[1])
                entry_N.delete(0, tk.END)
                entry_N.insert(0, params[4].split('=')[1])
                messagebox.showinfo("Parameters Loaded", "Simulation parameters loaded from log file.")
            else:
                messagebox.showwarning("Log File Error", "Invalid format of simulation parameters in log file.")
    except Exception as e:
        messagebox.showerror("Error", f"An error occurred while reading log file: {str(e)}")

def run_simulation():
    try:
        # Retrieve values from the GUI
        Bs = float(entry_Bs.get())  # Saturation induction (flux density), Tesla (T)
        Br = float(entry_Br.get())  # Residual induction, Tesla (T)
        Hc = float(entry_Hc.get())  # Coercivity, Amperes/meter (A/m)
        Hmax = float(entry_Hmax.get())  # Maximum scanning field, Amperes/meter (A/m)
        N = int(entry_N.get())  # Number of points in the graphs

        # Log input values
        logging.info(f"Simulation parameters: Bs={Bs}, Br={Br}, Hc={Hc}, Hmax={Hmax}, N={N}")

        # Clear log file
        open('simulation_log.log', 'w').close()

        # Write parameters from the current run to log file
        with open('simulation_log.log', 'a') as log_file:
            log_file.write(f"Simulation parameters: Bs={Bs}, Br={Br}, Hc={Hc}, Hmax={Hmax}, N={N}\n")

        # Calculate lists: H (A/m), BH-loop branches B1 (T) and B2(T), and the averaged curve B3 = (B1 + B2) / 2
        # Full (saturated) or minor (unsaturated) BH-loop
        H_values = [-Hmax + 2 * Hmax * i / (N - 1) for i in range(N)]  # Magnetising force, A/m
        # dB - branch vertical adjustment for drawing a minor loop
        dB = Bs * (H_values[N - 1] + Hc) / (abs(H_values[N - 1] + Hc) + Hc * (Bs / Br - 1.0))
        dB = (dB - (Bs * (H_values[N - 1] - Hc) / (abs(H_values[N - 1] - Hc) + Hc * (Bs / Br - 1.0)))) / 2.0
```

```
        # The following curves are already vertically adjusted:
        B1_values = [(Bs * (H + Hc) / (abs(H + Hc) + Hc * (Bs / Br - 1.0)) - dB) for H in H_values]  # Upper branch
        B2_values = [(Bs * (H - Hc) / (abs(H - Hc) + Hc * (Bs / Br - 1.0)) + dB) for H in H_values]  # Lower branch
        B3_values = [((B1 + B2) / 2.0) for B1, B2 in zip(B1_values, B2_values)]  # Middle curve

        # Plot BH-loop
        plt.figure()
        plt.plot(H_values, B1_values, label='B1')
        plt.plot(H_values, B2_values, label='B2')
        plt.xlabel('H, A/m')
        plt.ylabel('B, T')
        plt.title('BH-loop: both branches')
        plt.legend(loc='upper right')
        plt.grid(True)
        plt.minorticks_on()
        plt.grid(True, which='minor', linestyle=':', linewidth=0.25)
        plt.show()

        # Plot averaged BH-loop
        plt.figure()
        plt.plot(H_values, B3_values, label='Middle curve')
        plt.xlabel('H, A/m')
        plt.ylabel('B, T')
        plt.title('BH-curve: averaged branches')
        plt.legend(loc='upper right')
        plt.grid(True)
        plt.minorticks_on()
        plt.grid(True, which='minor', linestyle=':', linewidth=0.25)
        plt.show()

        # Save data for the whole BH-loop (both branches)
        with open('BH-loop_data.csv', mode='w', newline='') as file:
            writer = csv.writer(file)
            writer.writerow(['H, A/m', 'Upper B, T', 'Lower B, T'])
            for H, B1, B2 in zip(H_values, B1_values, B2_values):
                writer.writerow([H, B1, B2])

        # Save data for the averaged BH-loop (middle curve)
        with open('Averaged_BH-loop_data.csv', mode='w', newline='') as file:
            writer = csv.writer(file)
            writer.writerow(['H, A/m', 'B, T'])
            for H, B3 in zip(H_values, B3_values):
                writer.writerow([H, B3])

    except Exception as e:
        messagebox.showerror("Error", f"An error occurred: {str(e)}")

# Create a tkinter window
window = tk.Tk()
window.title("BH-loop Simulation")

# Create labels and entry fields for input values
tk.Label(window, text="Bs (T):").grid(row=0, column=0)
entry_Bs = tk.Entry(window)
entry_Bs.grid(row=0, column=1)

tk.Label(window, text="Br (T):").grid(row=1, column=0)
entry_Br = tk.Entry(window)
entry_Br.grid(row=1, column=1)

tk.Label(window, text="Hc (A/m):").grid(row=2, column=0)
entry_Hc = tk.Entry(window)
entry_Hc.grid(row=2, column=1)

tk.Label(window, text="Hmax (A/m):").grid(row=3, column=0)
entry_Hmax = tk.Entry(window)
entry_Hmax.grid(row=3, column=1)

tk.Label(window, text="N (Number of points):").grid(row=4, column=0)
entry_N = tk.Entry(window)
```

```
entry_N.grid(row=4, column=1)

# Load parameters from log file
btn_load_params = tk.Button(window, text="Load Parameters from Log", command=read_log_file)
btn_load_params.grid(row=5, column=0, columnspan=2, pady=10)

# Create Run and Stop buttons
btn_run = tk.Button(window, text="Run Simulation", command=run_simulation)
btn_run.grid(row=6, column=0, columnspan=2, pady=5)

btn_stop = tk.Button(window, text="Stop Simulation", command=window.destroy)
btn_stop.grid(row=7, column=0, columnspan=2)

# Start the tkinter event loop
window.mainloop()
```

FE21001-1301-010

FDK

FERRITE CORES
FOR TRANSFORMER & CHOKE COIL

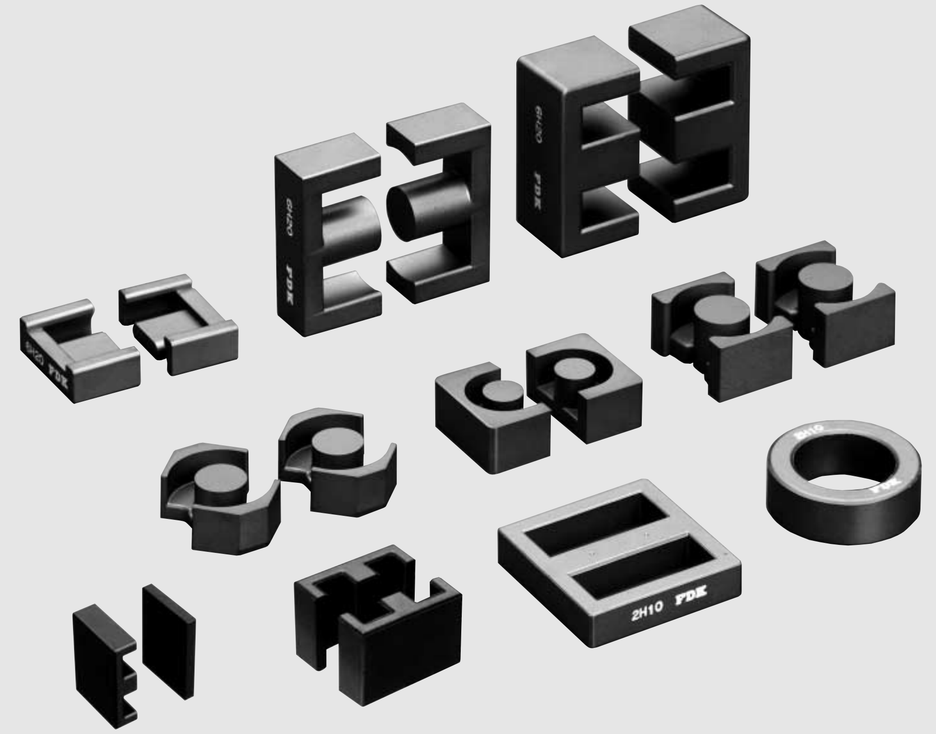

FDK CORPORATION

An introduction to FDK's ferrite cores

As a total manufacturer of ferrite products, FDK has developed diverse types of ferrite material and core, which satisfy the latest demands from electronics market. This catalogue presents a comprehensive list of FDK's ferrite cores for various application such as transformer & choke coils for switching power supply, common mode noise suppression coils, pulse transformer for telecommunication equipments etc.
In this Year 2000 Edition catalogue, following materials (including new materials) are introduced:

① 6H series material : for transformer & choke coils for switching power supply
② 7H series material : for transformer & choke coils for high-frequency(over 500 kHz) switching power supply
③ 2H series material : for common mode noise suppression coils and pulse transformers for telecommunications

Contents

Page

Standard material characteristics (Power material)

Property	Symbol		Condition	Unit	6H10	6H20	6H40	6H41	6H42	7H10	7H20
AC initial permeability	μi		0.1 MHz	—	2500	2300	2400	2500	3400	1500	1000
Saturation magnetic flux density	Bs (1000 A/m)		23 °C	mT	510	510	530	530	530	480	480
			100 °C		390	390	430	430	430	380	380
Residual magnetic flux density	Br		23 °C	mT	110	130	110	110	110	150	130
Coercivity	Hc		23 °C	A/m	13	13	10	10	10	30	25
Relative loss factor	tanδ/μi		0.1 MHz	$\times 10^{-6}$	<5	<5	<3	<3	<3	<5	<4
Core loss	200 mT	25 kHz	23 °C	kW/m^3	—	—	90	75	60	—	—
			40 °C		—	—	75	60	50	—	—
			60 °C		65	80	60	50	40	—	—
			80 °C		55	65	50	40	45	—	—
			100 °C		80	55	40	45	55	—	—
		100 kHz	23 °C	kW/m^3	—	—	650	550	450	—	—
			40 °C		—	—	550	450	350	—	—
			60 °C		450	550	450	350	300	—	—
			80 °C		400	450	350	300	325	—	—
			100 °C		500	400	300	325	375	—	—
	50 mT	500 kHz	60 °C	kW/m^3	—	—	—	—	—	100	50
			80 °C		—	—	—	—	—	80	40
			100 °C		—	—	—	—	—	100	50
		1 MHz	60 °C	kW/m^3	—	—	—	—	—	400	200
			80 °C		—	—	—	—	—	400	200
			100 °C		—	—	—	—	—	500	250
Temperature coefficient	αμr		20 °C~80 °C	$\times 10^{-6}$	8	8	8	8	8	8	8
Curie temperature	Tc		—	°C	>200	>200	>200	>200	>200	>200	>200
Resistivity	ρ		—	Ω · m	3	3	2	2	2	5	5
Apparent density	d		—	$\times 10^3\ kg/m^3$	4.8	4.8	4.9	4.9	4.9	4.8	4.8

Note: 1) The values were obtained with toroidal cores (FR25/15/5).
2) The values were obtained at 23±2 °C unless otherwise specified.
3) Initial permeability was measured at 10kHz, 0.8A/m.

Standard material 6H Series

6H series are FDK's standard power material with low core loss and high saturation flux density, and are suitable for wide range of transformers and choke coils for switching power supply.
6H20 is standard material with superb characteristcs and high cost performance. 6H10 has higher permeability than 6H20 in room temperature, and is suitable for ungapped cores for FF type transformers.
In addition to above, FDK has developed new materials with lower core loss and higher magnetic flux density, which satisfies latest requirements of digital and mobilie electronics.
Core loss of new 6H40 material is around 25 % lower than that of standard 6H20, and is suitable for transformers and choke coils for flat, low profile power supplies and AC/DC adaptors of electronic equipments (such as notebook PCs), which strictly require low temperature rise.
For transformers and choke coils of mobile electronic equipments, FDK has developed 6H41 material (bottom temperature of core loss curve 80 °C) and 6H42 (bottom temperature 50 °C), which enables low operation temperature of transformers. (This is key point for mobile equipments, which have frequent contact with human body.)

● μi vs. Freq.

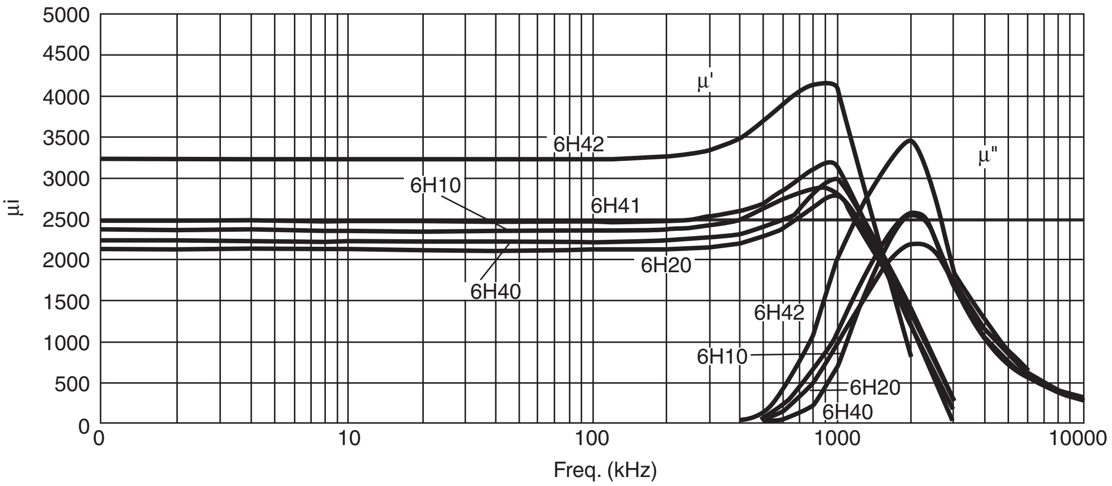

■Standard material 6H Series

●mi vs. Temp.

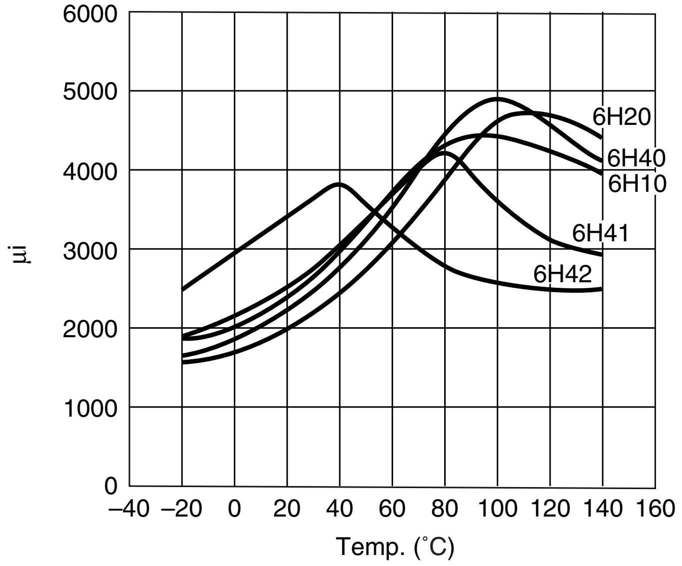

●Pcv vs. Temp.   50kHz, 150 mT

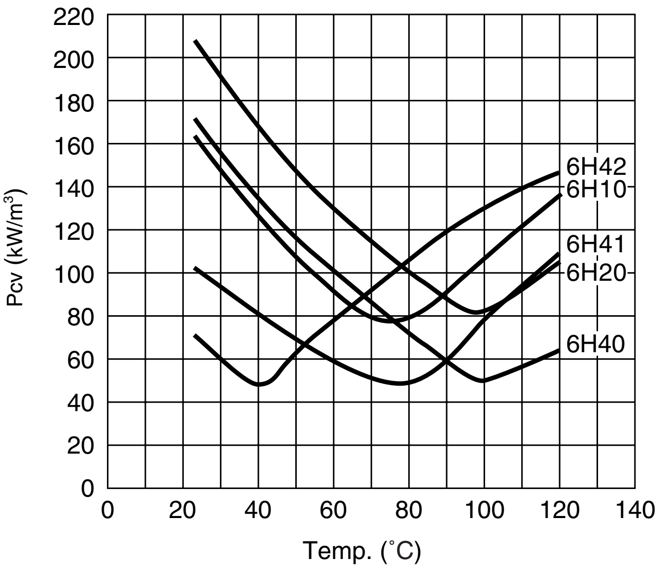

●Bm vs. Temp.

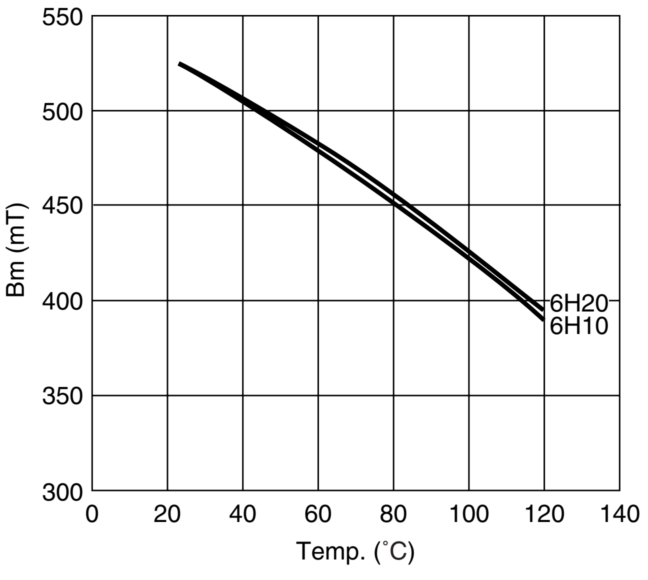

●Bm vs. Temp.

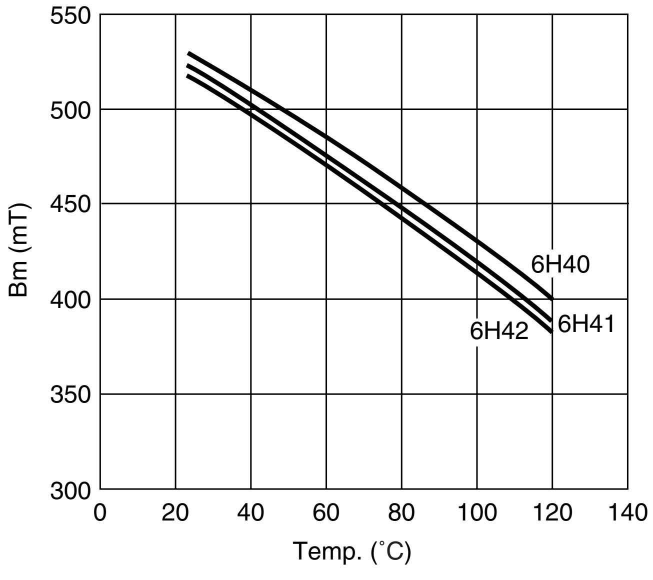

6H10

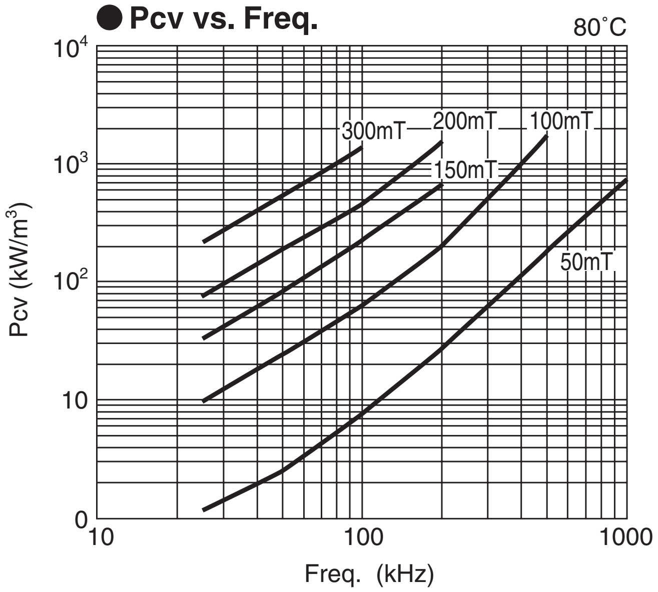
● Pcv vs. Freq.
80˚C
300mT
200mT
100mT
150mT
50mT
Pcv (kW/m³)
Freq. (kHz)
10
100
1000

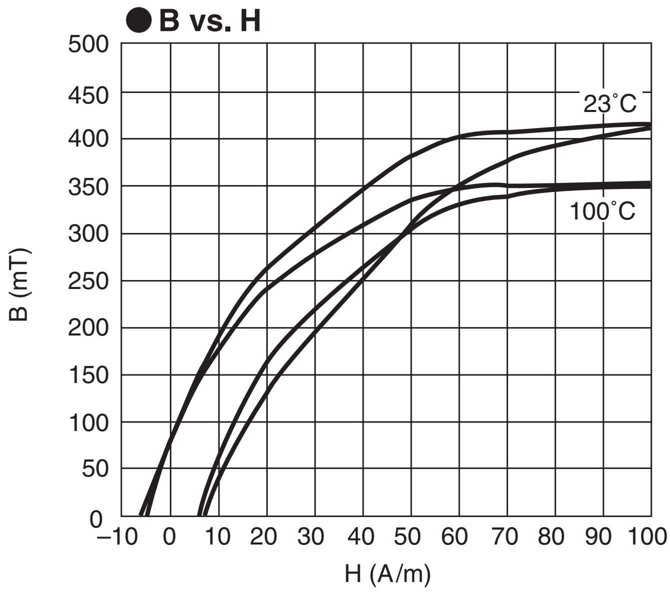
● B vs. H
23˚C
100˚C
B (mT)
H (A/m)

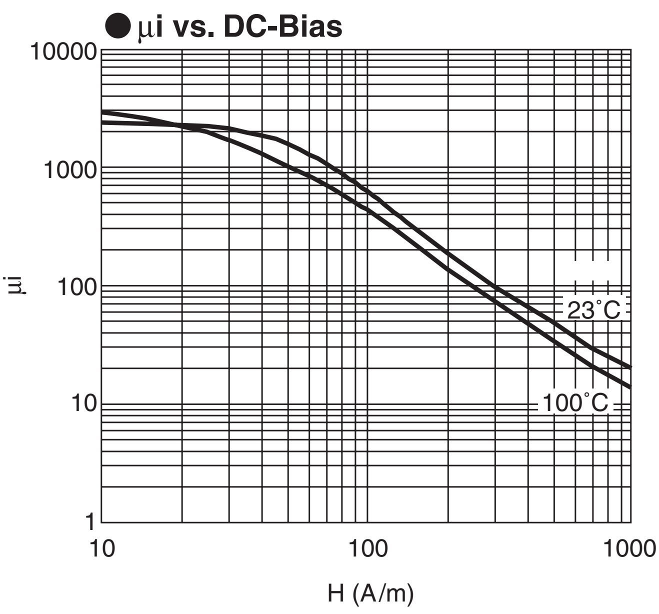
● μi vs. DC-Bias
23˚C
100˚C
μi
H (A/m)

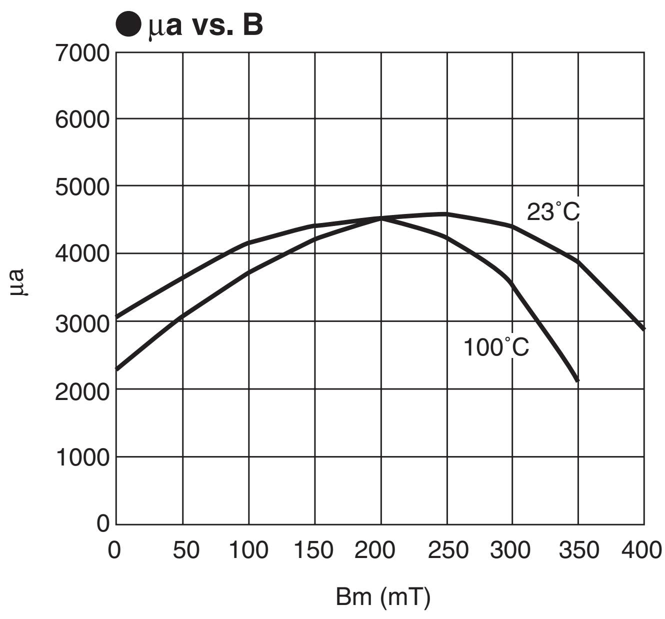
● μa vs. B
23˚C
100˚C
μa
Bm (mT)

6H20

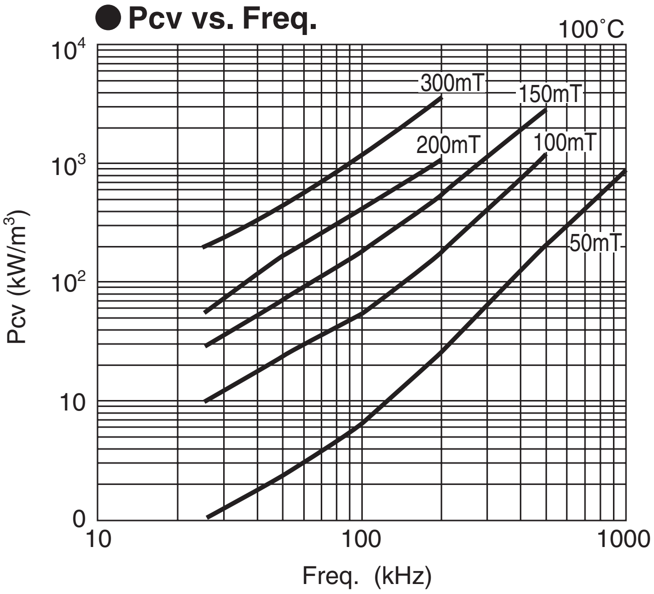
Pcv vs. Freq.
100˚C
300mT
150mT
200mT
100mT
50mT
10^4
10^3
10^2
10
0
10
100
1000
Pcv (kW/m^3)
Freq. (kHz)

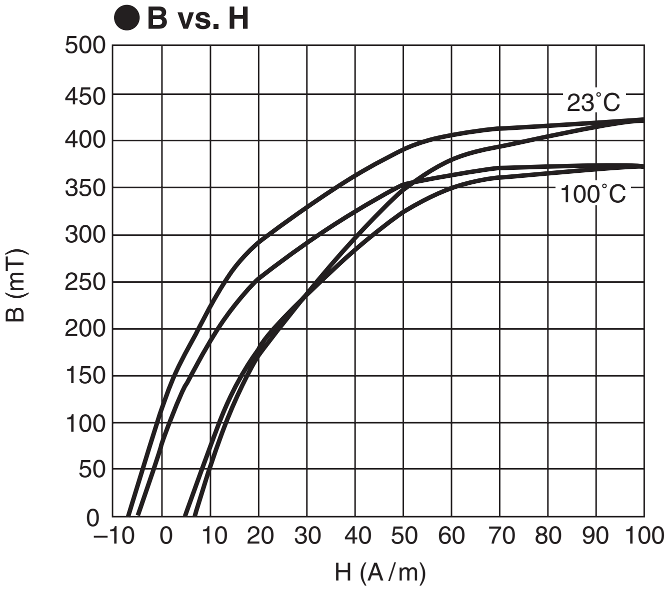
B vs. H
23˚C
100˚C
500
450
400
350
300
250
200
150
100
50
0
–10
0
10
20
30
40
50
60
70
80
90
100
B (mT)
H (A/m)

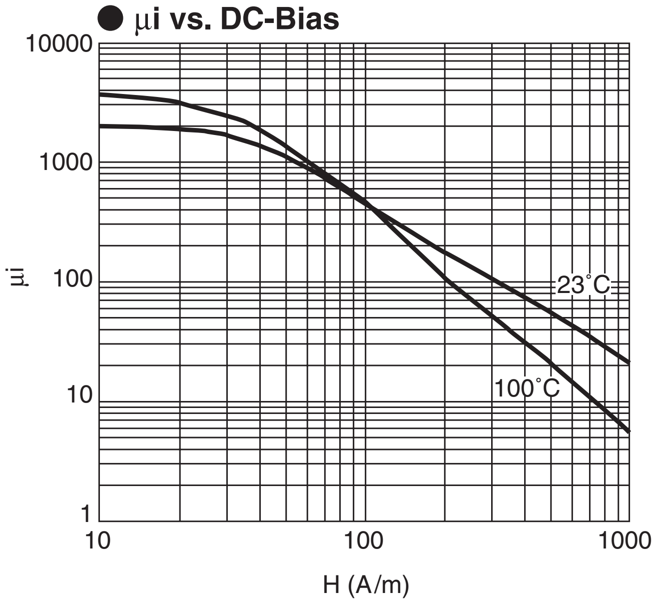
μi vs. DC-Bias
23˚C
100˚C
10000
1000
100
10
1
10
100
1000
μi
H (A/m)

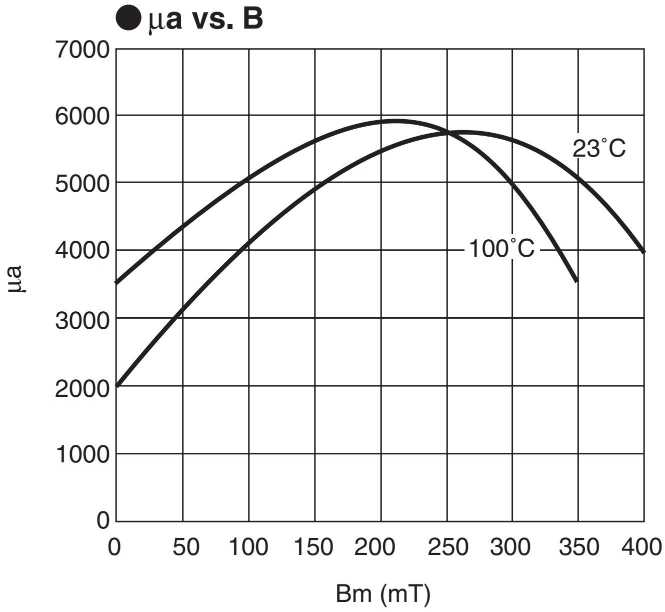
μa vs. B
23˚C
100˚C
7000
6000
5000
4000
3000
2000
1000
0
0
50
100
150
200
250
300
350
400
μa
Bm (mT)

6H40

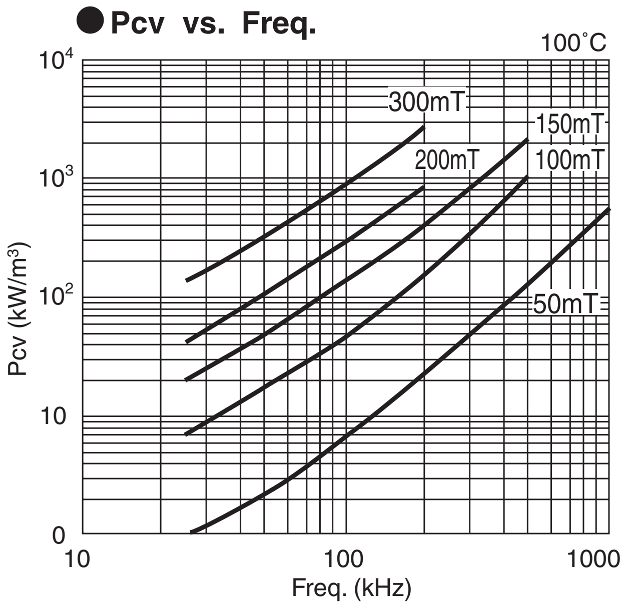
Pcv vs. Freq.
100˚C
300mT
150mT
200mT
100mT
50mT
Pcv (kW/m³)
Freq. (kHz)
10⁴
10³
10²
10
0
10
100
1000

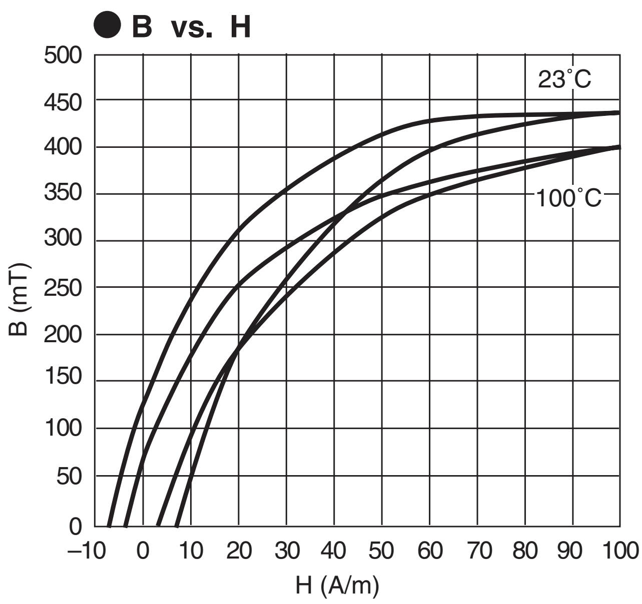
B vs. H
23˚C
100˚C
B (mT)
H (A/m)
500
450
400
350
300
250
200
150
100
50
0
–10
0
10
20
30
40
50
60
70
80
90
100

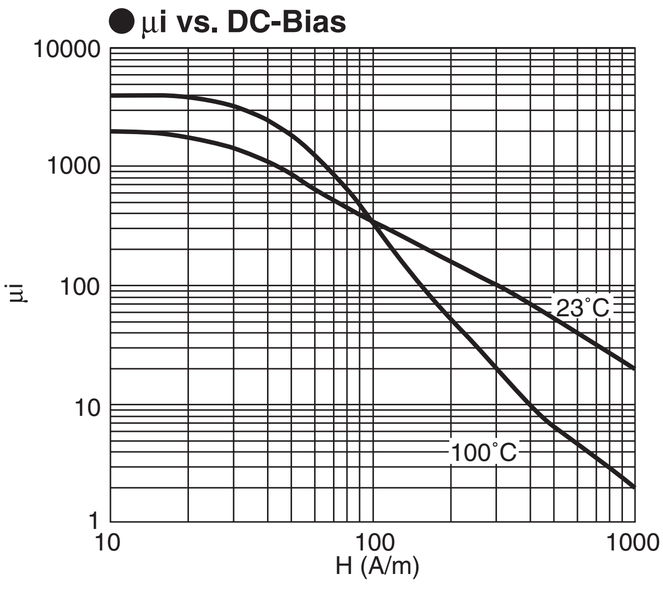
μi vs. DC-Bias
23˚C
100˚C
μi
H (A/m)
10000
1000
100
10
1
10
100
1000

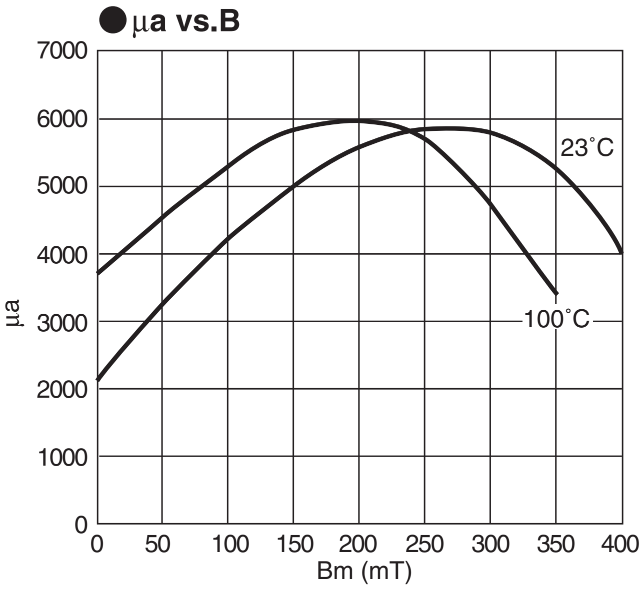
μa vs.B
23˚C
100˚C
μa
Bm (mT)
7000
6000
5000
4000
3000
2000
1000
0
0
50
100
150
200
250
300
350
400

6H41

● Pcv vs. Freq.

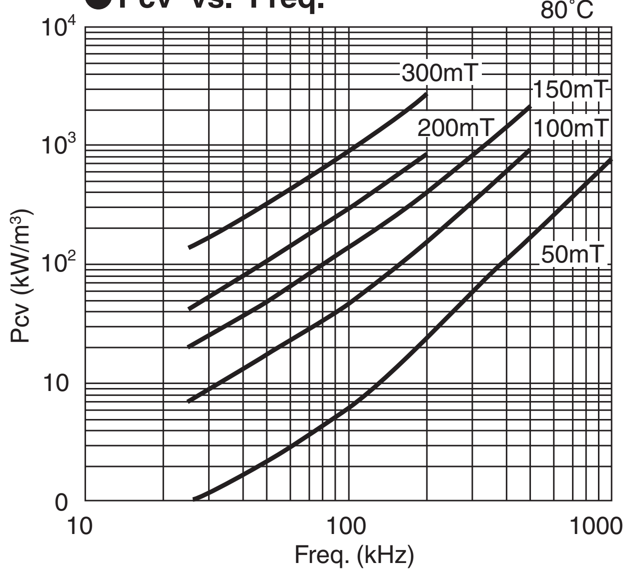

● B vs. H

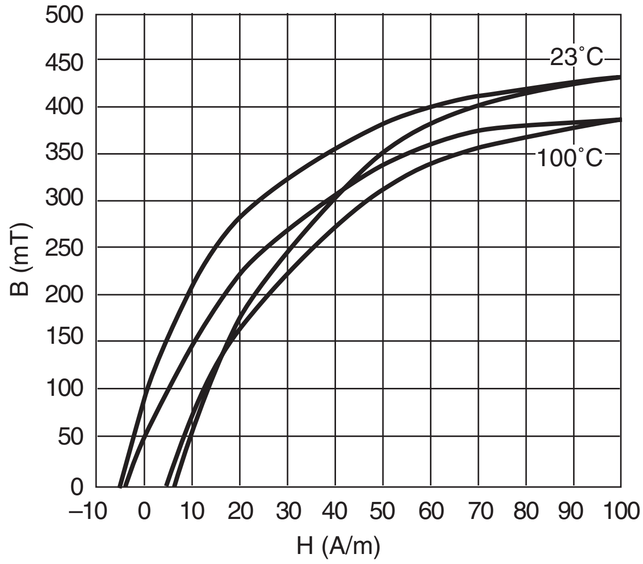

● μi vs. DC-Bias

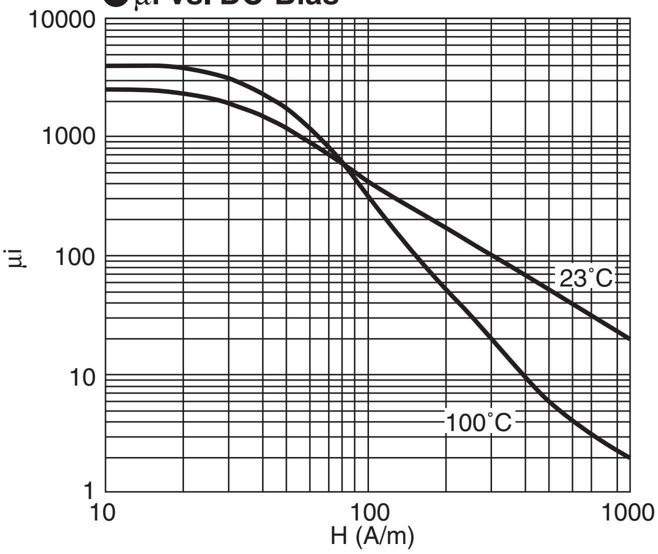

● μa vs.B

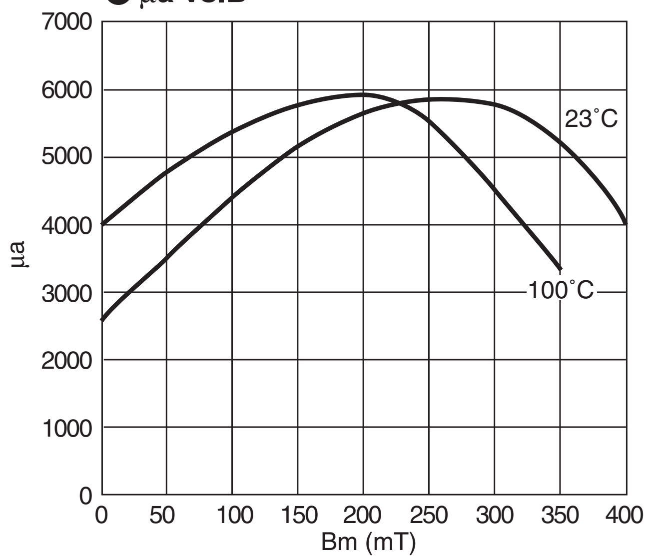

6H42

● **Pcv vs. Freq.**

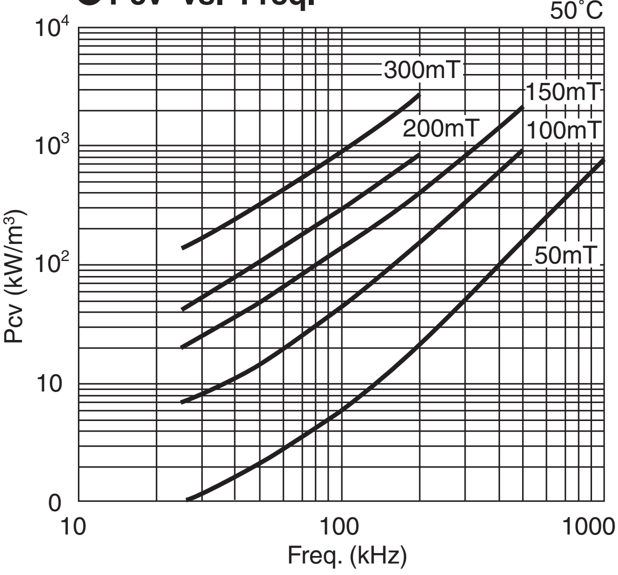

● **B vs. H**

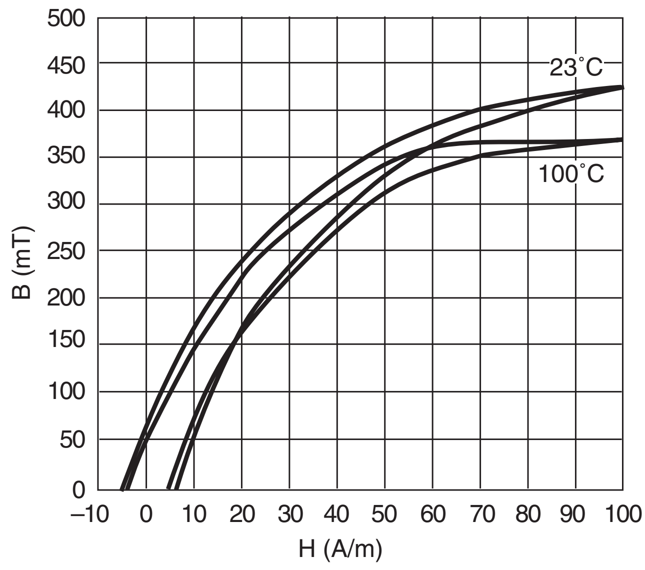

● **μi vs. DC-Bias**

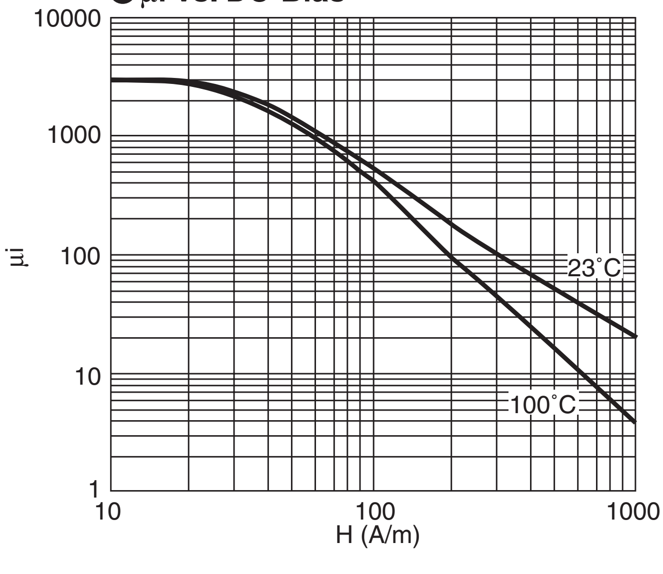

● **μa vs. B**

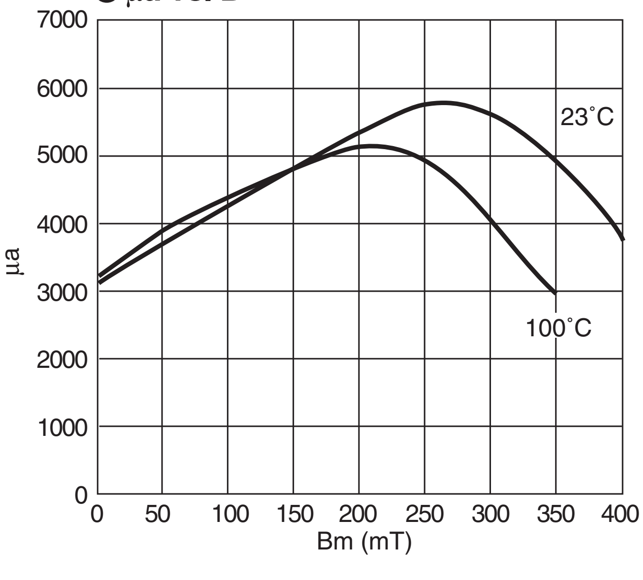

■High frequency material 7H Series

7H series are power material with advantage of low core loss in high frequency range, and suitable for transformers and choke coils of high frequency switching power supply.
7H10 is suitable for switching frequency over 500 kHz. Latest material 7H20 is suitable still higher frequency over 1000 kHz, and its core loss is around 50 % lower than 7H10.

● Pcv vs. Freq. 50mT, 80˚C

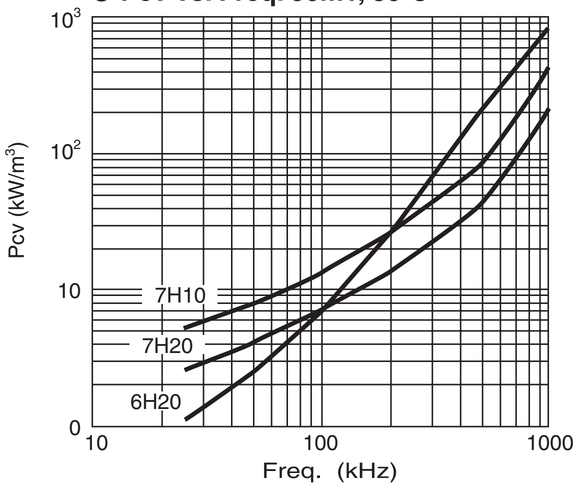

● μi vs. Freq.

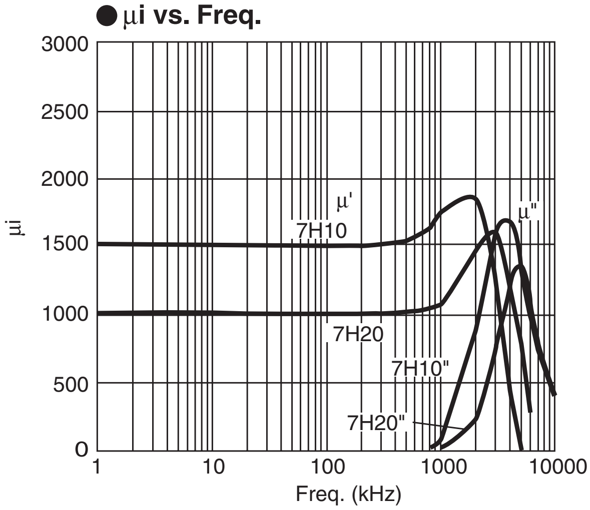

● μi vs. Temp.

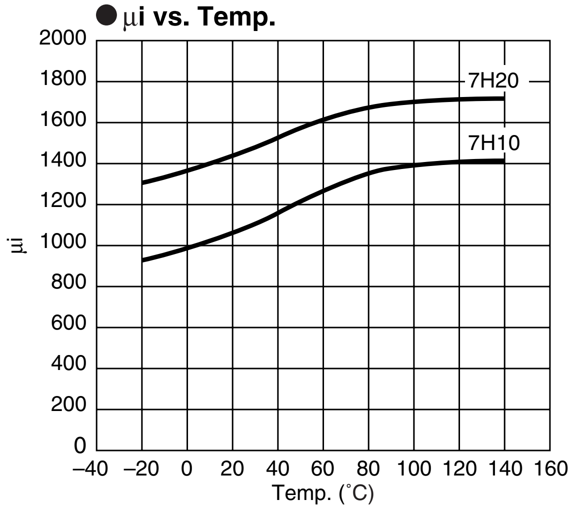

● Bm vs. Temp.

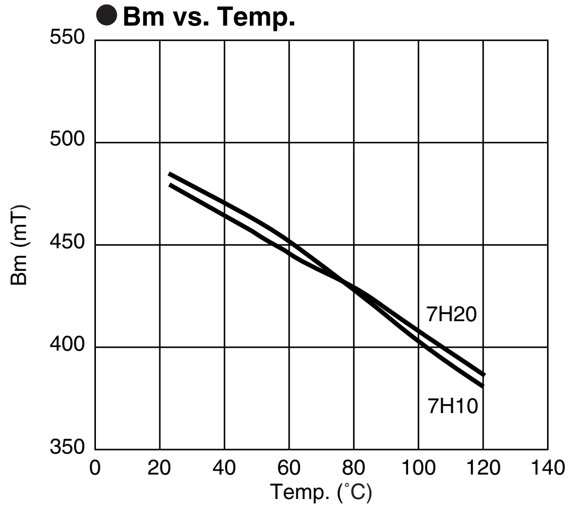

● Pcv. vs. Temp. 500kHz-50mT

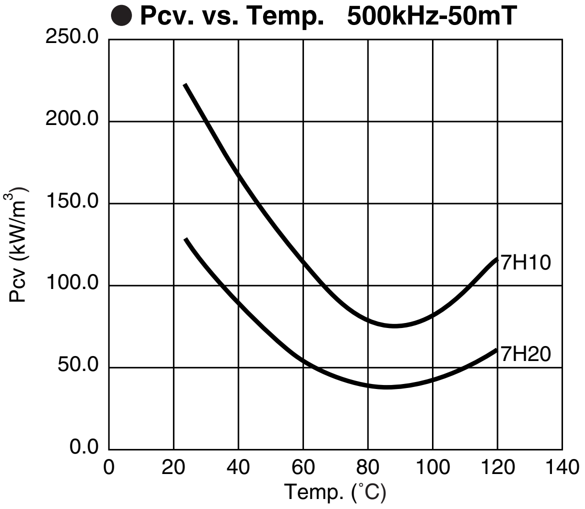

● Pcv. vs. Temp. 1000kHz-50mT

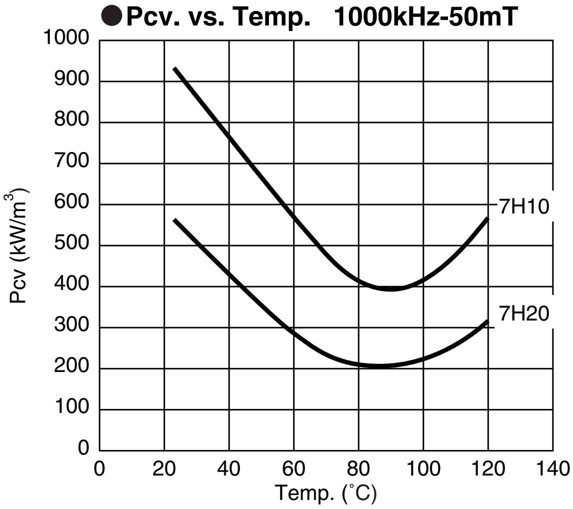

7H10

● Pcv vs. Freq.

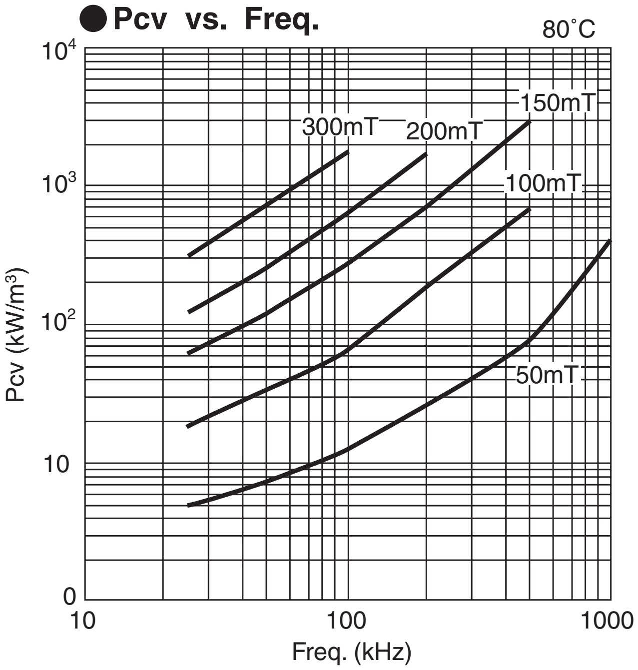

● B vs. H

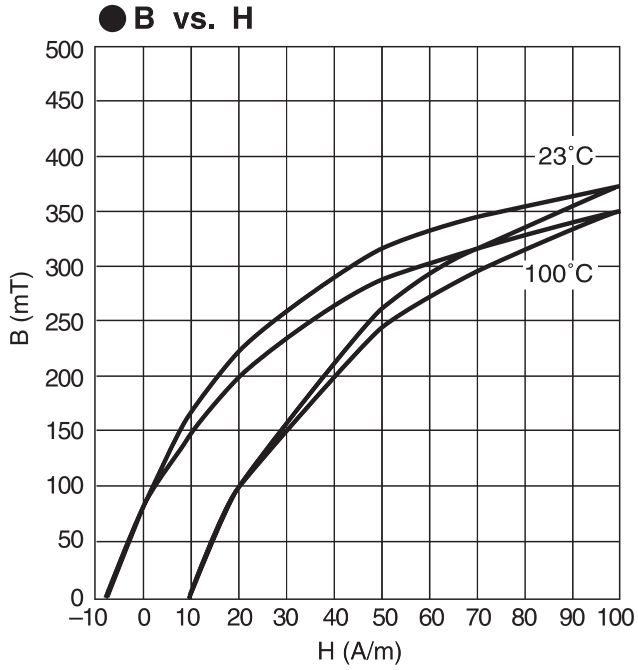

● μi vs. DC-Bias

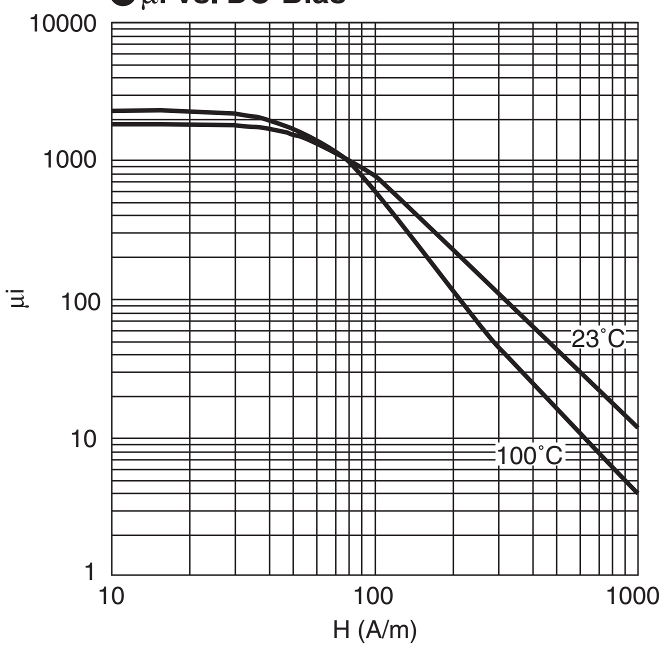

● μa vs. B

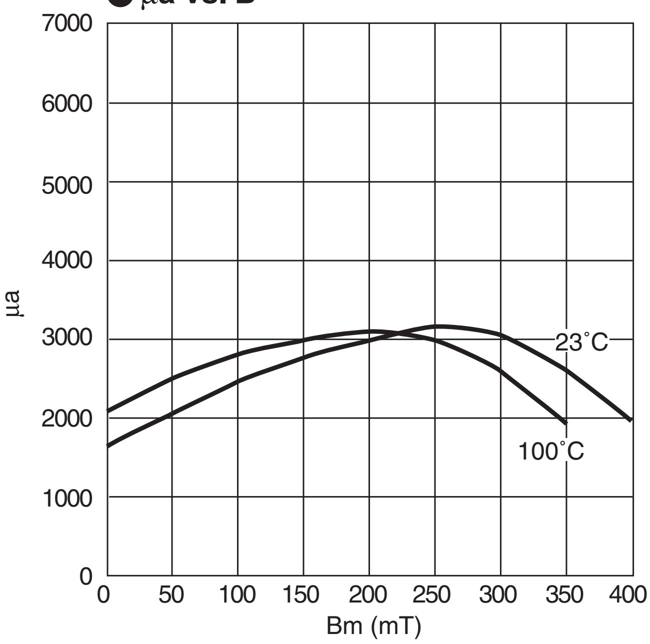

7H20

●Pcv vs. Freq.

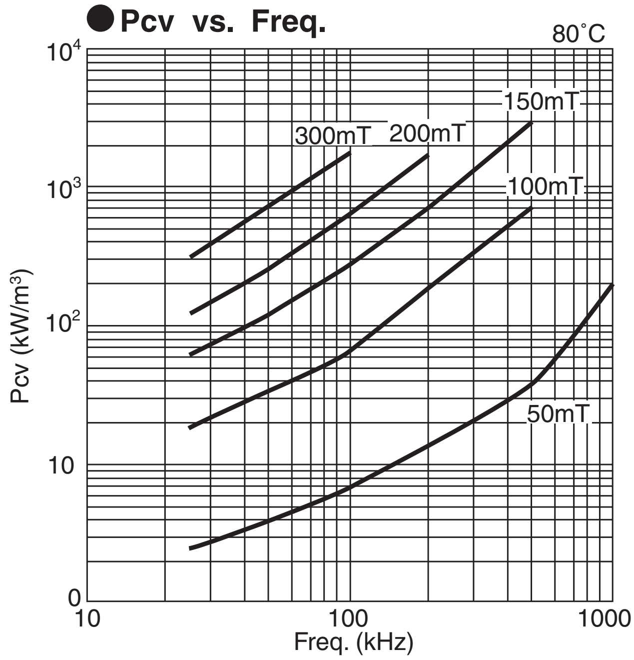

●B vs. H

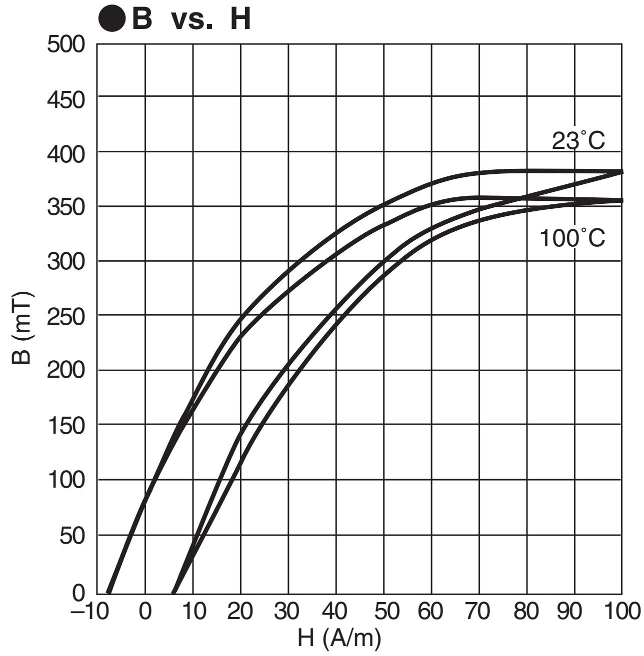

●μi vs. DC-Bias

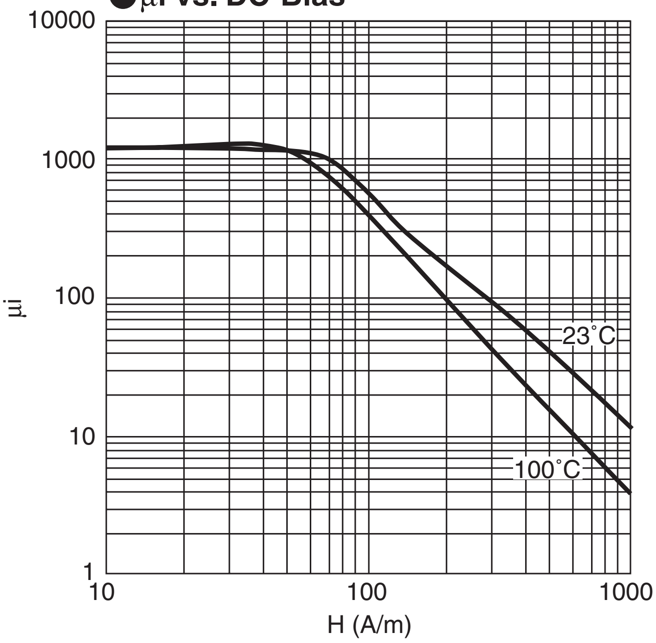

●μa vs.B

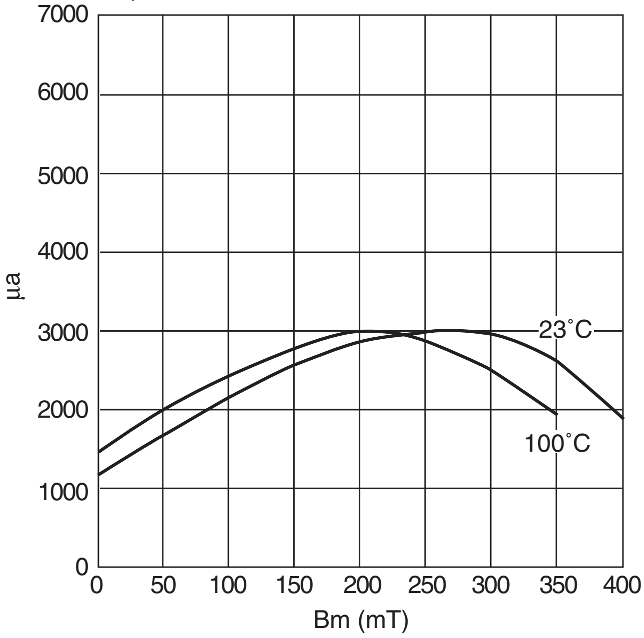

Standard material characteristics (High μ material)

Property	Symbol	Condition	Unit	2H03	2H04	2H06	2H07	2H10	2H15	2H15B
AC initial permeability	μi	0.01 MHz	—	2500 (±20%)	4500 (±20%)	6500 (±20%)	7500 (±20%)	10000 (±20%)	15000 (±20%)	10000 (±20%)
Relative loss factor	tanδ/μi	—	$\times10^{-6}$	<4 (100 kHz)	<10 (100 kHz)	<30 (100 kHz)	<5 (10 kHz)	<7 (10 kHz)	<10 (10 kHz)	<10 (10 kHz)
Temperature coefficient	αμr	–30°C~20 °C	$\times10^{-6}$	—	0~2.0	0~2.0	0~1.5	0~1.5	0.5~2.5	–1~1
		20 °C~55 °C		—	—	—	—	—	—	—
		20 °C~70 °C		—	0~2.0	0~2.0	–0.5~1.5	–0.5~1.5	–0.5~1.5	–0.5~2.0
Saturation magnetic flux density	Bs	1000 A/m 23 °C	mT	470	420	420	410	400	370	370
Residual magnetic flux density	Br	23 °C	mT	100	80	80	60	60	50	50
Coercivity	Hc	23 °C	A/m	12.8	8	8	4	3	2	2
Hysteresis material constant	ηB	0.01 MHz	510^{-6}/mT	—	<0.8	<0.8	<0.6	<1.0	(<1.0)	(<1.0)
Disaccommodation factor	DF	—	$\times10^{-6}$	—	<3.0	<3.0	<3.0	<2.0	<2.0	<2.0
Curie temperature	Tc	—	°C	>200	>140	>140	>130	>120	>100	>100
Resistivity	ρ	—	Ω · m	1	1	0.2	0.1	0.01	0.01	0.01
Apparent density	d	—	$\times10^3$ kg/m³	4.8	4.8	4.8	4.9	4.9	5.0	5.0

Note: 1) The values were obtained with toroidal cores (FR25/15/5).
2) The values were obtained at 23±2 °C unless otherwise specified.
3) Initial permeability was measured at 10kHz, 0.8A/m.

■ 2H Series

2H series are high permeability material with μ 2500~15000, which are suitable for common mode noise suppressor (conforming FCC, VDE, VCCI regulation) and for interface (pulse) transformers of digital telecommunication network systems.
2H07 (μ=7000) and 2H10 (μ=10000) are FDK's standard high permeability materials with superb characteristics and cost performance, and suitable for common mode noise suppressors. 2H10 shows superior characteristics in frequency lower than 500 kHz and suitable for noise suppression.
2H15 (μ=15000) and 2H15B (μ=10000) are the latest super permeability materials for interface (pulse) transformers. 2H15 is suitable for pulse transformers of telecommunication equipments for indoor use. 2H15B has specially stable temperature characteristics, and its permeability curve remains flat in temperature range from –30 °C up to +85 °C, thus makes it suitable for pulse transformers of telecommunication equipments of outdoor use.

● tanδ/μi vs. Freq.

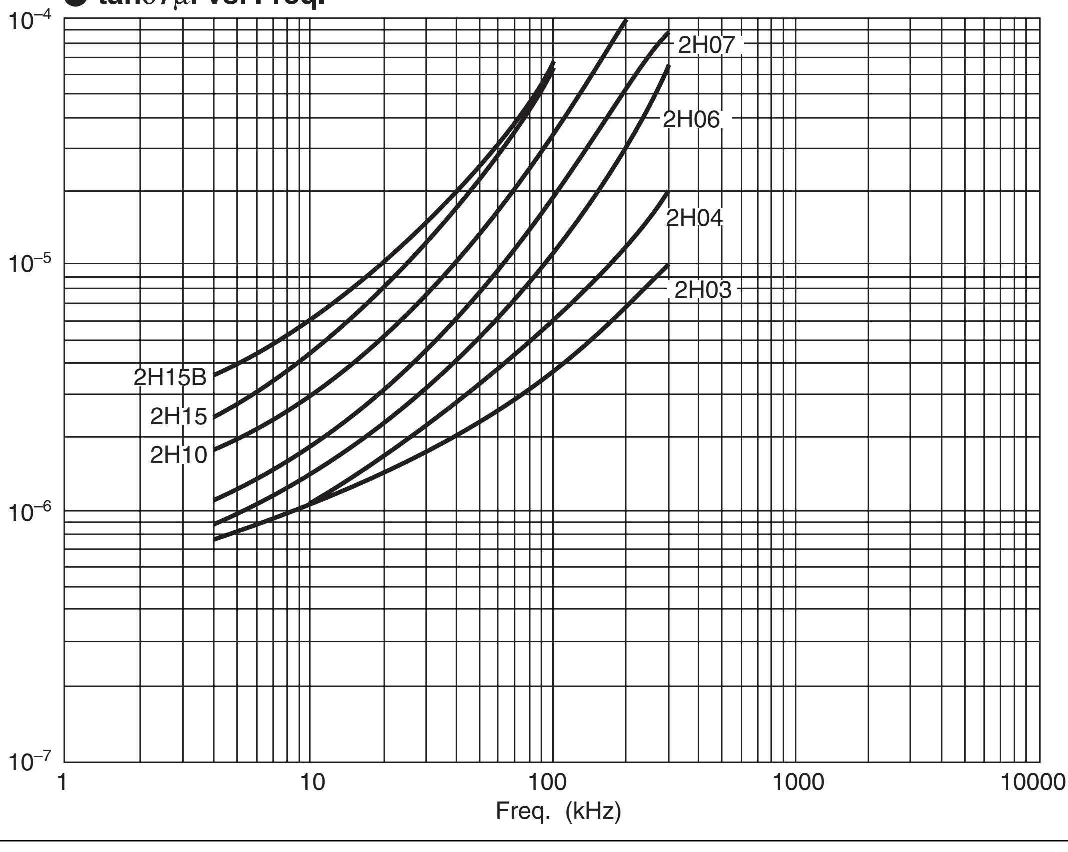

■2H Serise

●μi vs. Temp.

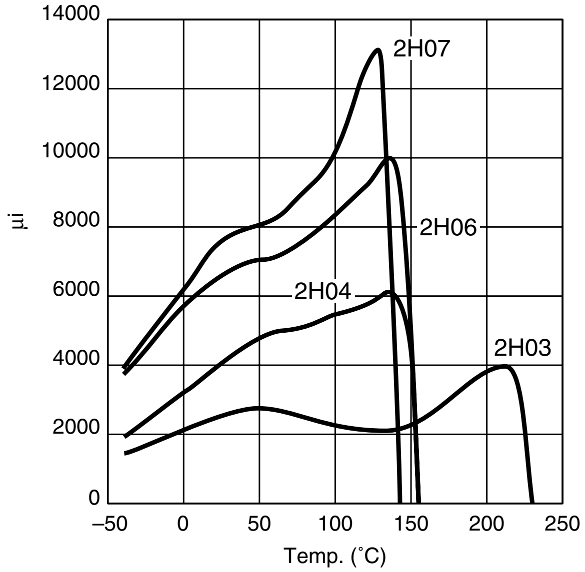

●μi vs. Temp.

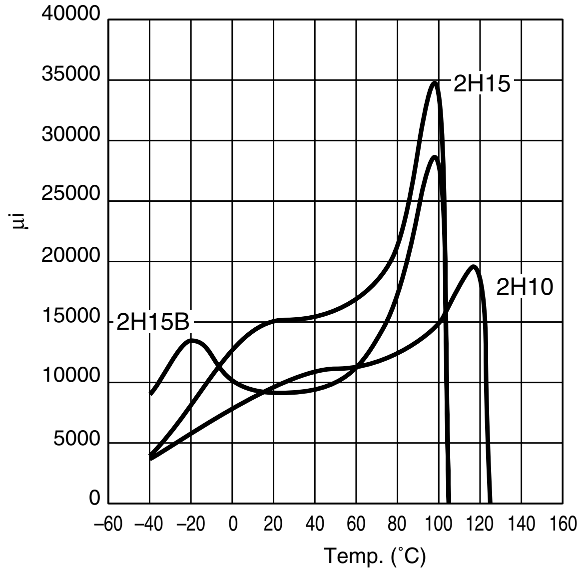

●μi vs.Freq.

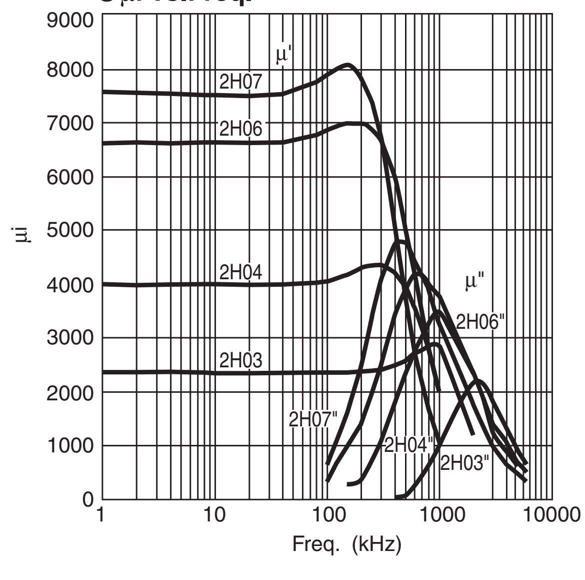

●μi vs.Freq.

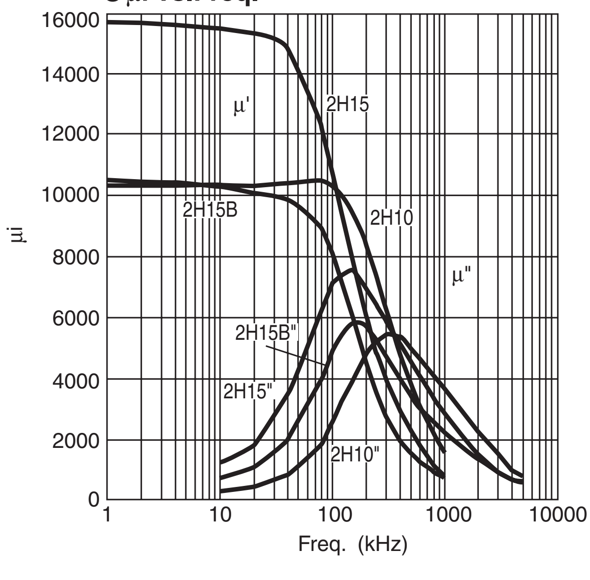

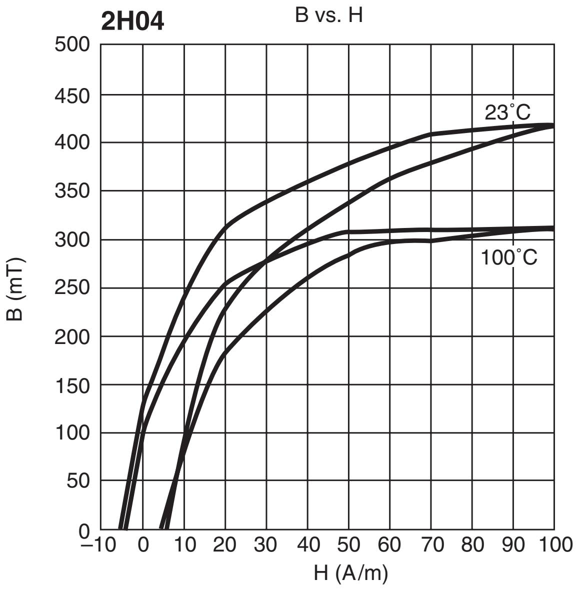
2H04
B vs. H
B (mT)
H (A/m)
23˚C
100˚C
500
450
400
350
300
250
200
150
100
50
0
–10 0 10 20 30 40 50 60 70 80 90 100

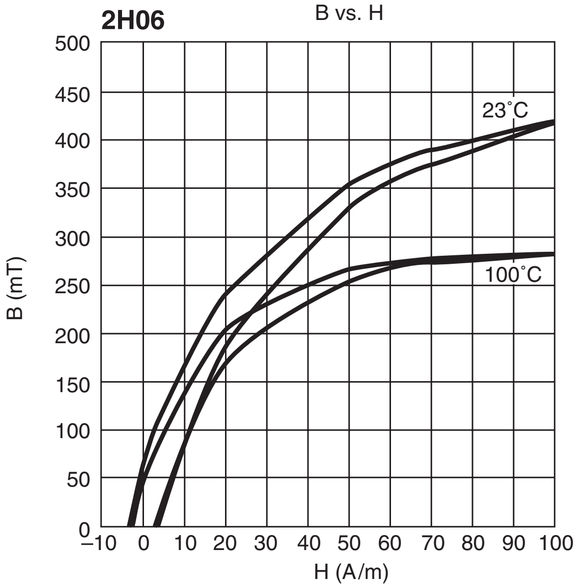
2H06
B vs. H
B (mT)
H (A/m)
23˚C
100˚C
500
450
400
350
300
250
200
150
100
50
0
–10 0 10 20 30 40 50 60 70 80 90 100

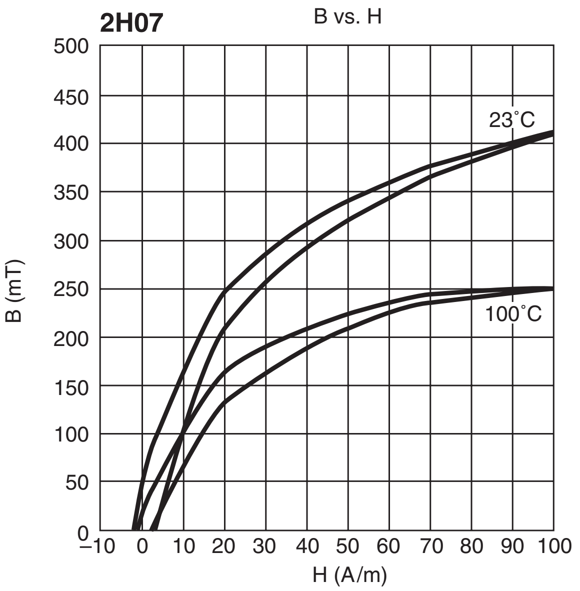
2H07
B vs. H
B (mT)
H (A/m)
23˚C
100˚C
500
450
400
350
300
250
200
150
100
50
0
–10 0 10 20 30 40 50 60 70 80 90 100

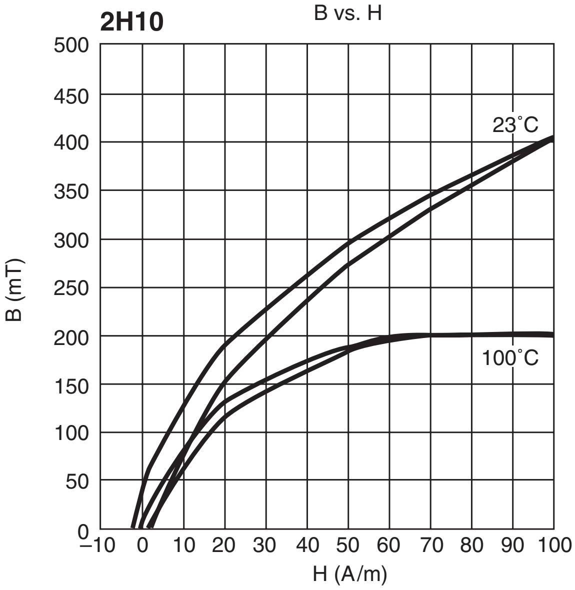
2H10
B vs. H
B (mT)
H (A/m)
23˚C
100˚C
500
450
400
350
300
250
200
150
100
50
0
–10 0 10 20 30 40 50 60 70 80 90 100

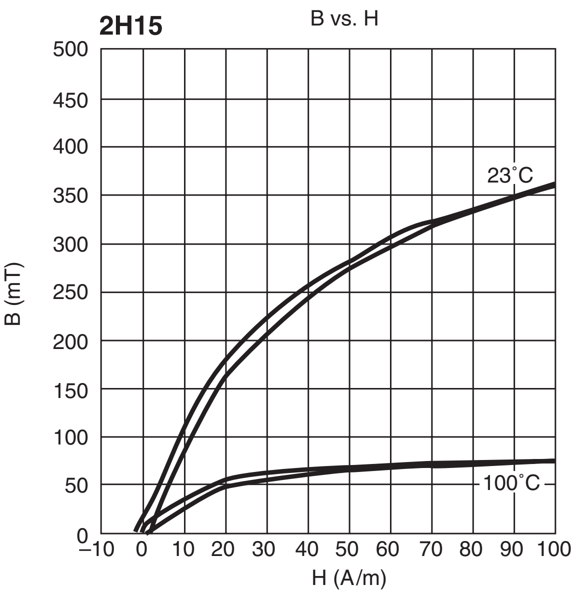
2H15
B vs. H
B (mT)
H (A/m)
23˚C
100˚C
500
450
400
350
300
250
200
150
100
50
0
–10 0 10 20 30 40 50 60 70 80 90 100

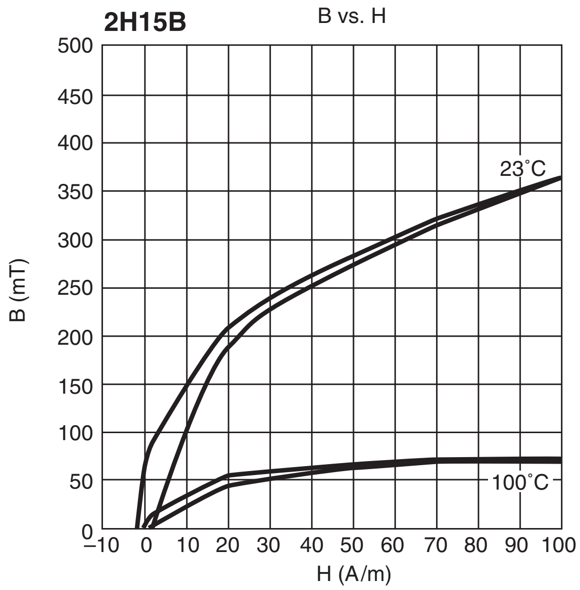
2H15B
B vs. H
B (mT)
H (A/m)
23˚C
100˚C
500
450
400
350
300
250
200
150
100
50
0
–10 0 10 20 30 40 50 60 70 80 90 100

Conventional type EER CORES (ETD)

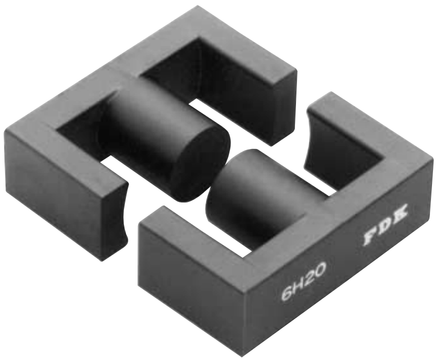

Features

①Wire winding is made easier by the cylindrical shape of the leg.
②A large surface area.
③ETD standard models available.

Applications

Switching regulators, choke coils, etc.

Designation

6H20 EER34/35

- 35: Core height
- 34: Core length
- EER: Shape
- 6H20: Material

Conventional type EER CORES (ETD)

Summary

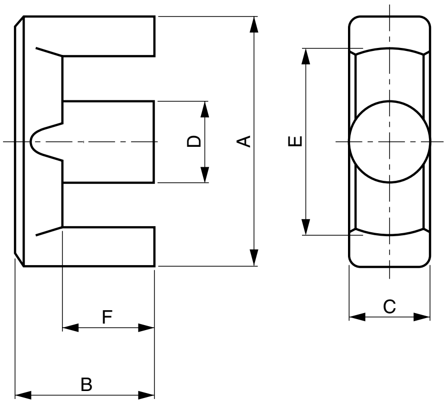

Product code	General standard		Dimensions (mm)					
	IEC	JIS	A	B	C	D	E	F
EER26/19B		FEER25.5A	25.5±0.5	9.3±0.2	7.5±0.2	7.2±0.15	19.8−0	6.2±0.1
EER28/18			28.6±0.5	8.5±0.25	11.4±0.25	$9.9^{+0.2}_{-0.15}$	21.2−0	5.25±0.25
EER28/28		FEER28.5A	28.6±0.5	14.0±0.2	11.4±0.25	9.9±0.2	21.2−0	$9.6^{+0.3}_{-0.2}$
EER28/34		FEER28.5B	28.6±0.5	16.9±0.25	11.4±0.25	9.9±0.25	21.2−0	12.6±0.3
EER29/20			$30.6^{+0}_{-1.4}$	10.1±0.2	$9.8^{+0}_{-0.6}$	$9.8^{+0}_{-0.6}$	$22.0^{+1.4}_{-0}$	6.1±0.2
EER29/32	ETD29	FEER29.8	$30.6^{+0}_{-1.4}$	$16.0^{+0}_{-0.4}$	$9.8^{+0}_{-0.6}$	$9.8^{+0}_{-0.6}$	$22.0^{+1.4}_{-0}$	$10.7^{+0.6}_{-0}$
EER34/26T			$34.0^{+1.0}_{-0.6}$	13.0±0.12	$11.1^{+0}_{-0.6}$	$11.1^{+0}_{-0.6}$	$25.6^{+1.4}_{-0}$	7.8±0.12
EER34/35	ETD34	FEER34.2	$35.0^{+0}_{-1.6}$	17.3±0.2	$11.1^{+0}_{-0.6}$	$11.1^{+0}_{-0.6}$	$25.6^{+1.4}_{-0}$	$11.8^{+0.6}_{-0}$
EER35/26			35.0±0.5	13.0±0.3	11.3±0.3	11.3±0.3	25.6−0	8.0±0.3
EER35/31			35.0±0.5	15.5±0.3	11.3±0.2	11.3±0.2	25.6−0	10.5±0.3
EER35/41		FEER35A	35.0±0.5	20.7±0.3	11.3±0.3	11.3±0.3	25.6−0	14.7±0.3
EER39/28			39.0±0.4	14.2±0.2	12.8±0.25	12.8±0.25	28.6−0	9.0±0.25
EER39/44		FEER39	39.0±0.4	22.2±0.2	12.8±0.25	12.8±0.25	28.6−0	17.0±0.25
EER39/45			39.0±0.4	22.7±0.2	12.8±0.25	$12.8^{+0.2}_{-0.25}$	28.6−0	$17.0^{+0.3}_{-0.1}$
EER39/40	ETD39	FEER39.1	$40.0^{+0}_{-1.8}$	19.8±0.2	$12.8^{+0}_{-0.6}$	$12.8^{+0}_{-0.6}$	$29.3^{+1.6}_{-0}$	$14.2^{+0.8}_{-0}$
EER40/18			40.0±0.7	$9.0^{+0}_{-0.2}$	13.3±0.3	13.3±0.3	28.8−0	4.0±0.15
EER40/45			40.0±0.7	22.4±0.3	13.3±0.3	13.3±0.3	28.8−0	15.4±0.3
EER40/55		FEER40	40.0±1.0	27.3±0.4	13.3±0.3	13.3±0.3	29.5±1.0	20.3±0.4
EER42/36			42.0±0.5	18.0±0.2	15.2±0.3	15.2±0.25	31.0±0.5	12.0±0.3
EER42/42		FEER42	42.0±0.5	21.2±0.2	15.2±0.25	15.2±0.25	31.0±0.5	$15.0^{+0.5}_{-0}$
EER42/42D			42.0±0.5	21.2±0.2	$20.0^{+0}_{-0.8}$	17.3±0.25	31.8−0	$15.0^{+0.5}_{-0}$
EER42/42B			42.0±0.5	21.6±0.2	15.2±0.25	15.2±0.25	31.0±0.5	$15.5^{+0.3}_{-0.1}$
EER42/45A			42.0±0.6	22.4±0.2	15.2±0.25	15.2±0.25	30.4−0	15.4±0.3
EER42/45			42.0±0.6	22.4±0.2	$15.5^{+0.25}_{-0.5}$	$15.5^{+0.25}_{-0.5}$	29.4−0	15.4±0.3
EER42/49			42.0±0.5	24.7±0.2	19.6±0.4	17.3±0.25	31.8−0	$18.5^{+0.5}_{-0}$
EER42/43			$43.0^{+0}_{-1.7}$	$21.8^{+0}_{-0.4}$	$15.0^{+0}_{-0.6}$	$15.0^{+0}_{-0.6}$	$30.4^{+1.2}_{-0}$	$15.6^{+0.7}_{-0}$
EER44/45	ETD44	FEER44	$45.0^{+0}_{-2.0}$	22.3±0.2	$15.2^{+0}_{-0.6}$	$15.2^{+0}_{-0.6}$	$32.5^{+1.6}_{-0}$	$16.1^{+0.8}_{-0}$
EER48/41			$49.0^{+0}_{-2.0}$	$21.2^{+0}_{-1.2}$	20.9±0.4	18.0±0.3	$37.2^{+1.1}_{-0}$	$14.7^{+0.6}_{-0}$
EER49/48			49.0±0.5	23.9±0.3	17.2±0.25	17.2±0.25	36.3−0	15.4±0.2
EER49/54			49.0±0.5	$26.8^{+0.4}_{-0}$	17.2±0.25	17.2±0.25	36.3−0	$18.3^{+0.4}_{-0}$
EER49/55			49.0±0.6	27.5±0.3	17.2±0.4	$17.2^{+0.2}_{-0.25}$	36.4−0	19.0±0.2
EER49/62		FEER49	49.0±0.5	$31.0^{+0.5}_{-0.1}$	17.2±0.4	17.2±0.2	36.4−0	$22.5^{+0.4}_{-0}$
EER49/49	ETD49	FEER48.7	$49.8^{+0}_{-2.2}$	$24.9^{+0}_{-0.4}$	$16.7^{+0}_{-0.6}$	$16.7^{+0}_{-0.6}$	$36.1^{+1.8}_{-0}$	$17.7^{+0.8}_{-0}$

Conventional type EER CORES

Product code	Magnetic parameter								AL (nH)	
	C_1 (mm^{-1})	Le (mm)	Ae (mm^2)	Ve (mm^3)	Ac (mm^2)	Amin. (mm^2)	Aw (mm^2)	W ($\times 10^{-3}$ kg)	6H20	2H10
EER26/19B	1.07	47.5	44.4	2110	44.2	42.5L	79.4	11.0	1920(±25%)	—
EER28/18	0.598	47.2	78.9	3720	77.0	77.0C	62.0	19.5	3500(±25%)	—
EER28/28	0.728	62.9	86.3	5430	77.0	77.0C	113	27.8	3000(±25%)	—
EER28/34	0.868	74.3	85.6	6360	77.0	77.0C	148	32.4	2600(±25%)	—
EER29/20	0.695	51.2	73.7	3770	70.9	70.9C	80.5	18.9	3000(±25%)	—
EER29/32	0.947	72.0	76.0	5740	70.9	70.9C	145	28.2	2300(±25%)	—
EER34/26T	0.654	62.4	95.4	5960	91.6	91.6C	121	31.8	4000(±25%)	—
EER34/35	0.815	79.0	97.0	7670	91.6	91.6C	188	38.0	2800(±25%)	—
EER35/26	0.569	61.5	108	6620	100	100C	118	35.0	3700(±25%)	—
EER35/31	0.677	72.4	107	7740	100	100C	156	38.9	3600(±25%)	—
EER35/41	0.817	90.1	110	9930	100	100C	218	52.7	2800(±25%)	—
EER39/28	0.525	70.4	134	9410	129	129C	146	51.0	4200(±25%)	—
EER39/44	0.759	101	133	13500	129	129C	279	68.0	2700(±25%)	—
EER39/45	0.750	102	136	13900	129	129C	277	69.7	3100(±25%)	—
EER39/40	0.741	92.6	125	11600	123	123C	257	57.2	2800(±25%)	—
EER40/18	0.346	48.5	140	6780	139	130B	64.8	36.2	5170(±25%)	—
EER40/45	0.634	97.2	153	14900	139	139C	249	75.9	3600(±25%)	—
EER40/55	0.768	117	152	17800	139	139C	329	89.0	2800(±25%)	—
EER42/36	0.459	83.6	182	15200	181	181C	190	78.0	4500(±25%)	—
EER42/42	0.527	96.3	183	17600	181	179B	242	92.5	4400(±25%)	—
EER42/42D	0.423	98.5	233	23000	235	233B	225	113	5300(±25%)	—
EER42/42B	0.531	97.7	184	17940	184	182B	246	91.0	4000(±25%)	—
EER42/45A	0.523	99.9	191	19100	181	181C	243	95.0	4800(±25%)	—
EER42/45	0.483	97.3	202	19600	189	189C	219	95.0	4800(±25%)	—
EER42/49	0.469	109	233	25400	235	231B	282	129	5000(±25%)	—
EER42/43	0.573	99.0	173	17100	170	165B	261	87.7	4100(±25%)	—
EER44/45	0.592	104	175	18000	174	173B	304	90.8	4000(±25%)	—
EER48/41	0.392	99.5	254	25300	254	251B	297	126	5800(±25%)	—
EER49/48	0.481	111	231	25500	232	228L	305	139	5600(±25%)	—
EER49/54	0.526	123	234	28800	232	228L	366	152	4400(±25%)	—
EER49/55	0.534	125	234	29300	232	228L	376	152	4400(±25%)	—
EER49/62	0.556	134	242	32500	232	230L	449	167	4300(±25%)	—
EER49/49	0.542	115	211	24200	209	209C	375	128	4400(±25%)	—

Conventional type EE CORES

Features

①Customers are invited to select the most suitable products from a wide selection of shapes.

Applications

Switching regulators, choke coils, transformers for strobo use, pulse transformers, etc.

Designation

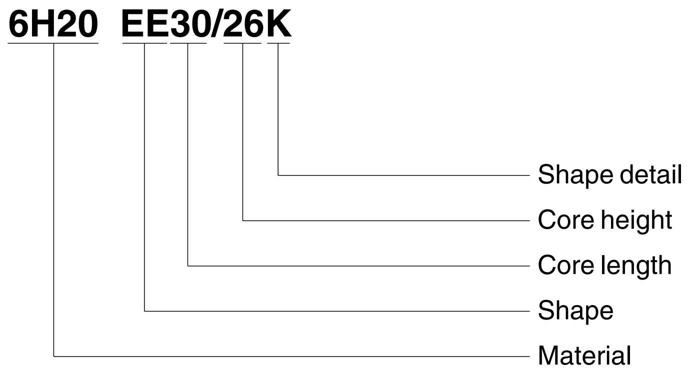

Conventional type EE CORES

Summary

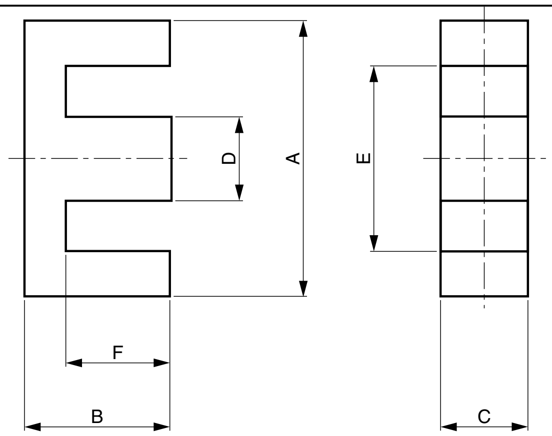

Product code	General standard		Dimensions (mm)					
	IEC	JIS	A	B	C	D	E	F
EE10/11		FEE10.2	10.2±0.2	5.5±0.1	4.75±0.15	2.45±0.15	7.8—0	$4.3^{+0.15}_{-0.075}$
EE12.5/15		FEE12.5	12.5±0.3	$7.6^{+0}_{-0.4}$	5.0±0.2	$2.6^{+0}_{-0.4}$	9.0—0	$4.9^{+0.4}_{-0}$
EE12.6/13	E13/4	FEE12.7A	$12.6^{+0.5}_{-0.4}$	$6.5^{+0}_{-0.2}$	$3.7^{+0}_{-0.3}$	$3.7^{+0}_{-0.3}$	$8.9^{+0.6}_{-0}$	$4.5^{+0.3}_{-0}$
EE13/11			13.0±0.3	$5.6^{+0.3}_{-0}$	6.5±0.2	3.8±0.15	9.8±0.3	$4.1^{+0.3}_{-0}$
EE13/12C			13.0±0.2	6.0±0.15	6.15±0.15	2.75±0.15	10.2±0.2	4.6±0.1
EE16/11			$16.0^{+0.7}_{-0.5}$	5.65±0.2	$7.4^{+0}_{-0.5}$	$4.7^{+0}_{-0.3}$	$11.3^{+0.8}_{-0}$	3.6±0.15
EE16/14K			16.0±0.3	$7.1^{+0.2}_{-0}$	$5.0^{+0}_{-0.4}$	$4.0^{+0}_{-0.4}$	12.0±0.3	$5.1^{+0.25}_{-0}$
EE16/14C		FEE16A	16.0±0.3	7.2±0.3	$5.0^{+0}_{-0.4}$	4.0±0.2	11.7—0	5.2±0.2
EE16/16			$16.0^{+0.7}_{-0.5}$	$8.2^{+0}_{-0.3}$	$4.7^{+0}_{-0.4}$	$4.7^{+0}_{-0.3}$	$11.3^{+0.6}_{-0}$	$5.7^{+0.4}_{-0}$
EE16/24		FEE16B	16.0±0.3	$12.0^{+0.4}_{-0}$	$5.0^{+0}_{-0.4}$	4.0±0.2	11.8—0	$10.0^{+0.4}_{-0}$
EE16/21			16.1±0.25	$10.5^{+0.4}_{-0}$	4.2±0.2	$4.4^{+0}_{-0.3}$	11.6—0	$8.0^{+0.4}_{-0}$
EE19/27		FEE19B	$19.0^{+0.4}_{-0.3}$	13.4±0.3	5.0±0.2	4.5±0.2	14.2—0	11.0±0.3
EE19/15			19.05±0.38	7.59±0.13	4.75±0.13	4.75±0.13	14.33±0.31	5.23±0.13
EE19/16K		FEE19A	19.1±0.3	$7.8^{+0.3}_{-0}$	$5.2^{+0}_{-0.4}$	$4.7^{+0}_{-0.3}$	14.2—0	$5.5^{+0.4}_{-0}$
EE20/20A	E20/6	FEE20.1	20.0±0.4	9.9±0.2	5.65±0.25	5.7±0.2	14.1—0	7.2±0.2
EE22/19		FEE22A	$22.0^{+0}_{-0.6}$	9.55±0.25	$6.0^{+0}_{-0.5}$	$6.0^{+0}_{-0.5}$	15.5—0	$5.3^{+0.4}_{-0}$
EE22/24C			$22.0^{+0}_{-0.6}$	11.9±0.25	$6.0^{+0}_{-0.5}$	$6.0^{+0}_{-0.5}$	15.5—0	$7.9^{+0.4}_{-0}$
EE22/29		FEE22B	22.0±0.5	$14.5^{+0.5}_{-0}$	$6.0^{+0}_{-0.5}$	$6.0^{+0}_{-0.5}$	16.0±0.5	$10.5^{+0.5}_{-0}$
EE24/31A			$24.5^{+0.4}_{-0.3}$	15.3±0.3	9.4±0.15	7.8±0.15	16.7—0	11.4±0.25
EE25/20			25.0±0.3	$10.0^{+0.3}_{-0}$	6.4±0.3	6.4±0.3	18.2—0	$6.5^{+0.3}_{-0}$
EE25/33			25.0±0.3	$16.3^{+0.5}_{-0}$	6.5±0.25	6.5±0.25	18.15—0	$13.0^{+0.4}_{-0}$
EE25/25B	E25/7	FEE25.1	25.05±0.75	12.55±0.25	7.2±0.3	7.25±0.25	17.5—0	8.95±0.25
EE25/19D			25.3±0.4	9.6±0.2	7.0±0.2	6.5±0.25	18.5—0	6.6±0.2
EE25/20B			25.3±0.4	9.95±0.2	6.6±0.25	6.4±0.2	19.0—0	6.75±0.15
EE25/23B			25.3±0.4	11.5±0.2	6.6±0.25	6.4±0.2	19.0—0	8.3±0.15
EE25/19Z		FEE25.4A	25.4±0.38	9.53±0.25	6.35±0.25	6.35±0.25	18.7—0	6.38±0.17
EE25/32Z		FEE25.4B	25.4±0.4	16.0±0.3	6.35±0.3	6.35±0.3	18.67—0	12.83±0.3
EE26/29A			26.0±0.3	$14.35^{+0.4}_{-0}$	8.0±0.15	7.3±0.2	18.6—0	10.7±0.15
EE26/33A			26.0±0.3	$16.35^{+0.4}_{-0}$	8.0±0.15	7.3±0.2	18.6—0	12.7±0.15
EE28/18			27.3±0.5	8.9±0.2	9.7±0.2	8.5±0.3	18.5—0	4.9±0.15
EE28/20			28.0±0.4	$10.0^{+0.25}_{-0}$	$11.0^{+0}_{-0.6}$	$7.5^{+0}_{-0.5}$	18.6—0	$6.0^{+0.25}_{-0}$
EE28/20B			28.0±0.5	$10.7^{+0.15}_{-0.1}$	12.0±0.3	7.2±0.3	18.6—0	$6.2^{+0.15}_{-0.1}$
EE28/25A			28.0±0.3	$12.5^{+0.35}_{-0.15}$	8.0±0.3	$8.0^{+0.1}_{-0.3}$	19.6—0	$8.5^{+0.25}_{-0.05}$

Conventional type EE CORES

Product code	Magnetic parameter								AL (nH)	
	C_1 (mm^{-1})	Le (mm)	Ae (mm^2)	Ve (mm^3)	Ac (mm^2)	Amin. (mm^2)	Aw (mm^2)	W ($\times 10^{-3}$ kg)	6H20	2H10
EE10/11	2.16	26.1	12.1	315	11.6	10.5L	24.0	1.4	850(±25%)	—
EE12.5/15	2.10	31.4	14.9	469	12.0	12.0C	35.2	2.3	900(±25%)	—
EE12.6/13	2.41	29.7	12.4	369	12.6	12.2L	26.3	1.9	800(±25%)	3500(±25%)
EE13/11	1.33	27.9	21.0	586	24.7	19.5B	25.5	3.1	1400(±25%)	—
EE13/12C	1.77	30.2	17.1	517	16.9	16.9C	34.3	2.5	1100(±25%)	—
EE16/11	0.848	28.0	33.0	924	32.5	29.3B	25.7	4.5	2200(±25%)	—
EE16/14K	1.87	35.2	18.9	663	18.2	18.2C	42.6	3.2	1100(±25%)	—
EE16/14C	1.83	35.1	19.2	674	19.2	19.2LBC	41.6	3.4	1100(±25%)	—
EE16/16	1.87	37.6	20.1	756	20.5	19.4B	41.6	3.6	1100(±25%)	—
EE16/24	2.87	55.1	19.2	1060	19.2	19.2LBC	81.6	5.3	800(±25%)	—
EE16/21	2.66	47.1	17.7	834	17.6	17.6LC	63.1	4.5	1500(±25%)	—
EE19/27	2.69	61.3	22.8	1400	22.5	22.5LC	110	7.0	850(±25%)	—
EE19/15	1.66	37.3	22.5	837	22.5	22.5LBC	50.1	4.2	1200(±25%)	—
EE19/16K	1.72	39.6	23.1	915	22.8	22.8C	55.7	4.6	1200(±25%)	—
EE20/20A	1.45	46.0	32.0	1490	32.2	31.6B	62.6	7.5	1550(±25%)	—
EE22/19	1.15	42.5	37.0	1570	33.1	33.1C	54.7	8.3	1850(±25%)	—
EE22/24C	1.46	52.4	35.9	1880	33.1	33.1C	80.6	9.7	1500(±25%)	—
EE22/29	1.73	63.4	36.0	2280	33.0	33.0C	108	11.6	1200(±25%)	—
EE24/31A	0.909	66.6	73.3	4880	73.3	70.5L	105	24.5	2550(±25%)	—
EE25/20	1.16	49.3	42.0	2070	40.8	40.8C	80.5	10.5	1600(±25%)	—
EE25/33	1.79	75.2	42.0	3160	42.2	41.6L	160	15.8	1300(±25%)	—
EE25/25B	1.11	57.7	51.7	2990	52.2	51.0L	95.8	15.0	2000(±25%)	—
EE25/19D	1.20	51.6	43.0	2232	45.5	42.0LB	84.5	10.6	1800(±25%)	—
EE25/20B	1.21	49.8	41.3	2060	42.2	39.6L	87.1	10.3	1800(±25%)	—
EE25/23B	1.37	56.0	41.0	2300	42.2	39.6L	107	11.5	1650(±25%)	—
EE25/19Z	1.20	48.1	40.2	1940	40.3	40.0B	81.0	10.3	1800(±25%)	9000($^{+35\%}_{-25\%}$)
EE25/32Z	1.84	74.0	40.3	2970	40.3	40.3LBC	163	14.8	1350(±25%)	—
EE26/29A	1.33	76.0	57.0	4330	58.4	56.0L	203	19.1	1800(±25%)	—
EE26/33A	1.48	84.0	56.9	4780	58.4	56.0L	241	21.3	1650(±25%)	—
EE28/18	0.535	42.9	80.2	3440	82.5	77.6B	51.0	17.2	4000(±25%)	—
EE28/20	0.559	48.2	86.2	4160	77.6	77.6C	72.0	23.0	4000(±25%)	—
EE28/20B	0.508	49.9	98.2	4910	86.4	86.4C	73.2	25.6	4500(±25%)	—
EE28/25A	0.931	59.0	63.4	3740	63.2	63.2C	104	19.1	2400(±25%)	—

Conventional type EE CORES

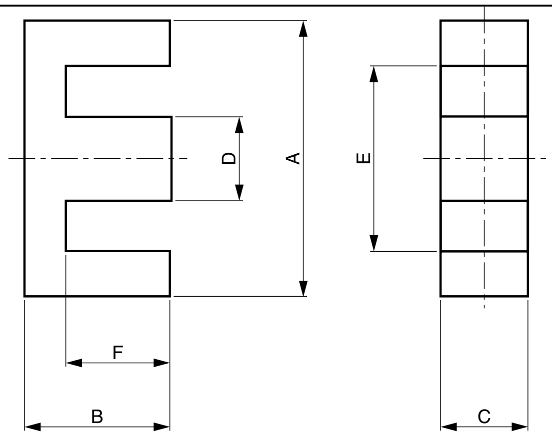

Product code	General standard		Dimensions (mm)					
	IEC	JIS	A	B	C	D	E	F
EE28/33		FEE28	28.0±0.4	$16.5^{+0.5}_{-0}$	$11.0^{+0}_{-0.6}$	$7.5^{+0}_{-0.5}$	18.6—0	$12.0^{+0.5}_{-0}$
EE28/28A			28.2±0.3	$14.0^{+0.4}_{-0}$	8.0±0.15	7.3±0.2	20.8—0	10.35±0.15
EE29/28			29.8±0.3	13.9±0.2	10.7±0.15	8.1±0.15	20.9—0	9.9±0.2
EE29/30MA			29.8±0.3	15.0	7.1±0.2	8.1±0.2	20.5—0	11.0±0.2
EE29/30M			29.8±0.5	15.0±0.2	$10.7^{+0.15}_{-0.3}$	8.1±0.2	20.5—0	11.0±0.2
EE30/26K		FEE30A	30.0±0.5	$13.0^{+0.3}_{-0}$	$11.0^{+0}_{-0.6}$	$11.0^{+0}_{-0.6}$	19.5—0	$8.0^{+0.3}_{-0}$
EE30/30A			30.0±0.5	14.9±0.25	6.9±0.3	6.9±0.2	19.5—0	10.15±0.2
EE30/31			$30.0^{+0.5}_{-0.2}$	15.6±0.2	7.5±0.2	10.5±0.2	20.0—0	10.6±0.15
EE30/42K		FEE30B	30.0±0.4	$21.0^{+0.5}_{-0}$	$11.0^{+0}_{-0.6}$	$11.0^{+0}_{-0.6}$	19.5—0	$16.0^{+0.5}_{-0}$
EE30/26B			30.1±0.3	13.13±0.12	10.69±0.3	10.69±0.27	20.0—0	8.13±0.12
EE31/26			30.5±0.5	13.1±0.15	9.4±0.3	9.4±0.3	21.6—0	$8.6^{+0.3}_{-0.1}$
EE32/32A	E32/9	FEE32.1	$32.0^{+0.9}_{-0.7}$	16.1±0.3	9.15±0.35	9.2±0.3	22.7—0	$11.6^{+0.3}_{-0.1}$
EE33/28A		FEE33A	33.0±0.7	14.1±0.25	12.7±0.3	9.7±0.3	$23.6^{+1.0}_{-0.25}$	9.6±0.25
EE33/33A			33.1±0.4	16.5±0.2	$9.0^{+0}_{-0.4}$	$9.0^{+0}_{-0.4}$	24.2—0	12.2±0.2
EE33/28B			33.2±0.5	14.15±0.15	12.7±0.3	9.8±0.3	23.7—0	9.65±0.15
EE34/28A			34.6±0.45	14.2±0.2	9.27±0.25	9.27±0.25	25.4—0	9.9±0.25
EE35/29A			34.93±0.5	14.43±0.25	9.53±0.25	9.53±0.25	25.04—0	9.68±0.25
EE35/35A			35.0±0.5	17.5±0.25	10.0±0.3	10.0±0.3	24.5—0	12.5±0.25
EE35/37			$35.0^{+0.7}_{-0.5}$	18.3±0.2	10.0±0.3	10.0±0.3	24.5—0	13.3±0.2
EE35/48		FEE35B	35.0±0.5	24.2±0.4	$10.3^{+0}_{-0.5}$	$10.3^{+0}_{-0.5}$	25.0±0.5	18.2±0.3
EE35/48C		FEE35C	$35.0^{+0.7}_{-0.5}$	24.2±0.4	11.7±0.3	10.0±0.3	24.5—0	18.2±0.3
EE40/34B			40.0±0.6	16.75±0.35	$12.0^{+0}_{-0.7}$	$12.0^{+0}_{-0.7}$	26.8—0	$10.55^{+0.2}_{-0}$
EE40/34A			40.0±0.5	$16.7^{+0.6}_{-0}$	$12.0^{+0}_{-0.7}$	$11.0^{+0}_{-0.6}$	27.4—0	$10.0^{+0.5}_{-0}$
EE40/34K		FEE40A	40.0±0.5	$16.7^{+0.6}_{-0}$	$11.0^{+0}_{-0.6}$	$11.0^{+0}_{-0.6}$	27.4—0	$10.0^{+0.5}_{-0}$
EE40/54K		FEE40B	40.0±0.5	$27.0^{+0.5}_{-0}$	$12.0^{+0}_{-0.7}$	$12.0^{+0}_{-0.7}$	26.8—0	$20.0^{+0.5}_{-0}$
EE40/35A			40.8±0.55	16.6±0.25	12.4±0.3	12.5±0.3	28.6—0	10.7±0.28
EE41/33			41.28±0.8	16.76±0.13	12.7±0.25	12.7±0.25	28.01—0	10.54±0.13
EE42/42-15W	E42/15	FEE42.2A	$42.0^{+1.0}_{-0.7}$	$21.2^{+0}_{-0.4}$	$15.2^{+0}_{-0.5}$	$12.2^{+0}_{-0.5}$	$29.5^{+1.2}_{-0}$	$14.8^{+0.7}_{-0}$
EE42/42-20W	E42/20	FEE42.2B	$42.0^{+1.0}_{-0.7}$	$21.2^{+0}_{-0.4}$	$20.0^{+0}_{-0.8}$	$12.2^{+0}_{-0.5}$	$29.5^{+1.2}_{-0}$	$14.8^{+0.7}_{-0}$
EE47/39A			47.1±0.5	19.6±0.25	15.6±0.3	15.6±0.3	31.7—0	12.4±0.3
EE49/48			49.07±0.64	23.77±0.25	15.62±0.43	15.62±0.25	31.37—0	$15.24^{+0.3}_{-0.15}$
EE50/66		FEE50B	50.0±0.7	$33.0^{+0.7}_{-0}$	$15.0^{+0}_{-0.8}$	$15.0^{+0}_{-0.8}$	33.5—0	$24.5^{+0.7}_{-0}$
EE55/55A	E55/21	FEE55.2A	$55.0^{+1.2}_{-0.9}$	$27.8^{+0}_{-0.6}$	$21.0^{+0}_{-0.6}$	$17.2^{+0}_{-0.5}$	$37.5^{+1.2}_{-0}$	$18.5^{+0.8}_{-0}$
EE55/55B	E55/25	FEE55.2B	$55.0^{+1.2}_{-0.9}$	$27.8^{+0}_{-0.6}$	$25.0^{+0}_{-0.8}$	$17.2^{+0}_{-0.5}$	$37.5^{+1.2}_{-0}$	$18.5^{+0.8}_{-0}$
EE56/47A			56.6±0.55	23.6±0.25	18.7±0.3	18.7±0.3	38.1—0	14.8±0.3
EE80/76			80.0±1.0	38.1±0.4	19.8±0.4	19.8±0.4	62.2	28.2±0.3

Conventional type EE CORES

Product code	Magnetic parameter								AL (nH)	
	C_1 (mm^{-1})	Le (mm)	Ae (mm^2)	Ve (mm^3)	Ac (mm^2)	Amin. (mm^2)	Aw (mm^2)	W ($\times10^{-3}$ kg)	6H20	2H10
EE28/33	0.844	73.6	87.2	6420	77.0	77.0C	145	32.1	2800(±25%)	—
EE28/28A	1.48	84.2	56.9	4790	58.4	56.0L	144	19.0	1650(±25%)	—
EE29/28	0.766	65.9	86.0	5670	86.7	85.6LB	136	28.6	2900(±25%)	—
EE29/30MA	1.07	92.1	86.0	7960	86.7	85.6LB	150	30.0	2300(±25%)	—
EE29/30M	1.61	92.1	57.3	5280	57.5	56.8LB	151	26.4	1500(±25%)	—
EE30/26K	0.528	57.9	110	6360	114	107L	75.8	32.2	4200(±25%)	—
EE30/30A	1.15	66.1	57.3	3790	47.6	47.6C	134	20.7	1900(±25%)	—
EE30/31	0.907	68.1	75.1	5110	78.8	72.0L	107	23.7	2600(±25%)	—
EE30/42K	0.823	90.2	110	9920	114	107LB	152	49.8	3000(±25%)	—
EE30/26B	0.621	61.3	97.6	5980	114	107LB	76.4	32.0	4200(±25%)	—
EE31/26	0.723	61.0	84.4	5150	88.4	79.9L	110	25.8	3150(±25%)	—
EE32/32A	0.886	74.8	84.4	6310	84.2	78.7L	167	31.0	2700(±25%)	—
EE33/28A	0.615	67.7	110	7520	123	114B	129	40.0	3800(±25%)	—
EE33/33A	1.02	78.1	76.3	5960	77.4	75.7LB	299	29.5	2600(±25%)	—
EE33/28B	0.561	65.6	117	7680	123	114LB	138	39.0	4150(±25%)	—
EE34/28A	0.852	69.9	82.1	5750	85.9	79.7B	164	29.5	2500(±25%)	—
EE35/29A	0.768	69.6	90.6	6300	90.8	90.5LB	154	32.2	3400(±25%)	—
EE35/35A	0.807	80.7	100	8070	100	100LBC	188	40.6	3000(±25%)	—
EE35/37	0.839	83.9	100	8390	100	100LBC	200	42.5	2600(±25%)	—
EE35/48	1.01	105	104	10800	100	100LC	273	54.0	2500(±25%)	—
EE35/48C	0.863	105	121	12700	117	117LC	273	63.5	2900(±25%)	—
EE40/34B	0.544	77.5	142	11000	137	137C	167	52.0	4200(±25%)	—
EE40/34A	0.557	77.4	139	10800	125	125C	177	56.4	4500(±25%)	—
EE40/34K	0.608	77.4	127	9860	114	114C	178	52.0	3800(±25%)	—
EE40/54K	0.808	117	145	17000	137	137C	323	85.0	3150(±25%)	—
EE40/35A	0.526	78.1	149	11600	155	145L	178	58.8	4250(±25%)	—
EE41/33	0.483	77.3	160	12400	161	158LB	169	63.0	4950(±25%)	—
EE42/42-15W	0.542	97.8	180	17600	180	180BC	276	87.0	4400(±25%)	—
EE42/42-20W	0.415	97.8	236	23000	235	235BC	276	118	5600(±25%)	—
EE47/39A	0.385	89.5	232	20800	243	223B	206	106	6000(±25%)	—
EE49/48	0.428	110	257	28200	245	245C	250	134	5900(±25%)	—
EE50/66	0.649	144	222	32000	213	213C	506	160	4000(±25%)	—
EE55/55A	0.350	124	353	43700	352	352C	400	218	6700(±25%)	—
EE55/55B	0.295	124	420	52000	417	417C	400	260	8650(±25%)	—
EE56/47A	0.316	107	345	36700	352	329B	292	189	6500(±25%)	—
EE80/76	0.491	185	377	69800	392	352L	1480	350	4800(±25%)	—

Conventional type EI CORES

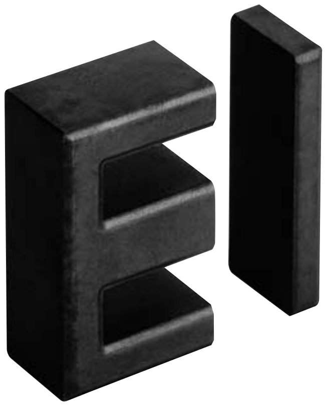

Features

①Wide selection of the shapes for customer's choice.

Applications

Transformers for switching power supply, Choke coil, Inverter, Converter, etc.

Designation

6H20 EI16/14K

- 6H20 — Material
- EI — Shape
- 16 — Core length
- 14 — Core height
- K — Shape detail

Conventional type EI CORES

Summary

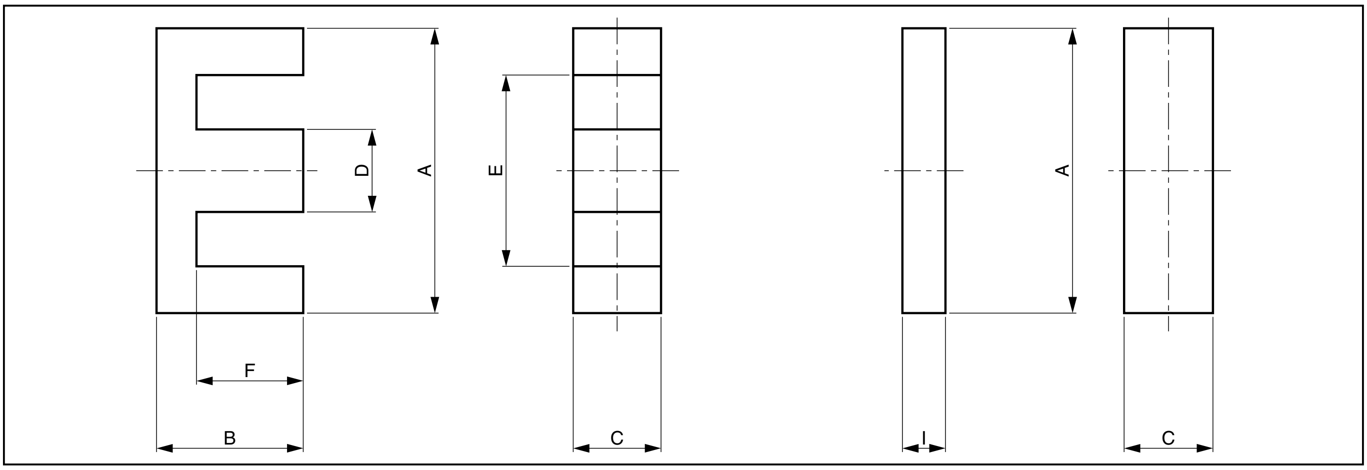

Product code	General standard		Dimensions (mm)						
	IEC	JIS	A	B	C	D	E	F	I
EI12.5/09		FEI12.5	12.5±0.3	$7.6^{+0}_{-0.4}$	5.0±0.2	$2.6^{+0}_{-0.4}$	9.0—0	$4.9^{+0.4}_{-0}$	1.5±0.15
EI16/14K		FEI16	16.0±0.3	$12.0^{+0.4}_{-0}$	$5.0^{+0}_{-0.4}$	4.0±0.2	11.8—0	$10.0^{+0.4}_{-0}$	2.0±0.2
EI19/16		FEI19	$19.0^{+0.4}_{-0.3}$	13.4±0.3	5.0±0.2	4.5±0.2	14.2—0	11.0±0.3	2.4±0.2
EI22/18		FEI22	22.0±0.5	$14.5^{+0.5}_{-0}$	$6.0^{+0}_{-0.5}$	$6.0^{+0}_{-0.5}$	16.0±0.5	$10.5^{+0.5}_{-0}$	4.0±0.2
EI25/19			25.0±0.3	$16.3^{+0.5}_{-0}$	6.5±0.25	6.5±0.25	18.15—0	$13.0^{+0.4}_{-0}$	3.0±0.2
EI25/19Z		FEI25.4	$25.4^{+0.5}_{-0.4}$	16.0±0.3	6.35±0.3	6.35±0.3	18.6—0	12.9±0.3	3.2±0.2
EI28/20		FEI28	28.0±0.4	$16.5^{+0.5}_{-0}$	$11.0^{+0}_{-0.6}$	$7.5^{+0}_{-0.5}$	18.6—0	$12.0^{+0.5}_{-0}$	3.5±0.2
EI30/26K		FEI30	30.0±0.4	$21.0^{+0.5}_{-0}$	$11.0^{+0}_{-0.6}$	$11.0^{+0}_{-0.6}$	19.5—0	$16.0^{+0.5}_{-0}$	5.5±0.2
EI35/29		FEI35A	35.0±0.5	24.2±0.4	$10.3^{+0}_{-0.5}$	$10.3^{+0}_{-0.5}$	25.0±0.5	18.2±0.3	5.0±0.2
EI40/35K		FEI40	40.2±0.5	$27.0^{+0.5}_{-0}$	$12.0^{+0}_{-0.7}$	$12.0^{+0}_{-0.7}$	27.3—0	$20.0^{+0.5}_{-0}$	7.5±0.3
EI50/42K		FEI50	50.0±0.7	$33.0^{+0.7}_{-}$	$15.0^{+0}_{-0.8}$	$15.0^{+0}_{-0.8}$	33.5—0	$24.5^{+0.7}_{-0}$	9.0±0.3

Product code	Magnetic parameter								AL (nH)
	C_1 (mm^{-1})	Le (mm)	Ae (mm^2)	Ve (mm^3)	Ac (mm^2)	Amin. (mm^2)	Aw (mm^2)	W (510^{-3} kg)	6H20
EI12.5/09	1.42	21.6	15.0	324	12.0	12.0C	35.2	1.9	1000(±25%)
EI16/14K	1.81	34.6	19.0	657	19.2	18.7L	82.6	3.3	1000(±25%)
EI19/16	1.71	39.3	23.0	903	22.5	22.5LC	55.0	4.5	1100(±25%)
EI22/18	1.11	41.9	37.0	1550	33.1	33.1C	110	8.3	1700(±25%)
EI25/19	1.17	48.5	42.0	2040	42.3	41.6L	160	10.1	1750(±25%)
EI25/19Z	1.20	48.3	40.2	1940	40.3	39.4B	81.7	9.7	1700(±25%)
EI28/20	0.569	48.4	84.0	4070	77.6	77.6C	144	22.0	3400(±25%)
EI30/26K	0.524	58.1	111	6450	114	107LB	151	32.3	4000(±25%)
EI35/29	0.660	67.3	102	6870	101	101LC	272	36.3	3000(±25%)
EI40/35K	0.522	76.8	148	11400	136	136C	323	59.2	4200(±25%)
EI50/42K	0.412	94.7	230	21800	213	213C	497	114	5000(±25%)

Conventional type　RM CORES

Features

①Products complying with IEC standard.
②A high-density mounting of elements on the substrate is possible.

Applications

Transformers for switching power supply, Choke coil, Filters, Inductors, etc.

Designation

6H20 RM6 G

- G — Core type No.
- RM6 — Shape
- 6H20 — Material

Conventional type RM CORES

Summary

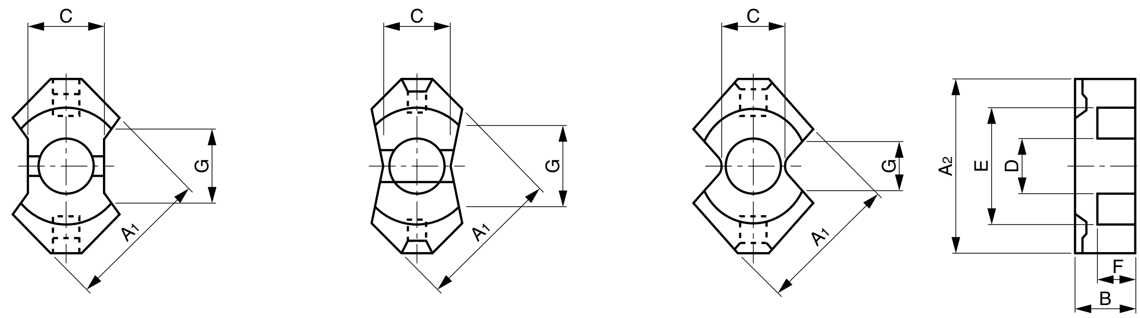

Type 1 Type 2 Type 3

Product code	Type	General standard		Dimensions (mm)							
		IEC	JIS	A_1	A_2	B	C	D	E	F	G
RM5G	1	RM5-ϕ	RM5-J	12.3 $^{+0}_{-0.4}$	14.9 $^{+0}_{-0.8}$	5.25 $^{+0}_{-0.1}$	6.8 $^{+0}_{-0.4}$	4.9 $^{+0}_{-0.2}$	10.2 $^{+0.4}_{-0}$	3.15 $^{+0.2}_{-0}$	6.0–0
RM6G	2	RM6-S-ϕ	RM6-S-J	14.7 $^{+0}_{-0.6}$	17.9 $^{+0}_{-0.6}$	6.25 $^{+0}_{-0.1}$	8.2 $^{+0}_{-0.4}$	6.4 $^{+0}_{-0.2}$	12.4 $^{+0.5}_{-0}$	4.0 $^{+0.2}_{-0}$	8.4–0
R6G	3	RM6-R-0	RM6-R	14.7 $^{+0}_{-0.5}$	17.7 $^{+0}_{-0.7}$	6.25 $^{+0}_{-0.1}$	—	6.2 $^{+0.2}_{-0}$	12.4 $^{+0.5}_{-0}$	4.0 $^{+0.2}_{-0}$	—
RM8G	1	RM8-ϕ	RM8-J	19.7 $^{+0}_{-0.7}$	23.2 $^{+0}_{-0.9}$	8.25 $^{+0}_{-0.1}$	11.0 $^{+0}_{-0.4}$	8.55 $^{+0}_{-0.3}$	17.0 $^{+0.6}_{-0}$	5.4 $^{+0.2}_{-0}$	10.5–0
RM10G	1	RM10-ϕ	RM10-J	24.7 $^{+0}_{-1.1}$	28.5 $^{+0}_{-1.3}$	9.35 $^{+0}_{-0.1}$	13.5 $^{+0}_{-0.5}$	10.9 $^{+0}_{-0.4}$	21.2 $^{+0.9}_{-0}$	6.2 $^{+0.3}_{-0}$	11.3–0
RM12GA	1			29.8 $^{+0}_{-1.2}$	37.6 $^{+0}_{-1.5}$	11.8 $^{+0}_{-0.1}$	—	12.8 $^{+0}_{-0.4}$	24.9 $^{+1.1}_{-0}$	8.4 $^{+0.3}_{-0}$	12.9–0
RM12G	1	RM12-ϕ	RM12-J	29.8 $^{+0}_{-1.2}$	37.6 $^{+0}_{-1.5}$	12.3 $^{+0}_{-0.1}$	—	12.8 $^{+0}_{-0.4}$	24.9 $^{+1.1}_{-0}$	8.4 $^{+0.3}_{-0}$	12.9–0

Product code	Magnetic parameter								AL (nH)		
	C_1 (mm^{-1})	Le (mm)	Ae (mm^2)	Ve (mm^3)	Ac (mm^2)	Amin. (mm^2)	Aw (mm^2)	W ($\times 10^{-3}$ kg)	6H20	2H07	2H10
RM5G	0.938	22.3	23.8	530	18.1	18.1C	18.2	3.2	2000($^{+30\%}_{-20\%}$)	3500(±30%)	6700($^{+40\%}_{-30\%}$)
RM6G	0.799	28.5	35.7	1020	31.2	30.7B	26.0	5.3	2400($^{+30\%}_{-20\%}$)	4300(±30%)	8600($^{+40\%}_{-30\%}$)
R6G	0.800	25.6	32.0	820	23.4	23.4C	26.0	5.2	—	—	8600($^{+40\%}_{-30\%}$)
RM8G	0.590	38.0	64.0	2400	55.4	55.0B	52.2	12.2	3300($^{+30\%}_{-20\%}$)	6000(±30%)	12500($^{+40\%}_{-30\%}$)
RM10G	0.453	45.0	99.0	4500	90.0	90.0C	69.5	22.0	4200($^{+30\%}_{-20\%}$)	—	—
RM12GA	0.374	56.0	150	8400	125	125C	113	44.1	5300($^{+30\%}_{-20\%}$)	—	—
RM12G	0.374	56.0	150	8400	125	125C	113	44.1	5300($^{+30\%}_{-20\%}$)	—	—

Conventional type EP CORES

Features

①Suitable for the designing of small-sized transformers.

②A high magnetic shield performance.

Applications

Wide band transformers, switching regulators, coils, etc.

Designation

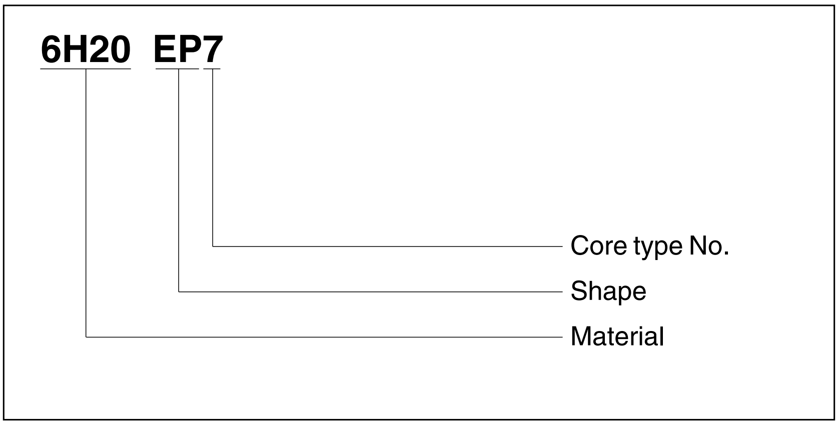

Conventional type EP CORES

Summary

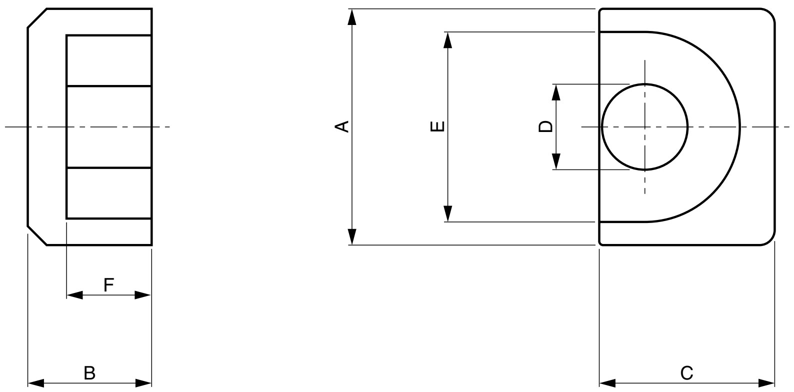

Product code	General standard		Dimensions (mm)					
	IEC	JIS	A	B	C	D	E	F
EP7	EP7	EP7	9.2±0.2	$3.75^{+0}_{-0.1}$	$6.5^{+0}_{-0.3}$	$3.4^{+0}_{-0.2}$	7.4±0.2	$2.5^{+0.2}_{-0}$
EP10	EP10	EP10	11.5±0.3	$5.2^{+0}_{-0.2}$	$7.85^{+0}_{-0.4}$	$3.45^{+0}_{-0.3}$	9.4±0.2	$3.6^{+0.2}_{-0}$
EP13	EP13	EP13	12.5±0.3	$6.5^{+0}_{-0.15}$	$9.0^{+0}_{-0.4}$	$4.5^{+0}_{-0.3}$	10.0±0.3	$4.5^{+0.2}_{-0}$
EP13B			12.5±0.4	6.5±0.15	$9.0^{+0}_{-0.4}$	$4.5^{+0}_{-0.4}$	9.9−0	$4.7^{+0.2}_{-0.1}$
EP17	EP17	EP17	18.0±0.4	$8.5^{+0}_{-0.3}$	$11.25^{+0}_{-0.5}$	$5.85^{+0}_{-0.35}$	12.0±0.4	$5.5^{+0.3}_{-0}$
EP20	EP20	EP20	24.0±0.5	$10.8^{+0}_{-0.2}$	$15.3^{+0}_{-0.7}$	$9.0^{+0}_{-0.5}$	16.5±0.4	$7.0^{+0.3}_{-0}$

Product code	Magnetic parameter								AL (nH)			
	C_1 (mm^{-1})	Le (mm)	Ae (mm^2)	Ve (mm^3)	Ac (mm^2)	Amin. (mm^2)	Aw (mm^2)	W ($\times 10^{-3}$ kg)	6H20	2H07	2H10	2H15
EP7	1.52	15.7	10.3	163	8.55	8.55C	10.7	1.3	1100($^{+30\%}_{-20\%}$)	2000(±30%)	5200($^{+40\%}_{-30\%}$)	—
EP10	1.70	19.2	11.3	218	8.55	8.55C	22.6	2.8	1100($^{+30\%}_{-20\%}$)	2000(±30%)	4800($^{+40\%}_{-30\%}$)	—
EP13	1.24	24.2	19.6	476	14.9	14.9C	26.0	4.8	1600($^{+30\%}_{-20\%}$)	3000(±30%)	7000($^{+40\%}_{-30\%}$)	8500($^{+40\%}_{-30\%}$)
EP13B	1.24	24.2	19.6	476	14.9	14.9C	26.0	4.8	—	—	—	7800(−0%)
EP17	0.840	28.5	33.9	964	25.3	25.3C	35.7	11.8	2400($^{+30\%}_{-20\%}$)	—	—	—
EP20	0.508	39.8	78.3	3110	60.1	60.1C	55.4	29.2	4000($^{+30\%}_{-20\%}$)	—	—	—

Conventional type PM CORES

Features

①8 basic shapes available.
②Suitable for high-density mounting.

Applications

Switching regulators, choke coils, etc.

Designation

6H20 PM3230

- 30 — Core height
- 32 — Core length
- PM — Shape
- 6H20 — Material

Conventional type PM CORES

Summary

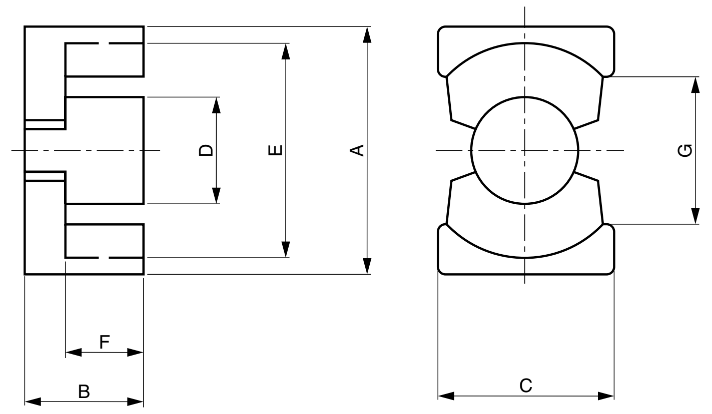

Product code	Dimensions (mm)						
	A	B	C	D	E	F	G
PM2010	20.5±0.4	4.95±0.05	14.0±0.4	$9.0^{+0}_{-0.4}$	18.0±0.4	2.03±0.13	12.0—0
PM2016	20.5±0.4	$8.2^{+0}_{-0.2}$	14.0±0.4	$9.0^{+0}_{-0.4}$	18.0±0.4	$5.0^{+0.5}_{-0}$	12.0—0
PM2020	20.5±0.4	$10.2^{+0}_{-0.2}$	14.0±0.4	$9.0^{+0}_{-0.4}$	18.0±0.4	$7.0^{+0.5}_{-0}$	12.0—0
PM2619	26.5±0.45	$9.7^{+0}_{-0.25}$	19.0±0.45	$12.2^{+0}_{-0.4}$	22.5±0.45	$5.1^{+0.5}_{-0}$	15.5—0
PM2620	26.5±0.45	$10.2^{+0}_{-0.25}$	19.0±0.45	$12.2^{+0}_{-0.4}$	22.5±0.45	$5.6^{+0.5}_{-0}$	15.5—0
PM2625	26.5±0.5	$12.5^{+0}_{-0.25}$	19.0±0.5	$12.2^{+0}_{-0.4}$	22.5±0.5	$7.9^{+0.5}_{-0}$	15.5—0
PM3220	32.0±0.5	$10.4^{+0}_{-0.25}$	22.0±0.5	$13.7^{+0}_{-0.5}$	27.5±0.5	$5.6^{+0.5}_{-0}$	19.0—0
PM3230	32.0±0.5	$15.3^{+0}_{-0.25}$	22.0±0.5	$13.7^{+0}_{-0.5}$	27.5±0.5	$10.5^{+0.5}_{-0}$	19.0—0
PM3530	$35.0^{+0.7}_{-0.5}$	$15.0^{+0}_{-0.25}$	26.0±0.5	$14.6^{+0}_{-0.5}$	32.0±0.5	$9.85^{+0.5}_{-0}$	23.5—0
PM3535	$35.0^{+0.7}_{-0.5}$	$17.5^{+0}_{-0.25}$	26.0±0.5	$14.6^{+0}_{-0.5}$	32.0±0.5	$12.35^{+0.5}_{-0}$	23.5—0

Product code	Magnetic parameter								AL (nH)	
	C_1 (mm^{-1})	Le (mm)	Ae (mm^2)	Ve (mm^3)	Ac (mm^2)	Amin. (mm^2)	Aw (mm^2)	W ($\times 10^{-3}$ kg)	6H20	7H10
PM2010	0.405	25.0	61.7	1540	60.8	60.8C	18.7	9.0	4200(±25%)	—
PM2016	0.605	37.4	62.0	2310	60.8	60.8C	47.4	13.0	3450(±25%)	—
PM2020	0.738	45.4	62.0	2790	60.8	60.8C	65.8	15.0	2900(±25%)	2100(±25%)
PM2619	0.366	43.5	119	5180	113	113C	56.2	29.8	5300(±25%)	—
PM2620	0.391	46.3	119	5490	113	113C	60.4	31.0	5500(±25%)	4050(±25%)
PM2625	0.472	55.5	118	6530	113	113C	84.5	34.7	4650(±25%)	—
PM3220	0.326	55.5	170	9420	142	142C	80.8	41.2	6750(±25%)	—
PM3230	0.464	74.6	161	12000	142	142C	150	56.6	4900(±25%)	—
PM3530	0.397	77.9	196	15300	162	162C	178	62.6	5000(±25%)	4000(±25%)
PM3535	0.448	87.9	196	17300	162	162C	221	71.4	5000(±25%)	3700(±25%)

Conventional type FR CORES

Features

①Customers are invited to select the most suitable products from a wide selection of shapes.

Applications

Line filters, pulse transformers, choke coils, various coils, etc.

Designation

2H06 FR10/6/4

- 4 — Core height
- 6 — Core inside diameter
- 10 — Core outside diameter
- FR — Shape
- 2H06 — Material

Conventional type FR CORES

Summary

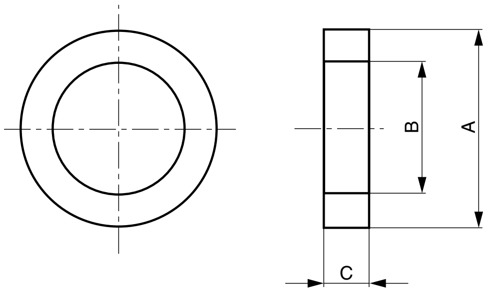

Product code	General standard		Dimensions (mm)			Magnetic parameter					AL (nH)			
	IEC	JIS	A	B	C	C_1 (mm^{-1})	Le (mm)	Ae (mm^2)	Ve (mm^3)	W ($\times 10^{-3}$ kg)	2H06	2H07	2H10	2H15
FR4/2.2/2.7			4.0±0.2	2.2±0.2	2.7±0.2	4.20	9.18	2.18	20.1	0.11	—	—	3000(±30%)	4500(±30%)
FR5.9/3.1/3.2			5.9±0.2	3.1±0.2	3.2±0.2	3.07	13.2	4.15	54.9	0.30	—	2800(±25%)	—	—
FR9.5/4.8/4.8			9.53±0.25	4.75±0.25	4.78±0.25	1.92	20.7	10.8	224	1.1	—	—	6600(±30%)	9900(±30%)
FR10/6/4	R10		10.0±0.3	6.0±0.3	4.0±0.2	3.07	24.0	7.80	187	1.0	$2500(^{+25\%}_{-40\%})$	2800(±25%)	4000(±30%)	—
FR11/5/3			11.0±0.3	5.0±0.2	3.0±0.2	2.67	22.7	8.54	194	1.1	2400(±25%)	3300(±25%)	4500(±30%)	—
FR12/6/4	FOR12	FOR12	12.0±0.4	6.0±0.3	4.0±0.3	2.26	26.1	11.5	301	1.5	$3500(^{+25\%}_{-40\%})$	3750(±25%)	5300(±30%)	—
FR12.5/8/8			12.5±0.3	8.0±0.3	8.0±0.3	1.76	31.2	17.7	552	2.8	$2800(^{+100\%}_{-0\%})$	4700(±25%)	—	—
FR12.7/8/6	T12.7		12.7±0.3	7.9±0.3	6.35±0.3	2.10	31.2	14.9	465	2.3	3000(±25%)	4200(±30%)	5500(±30%)	—
FR13/7/5			13.0±0.4	7.0±0.3	5.0±0.3	2.05	29.5	14.4	423	2.1	3200(±25%)	4400(±25%)	5900(±30%)	—
FR14/7.5/7			13.9±0.25	$7.57^{+0.3}_{-0.12}$	6.95±0.15	1.52	31.9	21.1	673	3.8	$4250(^{+30\%}_{-15\%})$	—	—	—
FR14/7/4	FOR14	FOR14	14.0±0.3	7.0±0.2	4.0±0.2	2.27	30.5	13.5	410	2.0	3000(±25%)	4100(±25%)	5000(±30%)	—
FR14/7/7			14.0±0.3	7.0±0.2	7.0±0.2	1.29	30.5	23.5	717	3.9	4625(−0%)	—	—	—
FR16/10/7			16.0±0.3	10.0±0.3	7.0±0.3	1.90	38.9	20.5	857	4.0	$2800(^{+40\%}_{-20\%})$	4800(±25%)	6400(±25%)	—
FR16/10/8	FOR16	FOR16	16.0±0.3	10.0±0.3	8.0±0.3	1.67	39.4	23.6	928	4.6	$3500(^{+25\%}_{-40\%})$	5600(±25%)	7500(±30%)	—
FR19/10/10	FOR19	FOR19	18.45±0.3	9.75±0.3	10.25±0.3	1.02	41.4	42.1	1740	9.2	6900(±25%)	9400(±30%)	12600(±30%)	—
FR20/12/4			19.95±0.3	12.05±0.3	4.15±0.3	3.00	48.1	16.0	770	3.9	$2100(^{+40\%}_{-20\%})$	$3000(^{+40\%}_{-20\%})$	—	—
FR20/12/8			19.95±0.3	12.05±0.3	8.0±0.3	1.55	48.2	30.9	1490	7.6	4500(±25%)	5600(±25%)	8100(±25%)	—
FR22/14/8			22.0±0.5	14.0±0.4	8.0±0.3	1.74	83.4	48.0	4000	8.7	2650(−0%)	5300(±25%)	7100(±30%)	—
FR22/14/10	FOR22	FOR22	22.0±0.3	14.0±0.3	10.0±0.3	1.41	54.7	38.8	2120	11.1	4900(±25%)	$6700(^{+40\%}_{-25\%})$	8900(±30%)	—
FR22/14/12.7			$22.0^{+0.25}_{-0.4}$	14.0±0.25	12.7±0.25	1.10	54.7	49.9	2730	14.3	$6250(^{+30\%}_{-15\%})$	—	—	—
FR25/15/10	R25		25.0±0.5	15.0±0.5	10.0±0.5	1.23	60.2	48.9	2940	15.0	5500(±25%)	7500(±25%)	10000(±30%)	—
FR25/15/12	FOR25	FOR25	25.0±0.5	15.0±0.5	12.0±0.3	1.03	60.2	58.7	3530	18.0	6500(±30%)	9000(±25%)	12000(±25%)	—
FR29/16/12			29.0±0.5	16.0±0.5	12.0±0.5	0.880	66.7	75.7	5050	26.5	7800(±25%)	—	—	—
FR31/20/10			$31.0^{+0}_{-0.8}$	$20.0^{+0.5}_{-0}$	$10.0^{+0}_{-0.6}$	1.63	77.7	47.5	3690	18.5	4400(±30%)	5900(±30%)	—	—
FR31/20/16			$31.0^{+0}_{-0.8}$	$20.0^{+0.5}_{-0}$	16.0±0.3	0.953	77.7	81.5	6330	31.7	$7000(^{+40\%}_{-20\%})$	$9900(^{+40\%}_{-25\%})$	—	—
FR38/19/13	FOR38	FOR38	38.0±0.7	19.0±0.5	13.0±0.4	0.697	82.7	119	9820	53.1	9300(±25%)	8600(−0%)	—	—
FR38/19/6	T38.1		38.0±0.7	19.0±0.5	6.35±0.35	1.43	82.7	57.8	4780	25.9	4400(±25%)	6000(±25%)	—	—
FR40/20/12			$40.0^{+0}_{-1.0}$	$20.0^{+0.5}_{-0}$	$12.0^{+0.6}_{-0}$	0.809	93.9	116	9780	53.3	$8000(^{+40\%}_{-20\%})$	11500(±25%)	—	—
FR50/25/10			$50.0^{+0}_{-1.2}$	$25.0^{+0.6}_{-0}$	$10.0^{+0.6}_{-0}$	0.959	117	122	14300	69.9	$6600(^{+40\%}_{-20\%})$	9900(±25%)	—	—
FR102/65/20			102±1.5	65.0±1.0	10.0±0.5	1.40	254	181	46000	233	—	$3540(^{+50\%}_{-10\%})$	—	—

Conventional type　FUR CORES

Features

①Most suitable for the designing of high inductance transformer in small size.

②Customers are invited to select the most suitable product from three shapes.

Applications

Line filters

Designation

2H07 FUR 3535

- 2H07 — Material
- FUR — Shape
- 35 — Core length
- 35 — Core height

Conventional type FUR CORES

Summary

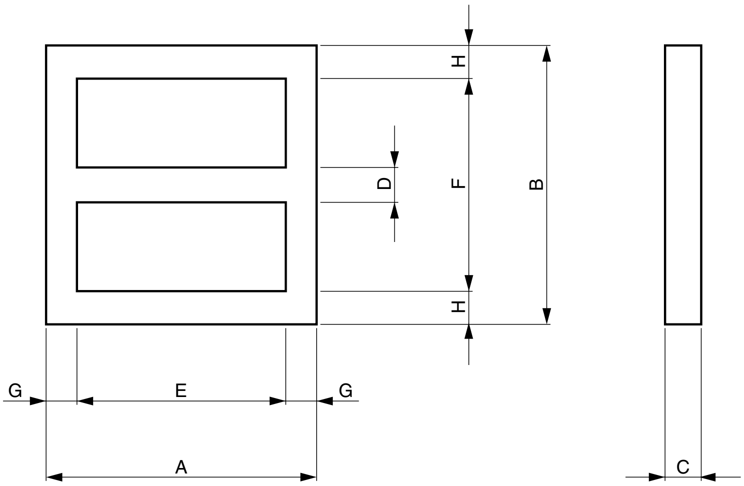

Product code	Dimensions (mm)							
	A	B	C	D	E	F	G	H
FUR2424	$24.0^{+0.7}_{-0.3}$	$24.0^{+0.7}_{-0.3}$	4.0±0.3	4.0±0.2	19.0—0	19.0—0	2.4±0.15	2.4±0.15
FUR2828	$28.2^{+0.8}_{-0.3}$	$28.2^{+0.8}_{-0.3}$	5.0±0.3	5.0±0.2	22.2—0	22.2—0	2.9±0.15	2.9±0.15
FUR3535	$35.0^{+0.9}_{-0.3}$	$35.0^{+0.9}_{-0.3}$	7.5±0.3	7.5±0.25	26.8—0	26.8—0	4.0±0.2	4.0±0.2

Product code	Magnetic parameter								AL (nH)	
	C_1 (mm^{-1})	Le (mm)	Ae (mm^2)	Ve (mm^3)	Ac (mm^2)	Amin. (mm^2)	Aw (mm^2)	W ($\times10^{-3}$ kg)	2H07	2H10
FUR2424	3.44	60.3	17.5	1050	16.0	16.0C	149	5.6	2600($^{+40\%}_{-25\%}$)	3600($^{+40\%}_{-25\%}$)
FUR2828	2.70	70.0	27.0	1890	25.0	25.0C	200	10.2	3550($^{+40\%}_{-25\%}$)	4690($^{+40\%}_{-25\%}$)
FUR3535	1.46	85.2	58.3	4960	56.3	56.3C	271	25.8	6000($^{+40\%}_{-25\%}$)	—

Conventional type FU CORES

Features

①Wide selection of the shapes for customer's choice.

Applications

Line filters, etc.

Designation

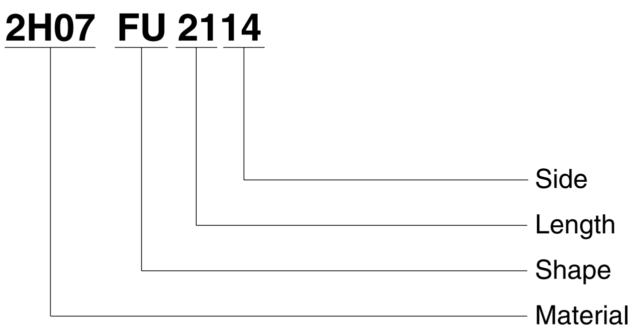

Conventional type FU CORES

Summary

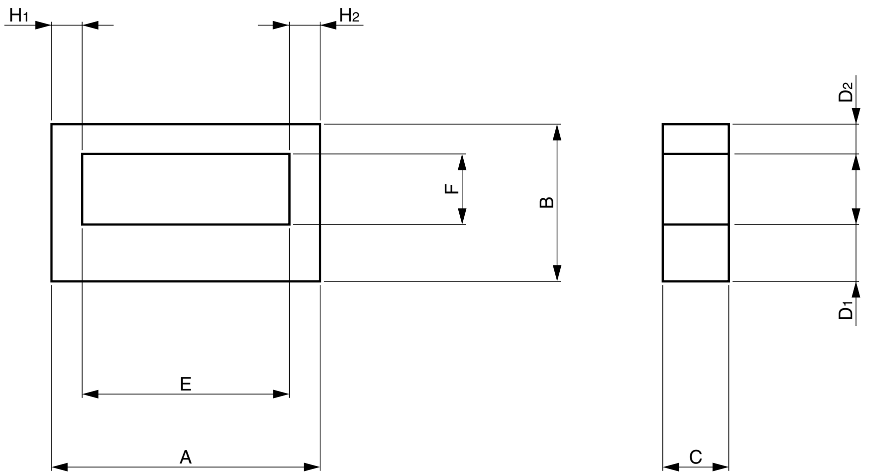

Product code	Dimensions (mm)								
	A	B	C	D_1	D_2	E	F	H_1	H_2
FU2014	20.5+0	14.0+0	4.1±0.2	$3.2^{+0.25}_{-0}$	$3.2^{+0.25}_{-0}$	$13.0^{+0.6}_{-0}$	$6.7^{+0.4}_{-0}$	$3.2^{+0.25}_{-0}$	$3.2^{+0.25}_{-0}$
FU2114	20.6±0.3	14.1±0.25	4.6±0.2	4.2±0.2	2.4±0.15	15.7—0	7.35—0	2.3±0.15	2.3±0.15
FU2216	21.5±0.3	15.6±0.2	3.75±0.2	3.7	5.0	15.5±0.2	6.9±0.2	—	—
FU2316	24.0+0	16.2+0	$4.6^{+0.3}_{-0.2}$	$3.6^{+0.25}_{-0}$	$3.6^{+0.25}_{-0}$	$15.6^{+0.7}_{-0}$	$8.1^{+0.4}_{-0}$	$3.6^{+0.25}_{-0}$	$3.6^{+0.25}_{-0}$
FU2618	25.6±0.4	17.6±0.3	5.2±0.25	5.2±0.15	3.4±0.15	19.5—0	8.7—0	2.9±0.15	2.9±0.15
FU3223	32.3+0	23.3+0	7.8±0.2	$6.3^{+0.3}_{-0}$	$6.3^{+0.3}_{-0}$	$18.5^{+0.9}_{-0}$	$9.6^{+0.5}_{-0}$	6.3±0.15	6.3±0.15

Product code	Magnetic parameter								AL (nH)	
	C_1 (mm^{-1})	Le (mm)	Ae (mm^2)	Ve (mm^3)	Ac (mm^2)	Amin. (mm^2)	Aw (mm^2)	W ($\times 10^{-3}$ kg)	2H07	2H10
FU2014	4.07	51.2	12.6	645	12.6	12.6	91.8	3.2	1950(±30%)	—
FU2114	4.37	52.9	12.1	638	19.3	10.6	120	3.8	2200($^{+40\%}_{-30\%}$)	2900($^{+40\%}_{-25\%}$)
FU2216	4.30	55.0	12.8	704	13.5	10.8	107	3.7	2500($^{+30\%}_{-15\%}$)	—
FU2316	3.88	62.1	15.5	963	15.5	15.5	132	4.7	2350(±30%)	—
FU2618	3.89	68.4	17.6	1200	22.4	15.1	178	6.5	2500($^{+30\%}_{-25\%}$)	3090($^{+30\%}_{-25\%}$)
FU3223	1.73	77.7	45.0	3500	45.8	44.6	187	16.5	5450(±30%)	—

Conventional type EED CORES

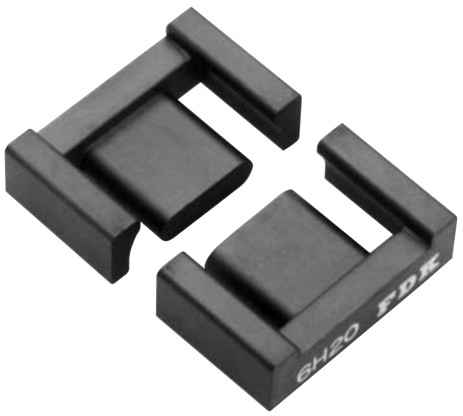

Features

①Most suitable for the designing of small sized transformer.

②Customers are invited to select the most suitable products from a wide selection of shapes.

Applications

Switching regulators, choke coils, etc.

Designation

6H20 EED 25/25 P

- 6H20 — Material
- EED — Shape
- 25 — Core length
- 25 — Core height
- P — Shape detail

Conventional type EED CORES

Summary

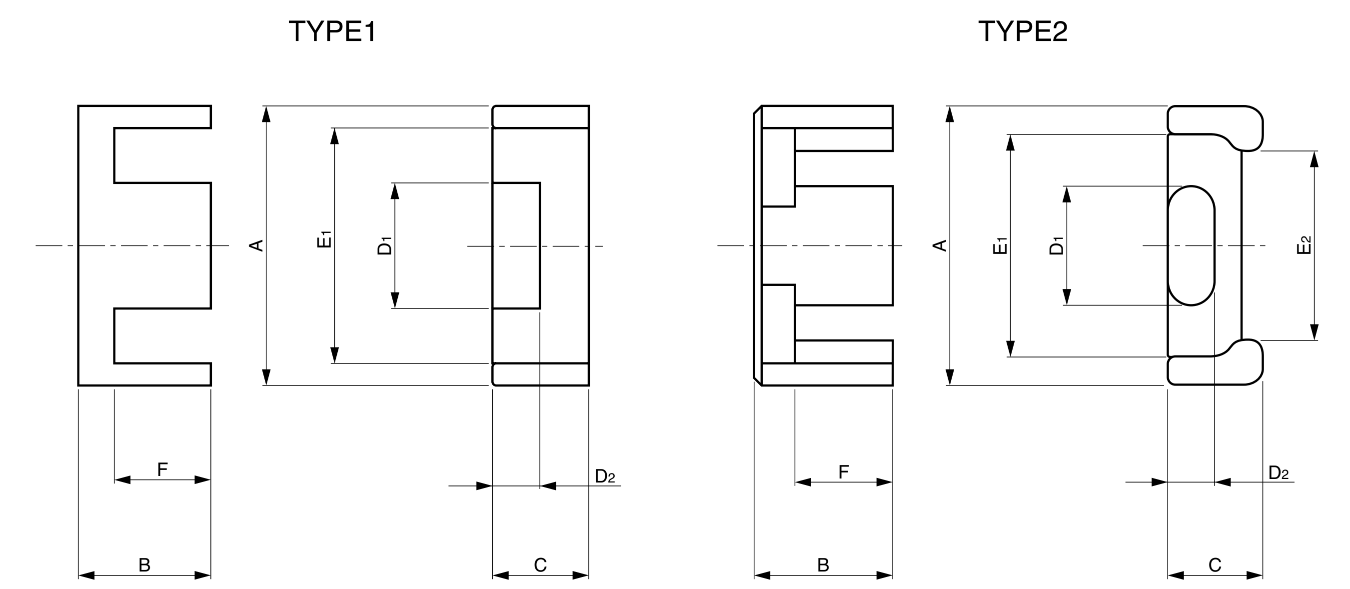

Product code	Type	General standard		Dimensions (mm)							
		IEC	JIS	A	B	C	D_1	D_2	E_1	E_2	F
EED12/12D	1			12.5±0.3	6.2±0.1	3.5±0.1	5.4±0.15	2.0±0.1	9.0±0.25	—	4.55±0.15
EED13/13P	2		FEEPC13	13.2±0.25	6.6±0.2	4.6±0.15	5.6±0.15	2.05±0.1	10.7±0.2	8.3—0	4.5±0.2
EED15/15D	1			15.0±0.4	7.5±0.15	4.65±0.15	5.3±0.15	2.4±0.1	11.0±0.35	—	5.5±0.25
EED16/15	2			$16.0^{+0.4}_{-0.2}$	$7.5^{+0.3}_{-0}$	$7.5^{+0.3}_{-0.1}$	$6.5^{+0}_{-0.2}$	$5.0^{+0}_{-0.2}$	$12.7^{+0.6}_{-0}$	$10.5^{+0.4}_{-0.2}$	$5.6^{+0.25}_{-0}$
EED16/15A	1			16.0±0.3	7.25±0.2	4.8±0.2	$6.1^{+0.05}_{-0.25}$	2.4±0.1	11.8—0	—	5.05±0.2
EED17/17P	2		FEEPC17	17.5±0.3	8.55±0.2	6.0±0.15	7.7±0.15	2.8±0.1	14.5±0.3	12.0±0.5	6.05±0.2
EED19/19P	2		FEEPC19	19.0±0.3	9.75±0.2	6.0±0.15	8.5±0.15	2.5±0.1	16.0±0.3	13.6±0.5	7.25±0.2
EED20/20D	1			20.0±0.55	10.0±0.15	6.65±0.15	8.9±0.2	3.6±0.15	15.4±0.5	—	7.7±0.25
EED25/25D	1			25.0±0.65	12.5±0.15	9.1±0.2	11.4±0.2	5.2±0.15	18.7±0.6	—	9.3±0.25
EED25/25P	2		FEEPC25	25.0±0.4	12.5±0.2	8.0±0.2	11.5±0.2	4.0±0.1	21.0±0.35	17.5±0.5	9.0±0.3
EED27/32P	2		FEEPC27	27.0±0.4	16.0±0.2	8.0±0.2	13.0±0.3	4.0±0.1	22.0±0.4	19.0±0.5	12.0±0.3
EED30/35P	2		FEEPC30	30.0±0.4	17.5±0.2	8.0±0.2	15.0±0.3	4.0±0.1	24.0±0.4	20.5±0.5	13.0±0.3

Product code	Magnetic parameter								AL (nH)
	C_1 (mm^{-1})	Le (mm)	Ae (mm^2)	Ve (mm^3)	Ac (mm^2)	Amin. (mm^2)	Aw (mm^2)	W ($\times 10^{-3}$ kg)	6H20
EED12/12D	2.50	28.5	11.4	325	10.7	10.7C	16.4	1.7	800(±25%)
EED13/13P	2.46	30.6	12.5	382	10.6	10.6C	23.0	2.1	870(±25%)
EED15/15D	2.27	34.0	15.0	510	12.2	12.2C	31.4	2.8	900(±25%)
EED16/15	1.28	36.5	28.6	1040	27.9	27.9C	37.8	5.1	1400(±25%)
EED16/15A	1.94	33.1	17.1	566	14.4	14.4C	30.6	3.1	1000(±25%)
EED17/17P	1.76	40.2	22.8	917	19.9	19.9C	41.1	4.5	1150(±25%)
EED19/19P	2.03	46.1	22.7	1050	19.9	19.9C	54.4	5.3	940(±25%)
EED20/20D	1.52	47.0	31.0	1460	31.0	31.0C	50.1	7.1	1500(±25%)
EED25/25D	0.980	57.0	58.0	3310	57.5	57.0L	67.9	16.6	2100(±25%)
EED25/25P	1.28	59.2	46.4	2750	42.6	42.6C	85.5	13.0	1600(±25%)
EED27/32P	1.34	73.1	54.6	4000	48.6	48.6C	108	18.0	1600(±25%)
EED30/35P	1.32	81.6	61.0	5040	56.6	56.6C	117	23.0	1600(±25%)

Low profile type

Features

①Suitable for the designing of low profiled transformers.

②Customers are invited to select the most suitable products from a wide selection of shapes.

Applications

DC-DC converters

Low profile type Small E CORES

Summary

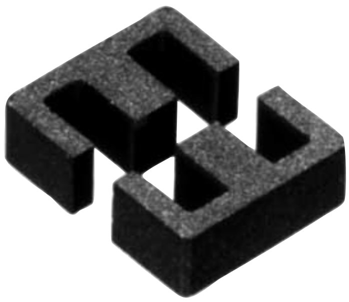

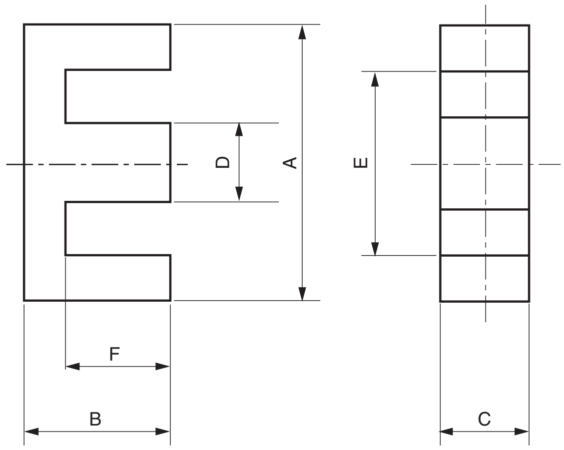

Product code	General standard		Dimensions (mm)					
	IEC	JIS	A	B	C	D	E	F
EE04/03			4.15±0.1	1.55±0.05	1.4±0.1	1.2±0.1	2.9±0.1	0.95±0.05
EE05/05	E5.3/2	FEE/5.25	5.25±0.05	2.65±0.05	1.95±0.05	1.35±0.05	3.85typ.	2typ.
EE07/06			6.5±0.3	3.0±0.15	1.8±0.15	1.5±0.15	4.5min.	2.1±0.15
EE09/08	E8.8/2	FEE/9	9.017typ.	3.937±0.127	1.905±0.102	1.905±0.127	5.207±0.127	2.159±0.127

Product code	Magnetic parameter							
	C_1 (mm^{-1})	Le (mm)	Ae (mm^2)	Ve (mm^3)	Ac (mm^2)	Amin. (mm^2)	Aw (mm^2)	W (g)
EE04/03	4.35	7.4	1.7	12.6	1.68	1.68BC	1.62	0.07
EE05/05	4.77	12.6	2.64	33.2	2.63	2.54B	5	0.17
EE07/06	4.7	14.2	3.02	42.9	2.7	2.70C	7.35	0.22
EE09/08	3.13	22.9	8.4	78	3.61	3.61C	7.23	0.4

Low profile type EE CORES

Summary

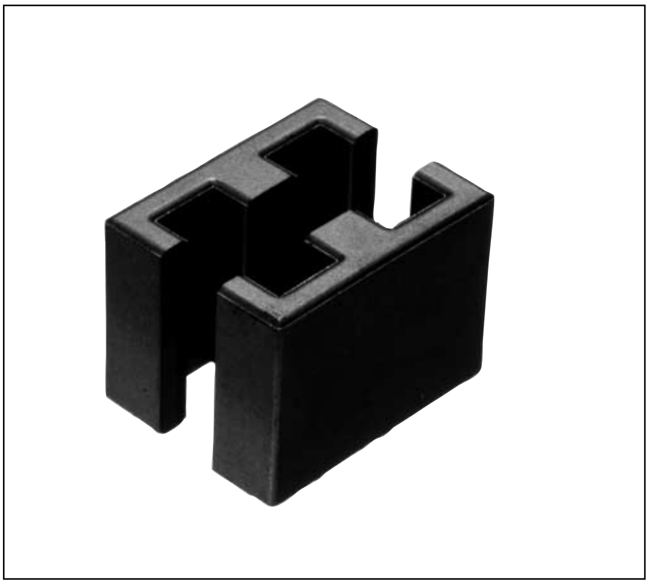

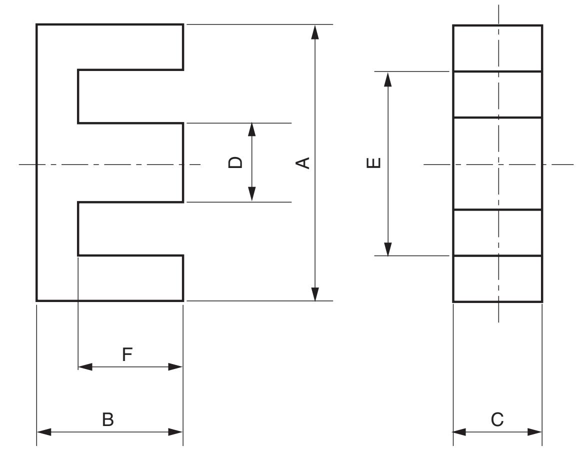

Product code	General standard		Dimensions (mm)					
	IEC	JIS	A	B	C	D	E	F
EE14/07	E/E14		14.0±0.3	3.5±0.1	5.0±0.1	3.0±0.1	11.0±0.25	2.0±0.1
EE18/08	E/E18		18.0±0.35	4.0±0.1	10.0±0.2	4.0±0.1	14.0±0.3	2.0±0.1
EE21/06			21.0±0.3	$2.9^{+0}_{-0.2}$	15.0±0.3	5.0±0.2	15.7min.	1.3±0.1
EE22/11A	E/E22		21.8±0.4	5.7±0.1	15.8±0.3	5.0±0.1	16.8±0.4	3.2±0.1

Product code	Magnetic parameter							
	C_1 (mm^{-1})	Le (mm)	Ae (mm^2)	Ve (mm^3)	Ac (mm^2)	Amin. (mm^2)	Aw (mm^2)	W (g)
EE14/07	1.45	20.7	14.3	296	15	13.9L	16	1.5
EE18/08	0.618	24.3	39.3	955	40	38.9L	20	4.8
EE21/06	0.418	21.6	51.7	1120	75	45B	13.9	5.6
EE22/11A	0.414	32.5	78.3	2540	79	77.9L	37.8	12.7

Low profile type EER CORES

Summary

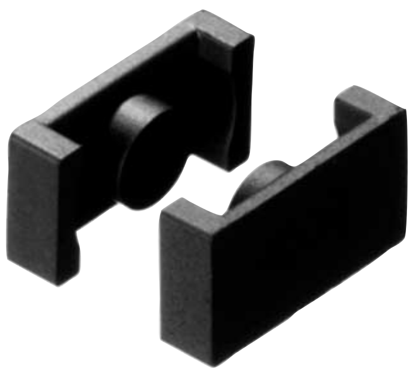

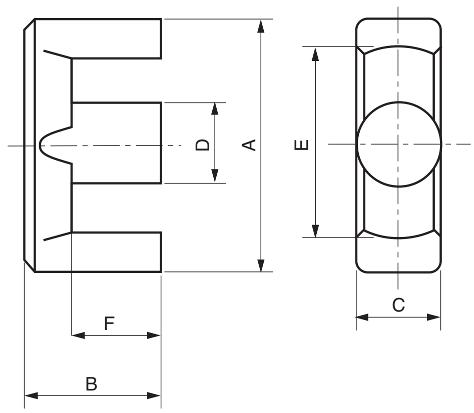

Product code	General standard		Dimensions (mm)					
	IEC	JIS	A	B	C	D	E	F
EER09/05			$9.5^{+0}_{-0.4}$	$2.4^{+0}_{-0.2}$	$5.2^{+0}_{-0.3}$	$3.5^{+0}_{-0.3}$	$7.7^{+0.4}_{-0}$	$1.5^{+0.2}_{-0}$
EER11/04			10.8±0.2	$2.0^{+0}_{-0.1}$	5.9±0.1	4.1±0.15	8.7min.	$1.0^{+0.15}_{-0}$
EER11/05			10.8±0.2	2.45±0.1	5.9±0.1	4.1±0.15	8.7min.	1.6±0.1
EER16/06			15.5±0.2	$3.2^{+0}_{-0.15}$	$7.0^{+0}_{-0.3}$	$5.2^{+0}_{-0.2}$	$11.7^{+0.4}_{-0}$	$1.85^{+0.2}_{-0}$
EER19/06A			19.08/20.09	2.93/3.12	7.19/7.59	5.47/5.96	14.38/15.39	1.27/1.47
EER24/06B			24.38±0.6	2.97±0.1	8.51±0.4	6.6±0.25	18.59±0.6	0.96±0.07
EER40/18			40.0±0.7	$9.0^{+0}_{-0.2}$	13.3±0.3	13.3±0.3	28.8min.	4.0±0.15

Product code	Magnetic parameter							
	C_1 (mm^{-1})	Le (mm)	Ae (mm^2)	Ve (mm^3)	Ac (mm^2)	Amin. (mm^2)	Aw (mm^2)	W (g)
EER09/05	1.73	13.8	7.96	110	8.81	7.07B	7.28	0.63
EER11/04	1.07	12.7	11.9	151	13.2	10.3B	5.27	0.9
EER11/05	1.24	14.7	11.9	175	13.2	10.3B	7.48	1
EER16/06	1.07	19.5	18.2	354	20.4	15.4B	11.1	2
EER19/06A	0.812	21.1	26	540	26	26CB	12.4	2.9
EER24/06B	0.656	23.6	36	840	34.2	34.2C	11.5	4.8
EER40/18	0.346	48.5	140	6780	139	130B	64.8	36.2

Low profile type EI CORES

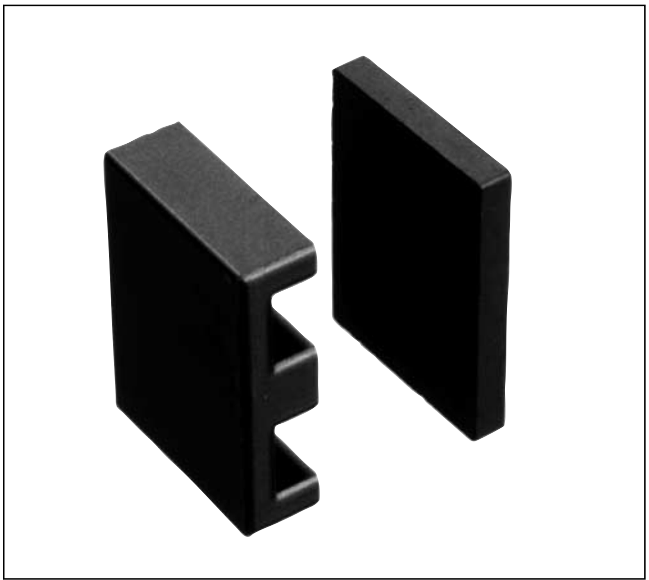

Summary

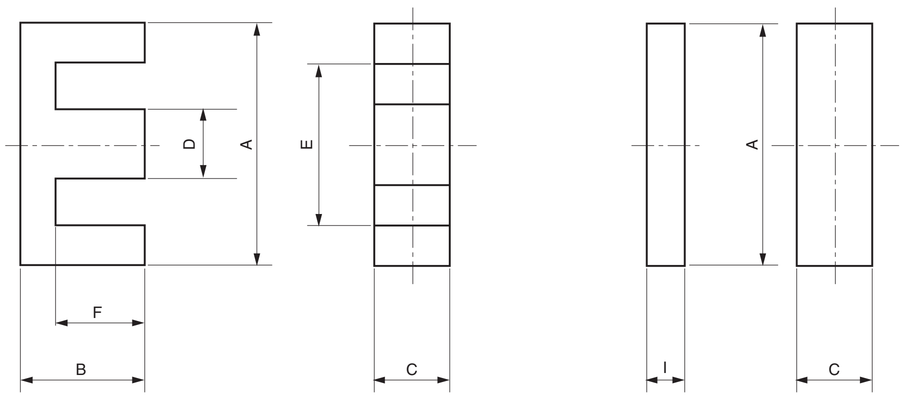

Product code	General standard		Dimensions (mm)						
	IEC	JIS	A	B	C	D	E	F	I
EI14/05	E/PLT14		14.0±0.3	3.5±0.1	5.0±0.1	3.0±0.1	11.0±0.25	2.0±0.1	1.5±0.1
EI18/06	E/PLT18		18.0±0.35	4.0±0.1	10.0±0.2	4.1±0.1	14.0±0.3	2.0±0.1	2.0±0.1
EI22/08			21.6±0.25	5.72±0.07	15.9±0.25	5.08±0.12	16.1min.	3.18±0.1	2.54±0.12
EI22/08A	E/PLT22		21.8±0.4	5.7±0.1	15.8±0.3	5.0±0.1	16.8±0.4	3.2±0.1	2.5v0.1

Product code	Magnetic parameter							
	C_1 (mm^{-1})	Le (mm)	Ae (mm^2)	Ve (mm^3)	Ac (mm^2)	Amin. (mm^2)	Aw (mm^2)	W (g)
EI14/05	1.15	16.7	14.5	242	15	13.9L	8	1.2
EI18/06	0.513	20.3	39.5	802	40	38.9L	10	4
EI22/08	0.32	25.8	80.5	2080	80.5	80.5LBC	15	10.8
EI22/08A	0.332	26.1	78.5	2050	79	77.9L	18.9	10.3

Low profile type　RM CORES

Summary

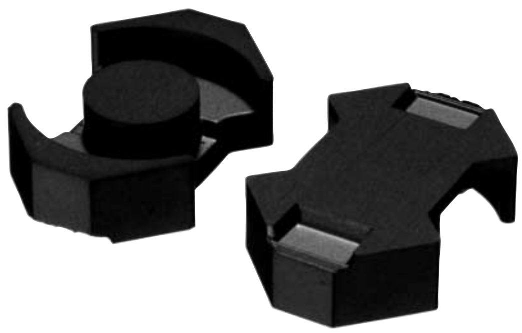

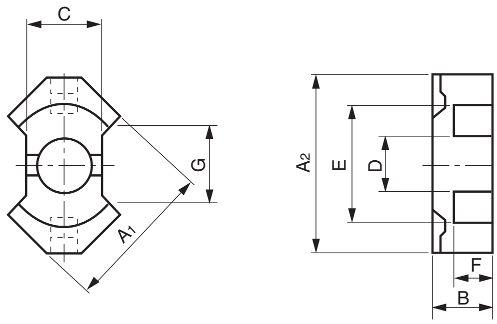

Product code	General standard		Dimensions (mm)							
	IEC	JIS	A1	A2	B	C	D	E	F	G
RM5GA			$12.3^{+0}_{-0.4}$	$14.9^{+0}_{-0.8}$	3.56±0.05	$6.8^{+0}_{-0.4}$	$4.9^{+0}_{-0.2}$	$10.2^{+0.4}_{-0}$	1.6±0.1	6.0min.
RM5GP	RM5/8		$12.3^{+0}_{-0.4}$	$14.9^{+0}_{-0.8}$	$3.9^{+0}_{-0.1}$	$6.8^{+0}_{-0.4}$	$4.9^{+0}_{-0.2}$	$10.2^{+0.4}_{-0}$	$1.8^{+0.2}_{-0}$	6.0min.
RM6GL			$14.7^{+0}_{-0.6}$	$17.9^{+0}_{-0.6}$	$3.55^{+0}_{-0.1}$	$8.2^{+0}_{-0.4}$	$6.4^{+0}_{-0.2}$	$12.4^{+0.5}_{-0}$	$1.35^{+0.2}_{-0}$	8.4min.
RM6GP	RM6/9		$14.7^{+0}_{-0.6}$	$17.9^{+0}_{-0.6}$	$4.5^{+0}_{-0.1}$	$8.2^{+0}_{-0.4}$	$6.4^{+0}_{-0.2}$	$12.4^{+0.5}_{-0}$	$2.25^{+0.2}_{-0}$	8.4min.
RM8GP	RM8/11		$19.7^{+0}_{-0.7}$	$23.2^{+0}_{-0.9}$	$5.8^{+0}_{-0.1}$	$11.0^{+0}_{-0.4}$	$8.55^{+0}_{-0.3}$	$17.0^{+0.6}_{-0}$	$2.95^{+0.2}_{-0}$	10.5min.
RM10GL			$24.7^{+0}_{-1.1}$	$28.5^{+0}_{-1.3}$	4.75±0.1	$13.5^{+0}_{-0.5}$	$10.9^{+0}_{-0.4}$	$21.2^{+0.9}_{-0}$	1.98±0.1	$11.3^{+1.3}_{-0}$
RM10GP	RM10/13		$24.7^{+0}_{-1.1}$	$28.5^{+0}_{-1.3}$	$6.5^{+0}_{-0.1}$	$13.5^{+0}_{-0.5}$	$10.9^{+0}_{-0.4}$	$21.2^{+0.9}_{-0}$	$3.35^{+0.2}_{-0}$	11.3min.
RM12GB			$29.8^{+0}_{-1.2}$	$37.6^{+0}_{-1.5}$	8.5±0.2	—	$12.8^{+0}_{-0.4}$	$24.9^{+1.1}_{-0}$	5.35±0.15	12.9min.
RM12GP	RM12/17		$29.8^{+0}_{-1.2}$	$37.6^{+0}_{-1.5}$	$8.4^{+0}_{-0.1}$	—	$12.8^{+0}_{-0.4}$	$24.9^{+1.1}_{-0}$	$4.5^{+0.25}_{-0}$	12.9min.

Product code	Magnetic parameter							
	C_1 (mm^{-1})	Le (mm)	Ae (mm^2)	Ve (mm^3)	Ac (mm^2)	Amin. (mm^2)	Aw (mm^2)	W (g)
RM5GA	0.794	18.9	23.8	450	18.1	18.1C	8.32	2.4
RM5GP	0.704	17.4	24.7	430	18.1	18.1C	9.5	2.6
RM6GL	0.496	17.7	35.7	632	31.2	30.7B	8.1	3.4
RM6GP	0.611	22	36	791	31.2	30.7B	13.5	4
RM8GP	0.409	27.7	67.6	1870	55.4	55B	24.9	9.2
RM10GL	0.271	26.8	99	2650	90	90C	20.3	13.2
RM10GP	0.334	33.4	100	3340	90	90C	34.5	17.2
RM12GB	0.271	26.8	99	2653	125	125C	20.4	13.2
RM12GP	0.279	41.3	148	6120	125	125C	54.5	33.6

FDK Web Site
http://www.fdk.co.jp

FDK CORPORATION

Electronics sales Div.
5-36-11, Shinbashi, Minato-ku, Tokyo 105-8677, Japan (Hamagomu Bldg.)
TEL: (81)-3-5473-2857 FAX: (81)-3-3431-9436

U.S.A. **FDK AMERICA, INC. CORPORATE OFFICE**
2270 North First Street, San Jose, California 95131-2022, U.S.A.
TEL: (1)-408-432-8331 FAX: (1)-408-435-7478

FDK AMERICA, INC. BOSTON OFFICE
411 Waverly Oaks Road, Suite 324, Waltham,
Massachusetts 02452-8437, U.S.A.
TEL: (1)-781-899-7700 FAX: (1)-781-899-7701

FDK AMERICA, INC. SAN DIEGO OFFICE
6540 Lusk Blvd Suite C274 San Diego,
California 92121-2766, U.S.A.
TEL: (1)-858-558-8368 FAX: (1)-858-558-6005

Europe **FDK ELECTRONICS GMBH**
Heerdter Lohweg 89, 40549 Düsseldorf, Germany
TEL: (49)-211-591574 FAX: (49)-211-593549

FDK ELECTRONICS UK LIMITED
Suite 4C Celect House 12A Fairbairn Road,
Kirkton North Livingston EH54 6TS,
Scotland, United Kingdom
TEL: (44)-1506-467981 FAX: (44)-1506-467982

Asia **FDK HONG KONG LTD.**
Suite 1601-1602, Tower 3, China Hong Kong City,
33 Canton Road, Tsim Sha Tsui, Kowloon, Hong Kong.
TEL: (852)-27999773 FAX: (852)-27554635

FDK SINGAPORE PTE., LTD.
4, Leng Kee Road, #06-07/08 SiS Building, Singapore. 159088,
Republic of Singapore
TEL: (65)-472-2328 FAX: (65)-472-5761

Printed in Japan